



---

# RESEARCH REPORT

---

Livorno, May 2012  
IFRF Doc. No F 73/y/02

## APPLICATION OF AN OPTICAL DIAGNOSTIC METHODOLOGY TO THE CHARACTERISATION OF SOLID FUEL COMBUSTION IN THE ISOTHERMAL PLUG FLOW REACTOR OPERATING IN CONVENTIONAL AND OXY-FUEL CONDITIONS

**ENEA, Pisa University, IFRF**

Prepared by

**S. Tarquini, C. Galletti, G. Coraggio, M. Faleni, L. Biasci  
R. Bruschi, F. Di Carlo, E. Giacomazzi, S. Giammartini**

<http://www.research.ifrf.net>

---

## **INTERNATIONAL FLAME RESEARCH FOUNDATION**

---

**REGISTERED OFFICE**  
c/o Presidenza Facoltà di  
Ingegneria, Via Diotallevi 2,  
56126, Pisa, Italy  
CF: 93059950506

**OPERATIONS CENTRE**  
Via Salvatore Orlando 5,  
57123 Livorno, Italy

**CONTACT NUMBERS**  
Tel: +39 0586 891678  
Fax: +39 0586 200045  
e-mail [info@ifrf.net](mailto:info@ifrf.net)  
<http://www.ifrf.net>

**BANK**  
IBAN: IT 06 M 06200 14011 000000586187  
Cassa di Risparmio Lucca Pisa Livorno  
Swift: BPALIT3LXXX  
VAT no.: 01807000508

## Acknowledgements

IFRF staff: L. Tognotti  
G. Coraggio  
L. Biasci  
M. Faleni  
L. Lupetti

ENEA staff R. Bruschi  
F. Di Carlo  
S. Gianmartini  
E. Giacomazzi

ENEL staff: D. Cecchini  
A. Birindelli  
M. Monticelli  
L. Carrai  
F. Costanzi  
R. Miliani

---

## Executive summary

Pulverized coal combustion is the most important source of electric power in the world, so a deep knowledge of this process is needed. In particular in last years important commitments were taken to reduce the enormous emission of carbonic dioxide due to fossil fuels combustion. To reach this purpose the process of Carbon Capture and Sequestration (CCS) is the most studied, even if is very effective only if flue gases are rich in CO<sub>2</sub>. One of the most promising technique to generate exhaust gases with a very high content of carbon dioxide is the oxy-fuel [1].

In last years the Electric System Research Division of ENEA (Italian Agency for Energy and Environment) has developed some optical probes (ODC – Optical Diagnostics of Combustion) useful in combustion diagnostics. They were already tested with good results in homogeneous combustion processes (i.e. natural gas oxidation) especially to study thermo-acoustic instabilities [6], but no applications were tested about heterogeneous combustion (i.e. pulverized coal oxidation). For this reason ENEA, IFRF and University of Pisa signed a contract of collaboration to carry out some experimental campaigns. The reactor used in the first periods of tests was an Entrained Flow Reactor (EFR), in particular the Isothermal Plug Flow Reactor (IPFR). This facility was chosen because of its very high heating rate, similar to real industrial boilers.

This report will provide a detailed description of the experimental equipment used for tests, of the conditions tested. In addition the procedures adopted for data analysis and the experimental results will be presented and discussed.

---

## Index

Acknowledgements.....	2
Executive summary.....	3
Index .....	4
1 Introduction.....	6
2 Objectives .....	7
3 Description of the experimental equipment.....	8
3.1 The Isothermal Plug Flow Reactor.....	8
3.2 The Optical Diagnostics of Combustion probes .....	11
3.3 Probes disposition .....	13
4 Operating conditions.....	15
4.1 Feed mode .....	15
4.2 Fuels .....	15
4.3 Process variables .....	16
4.4 Calculus of the equivalence ratio of volatiles oxidation .....	18
4.5 Calculus of the equivalence ratio .....	20
4.6 Calculus of the group number in each test.....	23
5 Signals analysis of continuous fed tests.....	28
5.1 Signals form and data treatment.....	28
5.2 Tests with coal.....	30
5.2.1 Validation of the probes capability to diagnose the pulverized coal transit .....	30
5.2.2 Effect of the reactor temperature .....	32
5.2.3 Effect of the oxygen gas fraction .....	34
5.2.4 Effect of the particles size.....	35
5.2.5 Effect of gaseous atmosphere composition.....	37
5.2.6 Effect of the carrier gas composition.....	38
5.2.7 Peaks analysis .....	40
5.3 Tests with char .....	46
5.3.1 Effect of the particles size.....	46
5.4 Tests with biomass .....	47
5.4.1 Effect of the oxygen gas fraction .....	47
6 Signals analysis of pulsed fed tests.....	49
6.1 Signals form and data treatment.....	49
6.2 Tests with coal.....	50
6.2.1 Effect of the reactor temperature .....	50

---

6.2.2	Effect of the oxygen gas fraction .....	52
6.2.3	Effect of the particles size.....	54
6.2.4	Effect of gaseous atmosphere composition.....	58
6.2.5	Determination of ignition delay .....	60
6.3	Tests with char .....	61
6.3.1	Effect of the particles size.....	61
6.4	Tests with biomass .....	63
6.4.1	Effect of the oxygen gas fraction .....	63
7	Data post-processing of signals of pulsed fed experimental tests.....	66
7.1	Evaluation of solid particles medium velocity .....	66
7.1.1	Adopted procedure.....	66
7.1.2	Experimental results.....	67
7.1.2.1	Tests with coal .....	67
7.1.2.2	Tests with char of coal .....	68
7.1.2.3	Tests with biomass .....	68
8	References.....	69

---

## 1 Introduction

Pulverized coal combustion is the most important source of electric power in the world, so a deep knowledge of this process is needed. In particular in last years important commitments were taken to reduce the enormous emission of carbonic dioxide due to fossil fuels combustion. To reach this purpose the process of Carbon Capture and Sequestration (CCS) is the most studied, even if is very effective only if flue gases are rich in  $\text{CO}_2$ . One of the most promising technique to generate exhaust gases with a very high content of carbon dioxide is the oxy-fuel [1]. In this case a mixture of oxygen and recycled flue gases is used instead of air for fuel oxidation. Consequently, a gas consisting of  $\text{CO}_2$  and  $\text{H}_2\text{O}$  is obtained, with a  $\text{CO}_2$  concentration ready for sequestration. Flue gases are recycled in order to make up the volume of the missing  $\text{N}_2$ . Obviously a preliminary treatment of separation of  $\text{O}_2$  from air is needed. Nowadays oxy-fuel has not still an industrial application because of the important differences from conventional combustion, so studies in this field are very useful. In particular in literature there are not many works on ignition and particle oxidation in oxy-fuel and most of them are about combustion of single coal particles [2]-[4]. Only in one case a dense feed stream is studied in oxy-fuel conditions [5].

In last years the Electric System Research Division of ENEA (Italian Agency for Energy and Environment) has developed some optical probes (ODC – Optical Diagnostics of Combustion) useful in combustion diagnostics. They were already tested with good results in homogeneous combustion processes (i.e. natural gas oxidation) especially to study thermo-acoustic instabilities [6], but no applications were tested about heterogeneous combustion (i.e. pulverized coal oxidation). For this reason ENEA, IFRF and University of Pisa signed a contract of collaboration to carry out some experimental campaigns. In this way ENEA could test the effectiveness of its probes in heterogeneous oxidation processes realized in pilot furnaces sited in ENEL Research's Experimental Area in Livorno. IFRF staff was responsible of the management of the reactors, while the University gave support in data analysis. The reactor used in the first periods of tests was an Entrained Flow Reactor (EFR), in particular the Isothermal Plug Flow Reactor (IPFR). This facility was chosen because of its very high heating rate, similar to real industrial boilers. This aspect is very important because heating rate influences volatiles yield, fraction of light gases generated, ignition delay and time of devolatilization (and volatiles oxidation) [7]. For this reason it is very important realize tests in facility with very high heating rate, with the purpose to obtain data for industrial applications. Obviously IPFR is a reactor with a very simple fluid-dynamics, so an important interaction between aerodynamics, chemistry and thermodynamics is not present.

---

## 2 Objectives

The general objectives of this report are:

- to describe the experimental equipment used for tests
  - to describe the experimental conditions tested
  - to describe the procedures adopted for data analysis
  - to report the experimental results.
-

### 3 Description of the experimental equipment

The experimental equipment is made of two parts:  
the pilot furnace (IPFR) where combustion processes happen  
the optical probes (ODC) that analyze combustion processes.

#### 3.1 The Isothermal Plug Flow Reactor

The Isothermal Plug Flow Reactor is a big drop tube reactor built in Netherlands in 1994 and transferred in Livorno in 2008. For a detailed description of the IPFR a previous report is available [8]. A scheme of IPFR is shown in Fig. 1. The IPFR is characterized by very high gas temperature (700-1400°C) and particles heating rates ( $10^4$ - $10^5$  K/s).

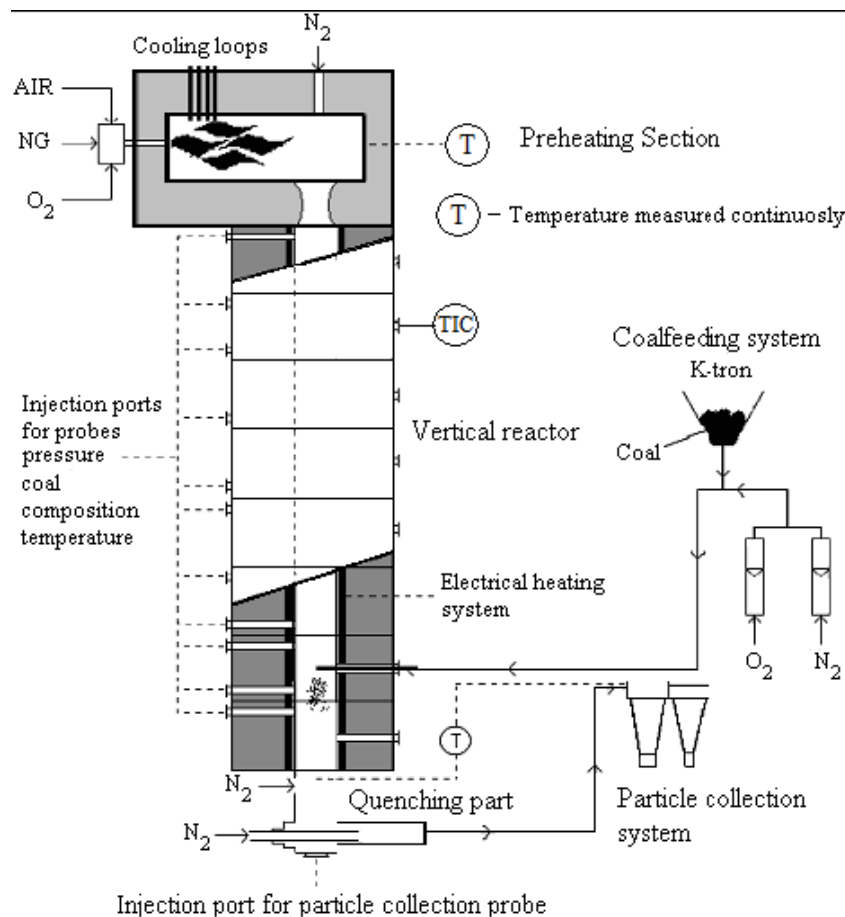


Fig. 1: Scheme and characteristics of IPFR

IPFR is made of three principal sections:  
a gas pre-heater  
a vertical section  
an exhaust line with particle collection system.

In the first section (the pre-heater) gases with different composition and temperature are generated, in order to create the desired atmosphere in the following vertical section. In this second zone the pulverized solid fuel (coal or biomass) is injected by a stream of carrier gas



and the heterogeneous oxidation process happens. At the bottom exhaust gases and burned solid particles are quenched with air or nitrogen (if collected) until 200°C and then treated in two cyclones and a bag filter before the discharge in atmosphere. Obviously there is the possibility to collect solid particles to analyze them on-line or off-line in laboratory. The main characteristics of IPFR are reported in Tab. 1.

Tab. 1: IPFR technical specification

CHARACTERISTIC	MEASURE
Reactor tube total length	4.5 m
Reactor tube operating length	4.0 m
Reactor tube inner diameter	150 mm
Number of operating modules	8
Number of feeding ports	19
Operating temperature	700-1400°C
Residence time	5–1500 ms
Max. gas flow rate	75 Nm <sup>3</sup> /h
Min. feeding rate of pulverized fuel	0.08 kg/h

The gas preheating section (Fig. 2) provides gases at desired composition and temperature realizing the oxidation of natural gas and oxygen in a horizontal chamber of 1 meter of length and 300 mm of diameter. The burner is an Aerodynamically Air Staged Burner (AASB) for natural gas. In this chamber many gas streams can be fed, in particular for conventional combustion natural gas and air are fed, while to create oxy-fuel conditions oxygen and carbon dioxide are fed instead of air. Carbon dioxide is used in substitution of recycled exhaust gases as really happens in oxy-fuel applications, this is possible because of carbon dioxide is the main constituent of flue gases. To regulate the gas composition a system of control acts on feed valves of the various streams to respect the indications given by the operator, in this way gases have the desired fraction of oxygen. To obtain the desired gas temperature a cold stream of nitrogen is added. Obviously to have a content of oxygen in exiting gas from this section is needed to realize natural gas oxidation in oxygen excess than the stoichiometric.

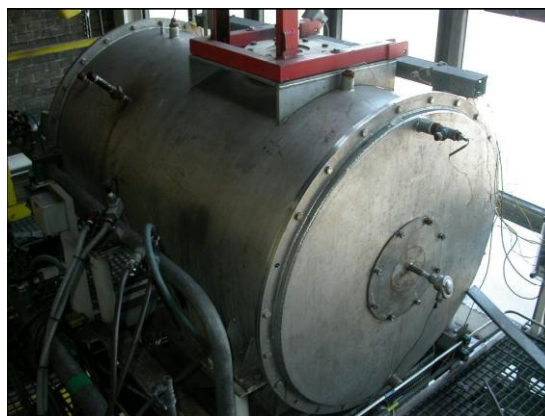


Fig. 2: Gas pre-heating section

The gases coming from the pre-heater section flow in the vertical section (Fig. 3). This is a long tube inserted in eight modules independently electrically heated to guarantee the condition of isothermal flow inside the reactor. Without these silicon carbide U-type heating elements gases' temperature tends to decrease along the reactor. Each module has several ports at different height which can be used to introduce the coal feed or measure instruments.

In these tests also the optical probes were inserted from those ports. Gases' temperature profile is monitored by several type B thermocouples.

Pulverized coal (or biomass) is injected in the reactor by a water cooled radial feed probe (Fig. 4) and is entrained by a carrier gas that can be nitrogen or a mixture of nitrogen and air in different percents. It is possible to feed the fuel from different height changing the port where the feed probe is inserted. Two kinds of coal feeds can be used: a continuous or a pulsed way. In the first case a K-tron mass flow controller provides the continuous coal flow in the carrier gas, while in the second case a small volume of coal is fed with a frequency chosen by the operator.



Fig. 3: Vertical section

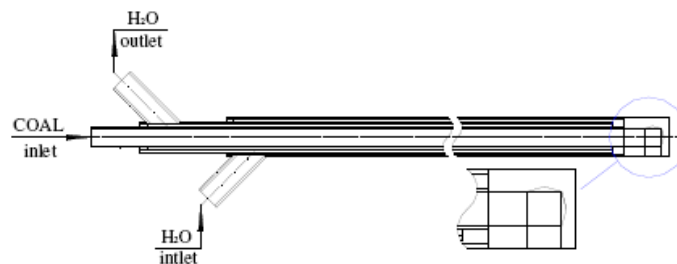


Fig. 4: Radial feeding probe

The scheme of the nineteen ports of the IPFR is shown in Fig. 5.

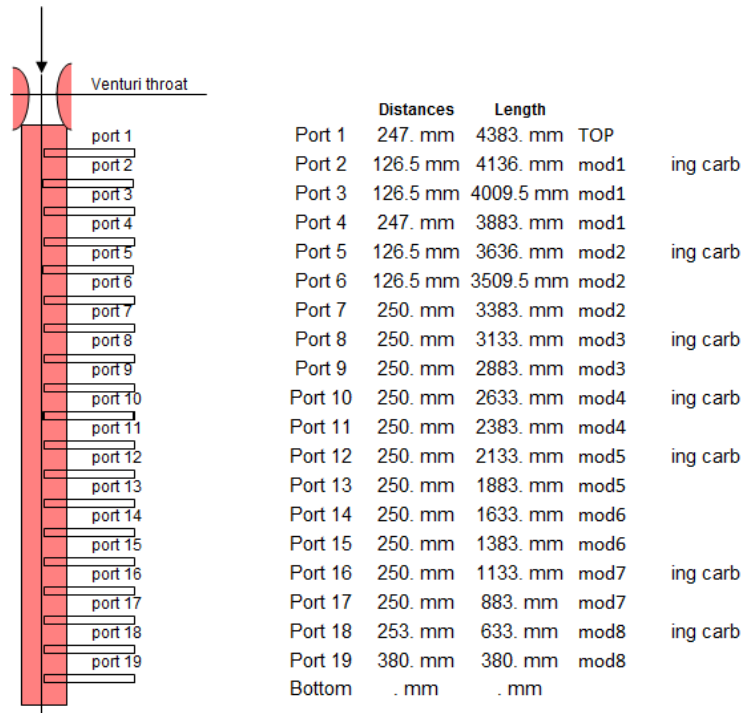


Fig. 5: Scheme of IPFR's ports

### 3.2 The Optical Diagnostics of Combustion probes

The ODC probes were developed by ENEA to monitor industrial combustion processes [9], [10]. ODC system (Fig. 6) is based on a photodiode which detects the radiant energy emitted by a combustion process in the spectral range from the UV to near IR (200 nm to 1100 nm). For gas combustion, such energy is the result of two effects: chemiluminescence of reactants and emission/absorption from combustion product. Hence such energy fluctuates in time and space, as a consequence of fluctuations of the flame, stemming from the interaction between the combustion process, the turbulent eddies and the acoustic field (that has no effects in this IPFR application).

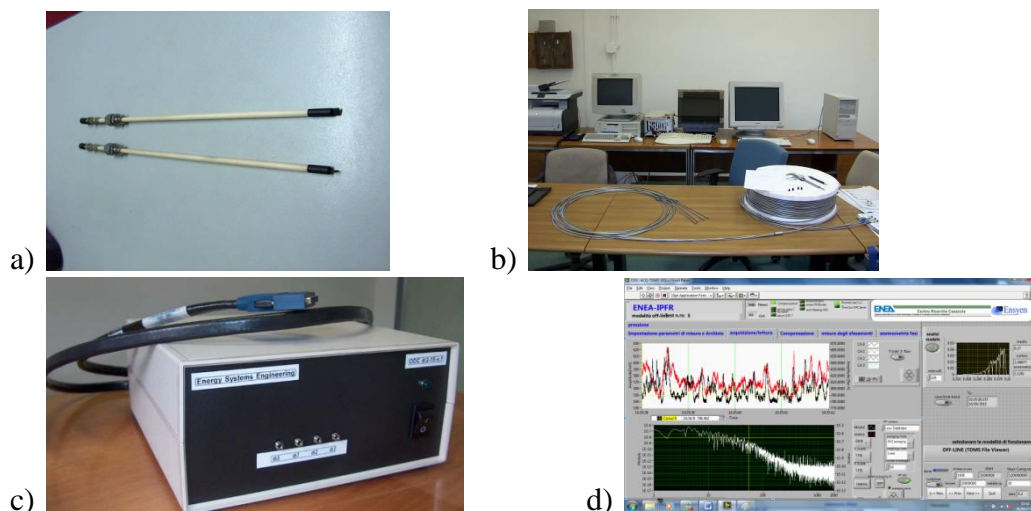


Fig. 6: Details of ODC system: the probes (a), the optical fibre (b), the transducer box (c) and the interactive panel LabView® (d)

The light emission's intensity is proportional to the rate of production of some molecules and this premises the use of the chemiluminescence to measure the reaction rate and the thermic release. The continuous component of the captured radiant energy is essentially a function of the thermic state of the combustion chamber. The signal detected by ODCs represents the trend of the luminosity and the peaks are the burst of flame of the combustion process which have the effect to increase the local luminosity from the thermic state of the walls (Fig. 7).

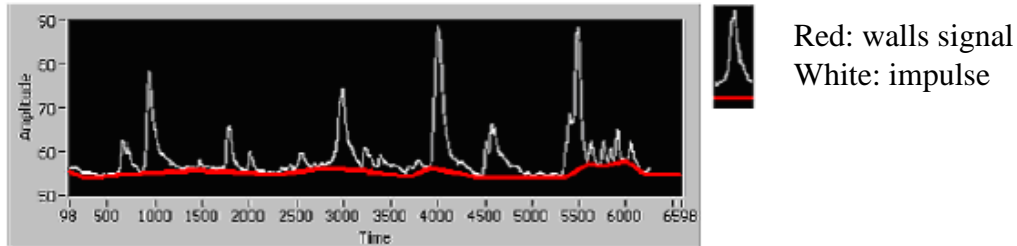


Fig. 7: An example of signal produced by the ODC system

The capability to monitor in real time e with little intrusiveness the events that cause these phenomena results strategic to obtain a consistent diagnostics of the flame stability. Due to this objective the combustion process is observed with an optical probe that transferred with an optical fibre the luminous signal to a transducer sited in a low interferences environment. The probe is made of two parts: a monocrystalline sapphire bar and a quartz optical fibre. Sapphire has the strategic function to have a very high refraction index which allows to consider it as an ideal optical fibre, beside it is an inert material until 2000 K and this premises the direct access to the combustion chamber. The optical sensor used is a UDT455HS with a sensible surface of 5 mm<sup>2</sup>, a spectral response from 200 to 1100 nm (UV-IR) and a frequency response higher than 5 MHz (Fig. 8). This last characteristic is needed to observe all the phenomena of a combustion process.

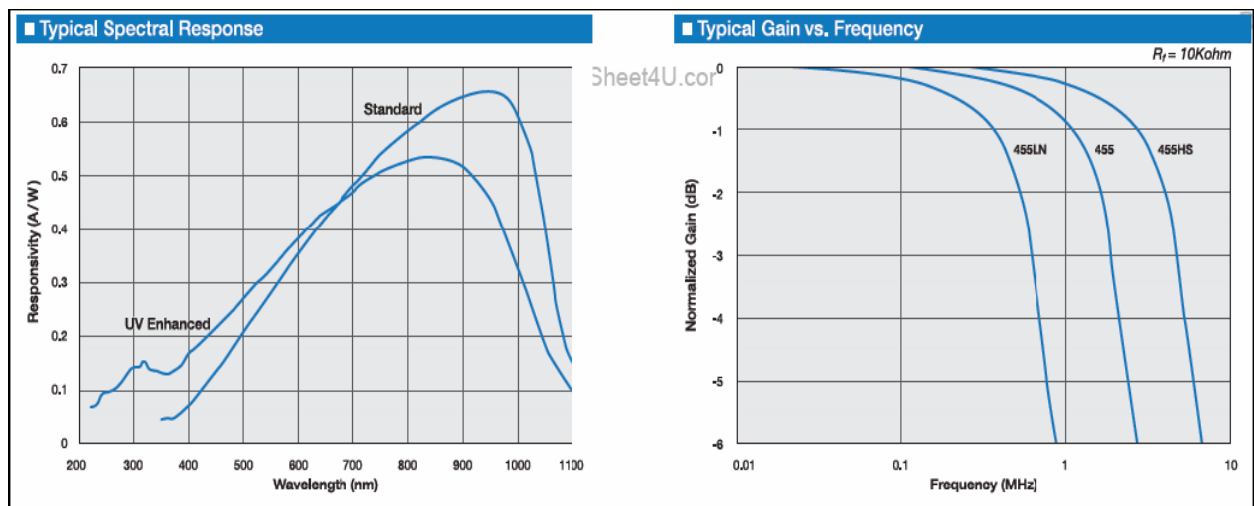


Fig. 8: Characteristics of the optical sensor UDT455HS and the ODC probes

The signal acquisition system is managed by an operator from computer by a connection with software LabView<sup>®</sup>. To have a high resolution of the converters on the signal dynamic component the system allows to compensate the signals for couples of probes. The

compensation is not automatic because setting before two values of compensation it is possible to avoid the introduction of not desired signals.

In case of coal combustion the radiant energy may come from the gaseous combustion process (volatiles oxidation), soot as well as from burning char particles. The main idea of ODC is thus to use the radiant energy as a nonintrusive and natural seeding to describe turbulent combustion. The analysis of the signal dynamics (i.e. variation with time) allows deriving important information on the flame behaviour.

### 3.3 Probes disposition

During both experimental campaigns four ODC probes were used with the purpose to monitor different zones of IPFR. In the first campaign (10-12 April 2011) the probes were inserted along the reactor at different heights from various ports. Instead during the second campaign (7 September 2011) one probe was inserted from the bottom of the reactor in axial position, while the other three probes were inserted in radial positions from the lateral ports. This last configuration was adopted to maximize the signals information for the pulsed tests (on September only this feed mode was made). Radial probes see the solid particles while they pass in front of them, so the detected signal gives a spatial information, deriving from the position of the probe. Obviously this is very interesting because it is possible to follow the combustion process for different distances from the coal injection point, then for different particles residence times. On the other hand the axial probe can see the particles from the moment they are injected inside the reactor to the moment they exit from the IPFR after the quench. For this reason the detected signal has a temporal information. Examining the signals from all four probes it is possible to join spatial and temporal informations and this allows to obtain a higher number of qualitative and quantitative informations from the post-processing data. The axial probe was inserted from the bottom of IPFR replacing the sampling probe that it was not used in these tests. The probes disposition in the two experimental campaigns is reported in Tab. 2.

**Tab. 2: Probes disposition during experimental campaigns**

Campaign	Probe position			
	Probe 1	Probe 2	Probe 3	Probe 4
April	Port 6	Port 7	Port 8	Port 9
September	From the bottom	Port 6	Port 8	Port 10

A scheme of the disposition adopted in September campaign is shown in Fig. 9.

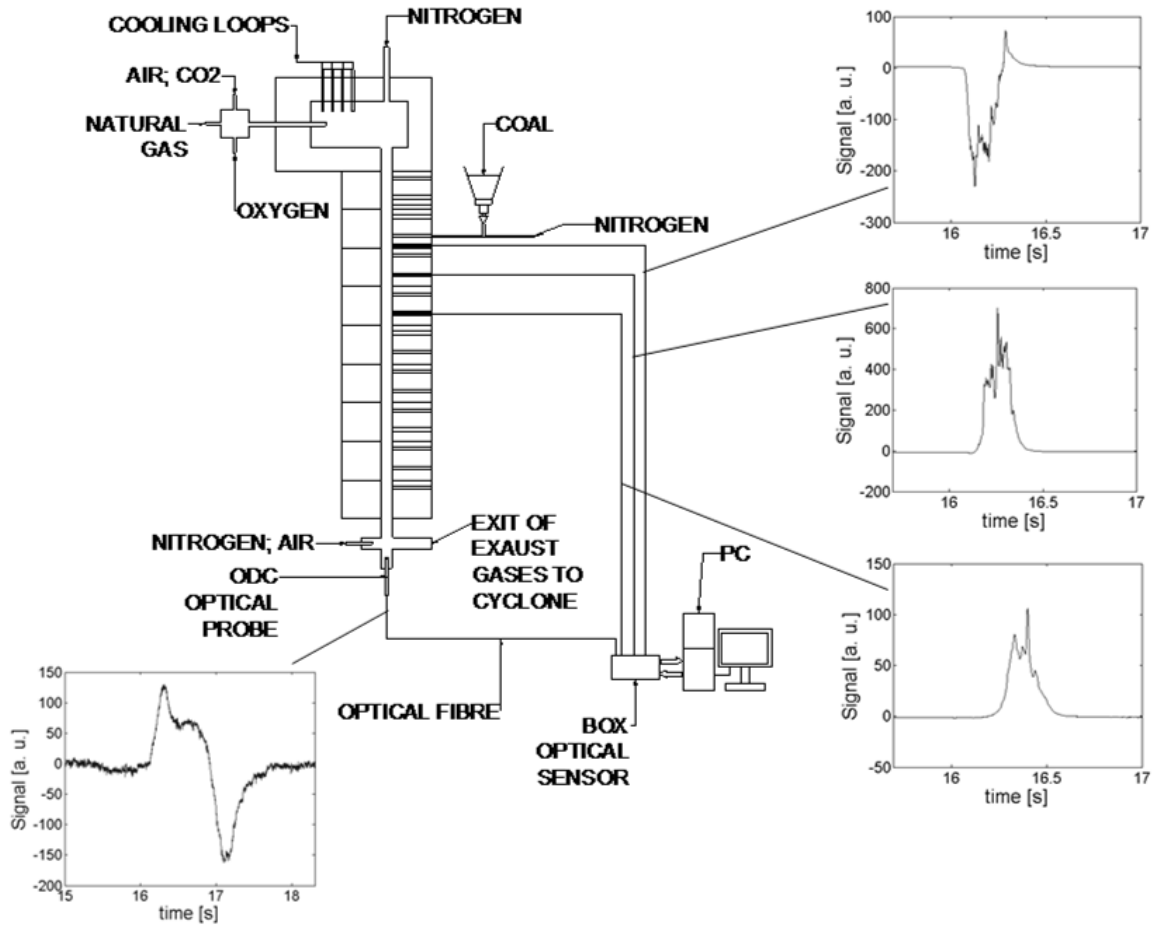


Fig. 9: Scheme of IPFR reactor and ODC probes in September campaign

## 4 Operating conditions

### 4.1 Feed mode

Two kinds of tests were made:

- devolatilization tests of the solid fuel
- char oxidation tests of char particles.

In both cases two modes of feed were tested:

- continuous feed
- pulsed feed.

Stationary and transitory tests were made (from no feed to continuous/pulsed feed) to verify the probes capability to detect the passage of coal/char/biomass in front of them.

In continuous feed tests a constant set point feed of 110 g/h was injected in the reactor. This condition is similar to real boilers feed. On the contrary during pulsed tests a little volume (250 mm<sup>3</sup>) of solid fuel was injected in IPFR every 6 seconds. In this way it was possible to discriminate the passage of the fuel in front of the probes and to follow the transit along the reactor. Obviously this kind of feed is not similar to an industrial boiler, but signals detected in these tests are easily understandable. In fact in this way it is possible to attribute a detected signal variation to the transit of the solid fuel and to the combustion processes that it is subjected inside the reactor. In pulsed feed tests it is possible to calculate a value of fuel mass flow considering the mass of the fuel volume injected during every pulse and the length of the pulse. The available discharge time is fixed in 2 seconds to flow away from the feed chamber and be entrained by the carrier gas inside the IPFR. Experimentally it was evaluated that the effective time needed to the little mass of fuel to be discharged into the reactor is only 0.5 seconds, then considering a density of the coal of 1.2 g/cm<sup>3</sup>, the massive feed flow is about 2160 g/h, a value very higher than continuous feed tests. As consequence of this it is easily understandable like in pulsed feed tests the fuel feed stream is very more dense of coal particles than in continuous feed ones. In the case of pulsed tests the signal detected by ODC probes was registered for a minimum of 40 pulses of fuel for every operating condition, in this way there is a sufficient statistic value.

### 4.2 Fuels

Three kinds of fuels were used during the tests:

- South African high volatiles bituminous pulverized coal sieved in two different ranges of particles size ( $d_p=38-90\ \mu\text{m}$  and  $d_p>125\ \mu\text{m}$ )
- char from the same coal previously produced in IPFR sieved in in two different ranges of particles size ( $d_p=45-90\ \mu\text{m}$  and  $d_p=90-125\ \mu\text{m}$ )
- squeezed and grinded sunflower's seeds as biomass with a wide range of particles size (Fig. 10).

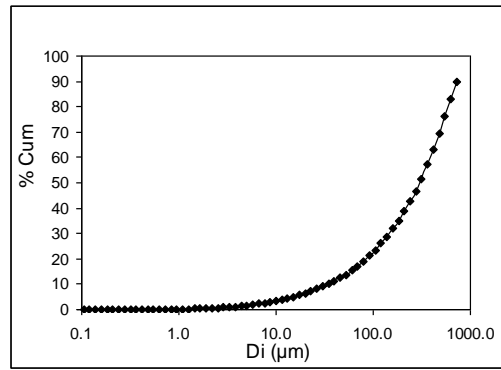


Fig. 10: Cumulative distribution of the biomass particles size

Fuels were previously analyzed in laboratory to know their ultimate and proximate composition.

**Tab. 3: Proximate and ultimate analysis of South African high volatiles bituminous coal**

	Moisture (% wet)	VM (% wet)	FC (% wet)	Ash (% dry)	C (% dry)	H (% dry)	N (% dry)	O (% dry)
$d_p=38-90$ $\mu\text{m}$	2.37	28.02	53.45	16.56	68.10	4.10	1.53	9.71
$d_p>125$ $\mu\text{m}$	2.97	28.02	55.60	13.82	69.43	4.44	1.63	10.68

**Tab. 4: Proximate and ultimate analysis of char produced from South African high volatiles bituminous coal**

	Moisture (% wet)	VM (% wet)	FC (% wet)	Ash (% dry)	C (% dry)	H (% dry)	N (% dry)	O (% dry)
$d_p=45-90$ $\mu\text{m}$	2.47	8.85	67.47	21.75	69.44	1.36	1.33	6.12
$d_p=90-125$ $\mu\text{m}$	5.05	8.82	67.23	19.90	71.29	1.59	1.38	5.84

**Tab. 5: Proximate and ultimate analysis of biomass**

Moisture (% wet)	VM (% wet)	FC (% wet)	Ash (% dry)	C (% dry)	H (% dry)	N (% dry)	O (% dry)
9.39	69.38	15.31	6.54	46.38	5.92	4.80	36.36

Of particular interest are tests on high volatiles bituminous coal because this is the most used class of coal for the global electric production.

### 4.3 Process variables

During the tests a lot of operating parameters were changed in order to investigate the real capability of the probes to follow the variation in the combustion process. In fact it is known how the combustion process changes varying an operating condition and this allows to corroborate the signals detected by the optical probes. Beside it is very interesting deriving informations in different conditions with the purpose to obtain qualitative and quantitative results from the data post-processing.

Many parameters were changed during the experimental tests, in particular:

temperature of hot gases inside the reactor (isothermal)



oxygen concentration in hot gases  
carrier gas composition  
diluent gas (conventional combustion process or oxy-fuel).

The hot gases temperature inside the reactor, coming from the gas pre-heater, is a very important variable to determine the combustion process in its stages. In fact the particles thermic history is a function of hot gas temperature and heating rate. Two values of temperature were tested (900-1100°C) in order to analyze the signal for two different thermic state. That values should be sufficiently different to allow a variation in the detected signal. Growing the gas temperature a faster particles heating velocity is expected and then the time to reach the devolatilization should be lower. In the same way also the ignition delay and the length of the char oxidation should decrease. It is important to note that the profile of temperature inside the IPFR reactor is isothermal, with little differences of about 10-20°C (Fig. 11).

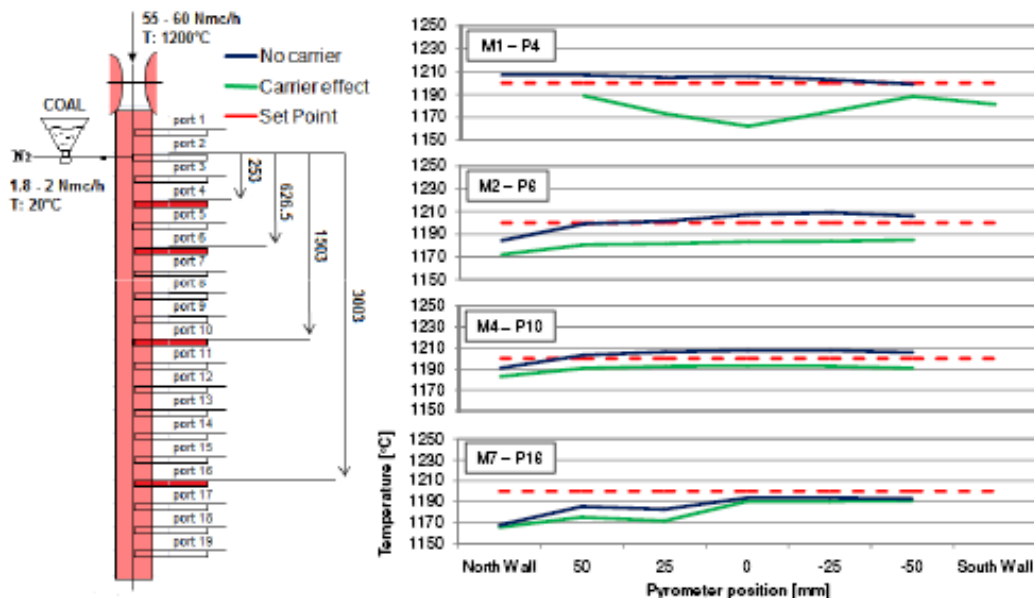


Fig. 11: Profiles of temperature inside IPFR with/without carrier gas

The oxygen concentration in hot oxidizing gases ( $Y_{O_2}$ ) has a great influence on the capability of volatiles and char to ignite. Obviously, on the base of the Fick's diffusion law, higher is the oxygen concentration and faster is the mass transport of oxygen from the bulk to solid coal particle. If volatiles ejected from it meet an oxidant gas can ignite generating a flame front sited in the gas phase. A diffusive and luminous flame origins and it is fed by volatiles ejected from the solid coal particle and by oxygen diffused from the gas bulk. On the contrary the following char oxidation is sited on the solid particle surface. In both cases, however, oxygen gas concentration is an important operating parameter because of ODC probes detect a luminous emission signal that is given by the combustion reactions, so if there is not enough oxygen and consequently there is not ignition, probes can't detect the devolatilization phase. Four different values of oxygen concentration in hot gases were used in experimental tests ( $Y_{O_2}=0.5; 3; 6; 9\%$ ).

For the gas carrier two different composition were tested during the campaign of April: a carrier made of all nitrogen and a stream made for 50% of nitrogen and 50% of air, so the oxygen content was about 10%. In the second case then additional oxygen is injected in the reactor. On September campaign this condition was not tested.

For the importance of oxy-fuel in Carbon Capture and Sequestration a set of tests were conducted in oxy-fuel conditions. In fact in the gas pre-heater it is possible to produce gases

with a high fraction of nitrogen as diluent gas using air, and this is the case of conventional combustion, but is also possible to feed pure oxygen and carbon dioxide to simulate oxy-fuel. Obviously that conditions are present also in the following vertical section of the IPFR where coal is injected. Both with nitrogen and carbon dioxide as diluent gas the oxygen fraction was changed in order to investigate the effect on the signals and then on the combustion process. All the operating alternatives tested during the experimental campaigns are listed in the following Tab. 6.

**Tab. 6: Possible alternatives in process variables**

Operating variable	Alternatives
Temperature of oxidizing gases	T=900°C / T=1100°C
Oxygen concentration in oxidizing gases	Y <sub>O2</sub> =0.5% / Y <sub>O2</sub> =3% / Y <sub>O2</sub> =6% / Y <sub>O2</sub> =9%
Composition of carrier gas	Y <sub>N2cg</sub> =100% / Y <sub>N2cg</sub> =90% , Y <sub>O2cg</sub> =10%
Environment of combustion	Conventional (in N <sub>2</sub> ) / Oxy-fuel (in CO <sub>2</sub> )

Really in cases of char or biomass feed not all the possible alternatives were tested because the main purpose of the experimental campaigns was the study of the ODC signals during the initial stages of the coal combustion process, then devolatilization tests were more interesting. The volumetric gas flow from the pre-heater it was not a constant during the tests, because it is a function of the desired set point values of gas temperature/oxygen concentration and diluent gas. In fact all the gas flows fed to the pre-heater are regulated to obtain the desired characteristic of the hot oxidizing gases. For this reason also the gas velocity inside the reactor is different from a tested condition to another, with typical values of 2.5-3 m/s in case of conventional combustion and 1.1-1.2 m/s in case of oxy-fuel. It is clear as in oxy-fuel the volumetric gas flow is very lower, this is caused by a temporary difficulty in the feed of pure oxygen and carbon dioxide. Works of improvement of the plant are in course to solve this limitation. It must be noted as solid particles are injected in the IPFR by the carrier gas at a speed of 9.3 m/s, much faster than hot oxidizing gases.

#### 4.4 Calculus of the equivalence ratio of volatiles oxidation

Most of the tests were made in order to analyze volatiles oxidation. For this reason it is very interesting to calculate an equivalence ratio for the stage of volatiles oxidation. The equivalence ratio of volatiles oxidation ( $\Phi_v$ ) is defined as the ratio between the stoichiometric oxygen amount and available one as shown in Eq. 1.

$$\phi_v = \frac{O_{2sto}}{O_{2aiv}} \quad (1)$$

where:

$O_{2sto}$ . are the moles of stoichiometric oxygen needed for the volatiles oxidation of the fed coal

$O_{2aiv}$ . are the moles of available oxygen for the oxidation in tested condition.

The stoichiometric oxygen were calculated as the needed amount to oxidize the volatiles matter ejected from the coal particles. To estimate the oxidation process the volatiles oxidation model used by Fluent<sup>®</sup> was used. In Fluent volatiles are modelled with a formula obtained from the proximate coal composition given. As coal composition values reported in Tab. 3 for the small size ( $d_p=38-90 \mu m$ ). The formula used in this evaluation is:

$$C_{1.39}H_{1.69}O_{0.67}N_{0.0452} \quad (2)$$

From this formula it is possible to estimate the volatiles molecular weight and then it is easy to calculate the moles of volatiles contained in the volume of coal fed in pulsed tests. Previously it was said that in pulsed fed tests the coal feed stream is very denser of particles

than the continuous case, and then it is sufficient the evaluation it the denser case to be conservative. Moles of volatiles fed for every pulse ( $N_{vol}$ ) of coal can be calculated as:

$$N_{vol} = \frac{V_{coal} * \rho_{coal} * VM}{PM_{vol}} \quad (3)$$

where:

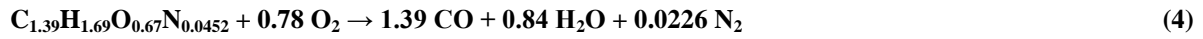
$V_{coal}$  is the volume of coal fed in pulsed tests (250 mm<sup>3</sup>)

$\rho_{coal}$  is the bulk density of the coal (1.2 g/cm<sup>3</sup>)

VM is the massive volatiles percent of volatiles matter in coal fed (Tab. 3)

$PM_{vol}$  is the volatiles molecular weight ( $PM_{vol}=29.72$  g/mol).

Volatiles oxidation is modelled with two stages: a preliminary oxidation of the volatiles to carbon monoxide and the following oxidation to carbon dioxide as shown in Eq. 4 and Eq. 5.



On the base of this reactions scheme the needed oxygen for both reactions was calculated, and the sum corresponds to the stoichiometric value ( $O_{2sto}$ ). In particular:

$$O_{2read} = 0.78 * N_{vol} \quad (6)$$

$$N_{CO} = 1.39 * N_{vol} \quad (7)$$

$$O_{2read2} = 0.5 * N_{CO} \quad (8)$$

$$O_{2sto} = O_{2read} + O_{2read2} \quad (9)$$

where:

$O_{2read1}$  are the moles of oxygen needed for the reaction of volatiles oxidation to carbon monoxide

$N_{CO}$  are the moles of carbon monoxide formed in the first reaction and oxidized to carbon dioxide in the following reaction

$O_{2read2}$  are the moles of oxygen needed for the oxidation of the carbon monoxide to carbon dioxide

$O_{sto}$  are the stoichiometric moles of oxygen needed for both reactions.

The available oxygen amount was evaluated considering all the oxygen amount contained in the IPFR reactor while coal particles are inside it. This approach is justified because volatiles oxidation is a gas reaction that happens along the reactor while coal particles are entrained from the top to the bottom. With this assumption a residence time ( $\tau$ ) of the coal particles inside the IPFR must be evaluated. From the signals registered by the bottom ODC probe a residence time of 0.8 seconds for coal combustion in conventional conditions was estimated. On the other hand in oxy-fuel a higher value of residence time is expected because of the lower volumetric gas flow used in these conditions, in fact the residence time is about 1.7 seconds in oxy-fuel. The available oxygen is evaluated as:

$$O_{2ava.} = \tau * G_{gas} * Y_{O2w} \quad (10)$$

where:

$G_{gas}$  is the molar gas flow in each test

$Y_{O2w}$  is the molar oxygen gas fraction in each test (wet).

Values of equivalence ratio for volatiles oxidation stage calculated for pulsed fed tests are shown in Tab. 7 and Tab. 8.

**Tab. 7: Values of equivalence ratio for volatiles oxidation stage for coal particles size  $d_p > 125 \mu\text{m}$**

T (°C)	Diluent gas	$Y_{O_2}$ (%dry)	$Y_{O_2w}$ (%wet)	$G_{\text{gas}}$ (mol/s)	$\tau$ (s)	$O_{2\text{sto.}}$ (mol)	$O_{2\text{ava.}}$ (mol)	$\Phi_v$
1100	N <sub>2</sub>	3	2.59	0.405	0.8	0.0149	0.0084	1.778
1100	N <sub>2</sub>	6	5.28	0.464	0.8	0.0149	0.0196	0.760
1100	N <sub>2</sub>	9	7.97	0.490	0.8	0.0149	0.0313	0.476
900	N <sub>2</sub>	3	2.56	0.389	0.8	0.0149	0.0080	1.868
900	N <sub>2</sub>	6	5.28	0.473	0.8	0.0149	0.0200	0.745

**Tab. 8: Values of equivalence ratio for volatiles oxidation stage for coal particles size  $d_p = 38-90 \mu\text{m}$**

T (°C)	Diluent gas	$Y_{O_2}$ (%dry)	$Y_{O_2w}$ (%wet)	$G_{\text{gas}}$ (mol/s)	$\tau$ (s)	$O_{2\text{sto.}}$ (mol)	$O_{2\text{ava.}}$ (mol)	$\Phi_v$
1100	N <sub>2</sub>	3	2.59	0.411	0.8	0.0149	0.0085	1.753
1100	N <sub>2</sub>	6	5.29	0.475	0.8	0.0149	0.0201	0.741
1100	N <sub>2</sub>	9	7.97	0.497	0.8	0.0149	0.0317	0.469
1100	CO <sub>2</sub>	3	1.86	0.183	1.7	0.0149	0.0058	2.578
1100	CO <sub>2</sub>	6	4.13	0.187	1.7	0.0149	0.0131	1.132
1100	CO <sub>2</sub>	9	6.91	0.193	1.7	0.0149	0.0226	0.658
900	N <sub>2</sub>	3	2.65	0.507	0.8	0.0149	0.0107	1.388
900	N <sub>2</sub>	6	5.28	0.473	0.8	0.0149	0.0200	0.745

It is possible seeing like for high oxygen fraction ( $Y_{O_2}=6\%$ ; 9% dry) the hot gases coming from the pre-heater have an oxygen content higher than the stoichiometric one ( $\Phi_v < 1$ ), then in those tests there is an excess of oxygen. On the other hand for low oxygen fraction ( $Y_{O_2}=3\%$ ) the environment has less oxygen than the stoichiometric ( $\Phi_v > 1$ ) and then volatiles oxidation is not complete. Obviously this doesn't mean that volatiles oxidation doesn't happen, but only that is partial. This last case is not representative of an industrial case, because little applications are in oxygen defect, but it was useful to have more cases with different gas oxygen concentration to evaluate this effect on the ODCs signals.

#### 4.5 Calculus of the equivalence ratio

The equivalence ratio ( $\Phi_c$ ) is the ratio between the oxygen needed for the oxidation of volatiles matter and char and the available oxygen in experimental tests.

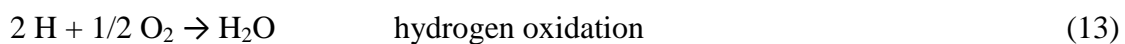
$$\phi_c = \frac{O_{2\text{sto}}}{O_{2\text{aiv}}} \quad (11)$$

where:

$O_{2\text{sto.}}$  are the moles of stoichiometric oxygen needed for the volatiles and char oxidation of the fed coal

$O_{2\text{aiv.}}$  are the moles of available oxygen for the oxidation in tested condition.

To calculate the needed oxygen it is possible considering the complete oxidation of the carbon and the hydrogen present in the coal composition. In this case two are the reactions to consider:



For the ultimate fuel composition seeing Tab. 3-Tab. 5.

The procedure utilized for the calculus of the equivalence ratio is different between the case of continuous feed or pulsed feed.

In case of tests with continuous feed a molar flow of carbon and hydrogen entering with the fuel feed is calculated on the base of the massive flow of pulverized coal/biomass fed. These molar amount of carbon and hydrogen have to be oxidized according to reactions (12) and (13). To keep count of this the following equation have to be used:

$$O_{2read} = N_C \quad (14)$$

$$O_{2react} = \frac{N_H}{4} \quad (15)$$

$$O_{2sto.c} = O_{2react1} + O_{2react2} - O_{2fuel} \quad (16)$$

where:

$O_{2react1}$  is the molar flow of oxygen needed for the reaction of carbon oxidation

$N_C$  is the molar flow of carbon fed with the feed stream

$O_{2react2}$  is the molar flow of oxygen needed for the reaction of hydrogen oxidation

$N_H$  is the molar flow of hydrogen fed with the feed stream

$O_{2sto.c}$  is the stoichiometric molar flow of oxygen needed for continuous feed stream

$O_{2fuel}$  is the molar flow of oxygen entering with the fuel feed and that acts in carbon and hydrogen reactions.

The available oxygen amount for continuous fed tests ( $O_{2ava.c}$ ) was evaluated considering the massive flow of oxygen entering with the hot gases coming from the pre-heater. In particular:

$$O_{2ava.c} = G_{gas} * Y_{O2w} \quad (17)$$

where:

$G_{gas}$  is the molar gas flow in each test

$Y_{O2w}$  is the molar oxygen gas fraction in each test (wet).

Values of equivalence ratio for volatiles and char oxidation stages calculated for continuous fed tests ( $\Phi_c$ ) are shown in Tab. 9-Tab. 13.

**Tab. 9: Values of equivalence ratio for volatiles and char oxidation stages for coal particles size  $d_p > 125 \mu m$  in continuous fed tests**

T (°C)	Diluent gas	$Y_{O2}$ (% dry)	$Y_{O2w}$ (% wet)	$G_{gas}$ (mol/s)	$O_{2sto.c}$ (mol/s)	$O_{2ava.c}$ (mol/s)	$\Phi_c$
1100	N <sub>2</sub>	0.5	0.42	0.341	0.0020	0.0014	1.413
1100	N <sub>2</sub>	3	2.55	0.385	0.0020	0.0098	0.204
1100	N <sub>2</sub>	6	5.20	0.432	0.0020	0.0225	0.089
1100	CO <sub>2</sub>	6	5.70	0.190	0.0020	0.0108	0.185
900	N <sub>2</sub>	0.5	0.43	0.403	0.0020	0.0017	1.170
900	N <sub>2</sub>	3	2.61	0.444	0.0020	0.0116	0.173
900	N <sub>2</sub>	6	5.34	0.519	0.0020	0.0277	0.072

**Tab. 10: Values of equivalence ratio for volatiles and char oxidation stages for coal particles size  $d_p=38-90 \mu\text{m}$  in continuous fed tests**

T (°C)	Diluent gas	$Y_{O_2}$ (% dry)	$Y_{O_{2w}}$ (% wet)	$G_{\text{gas}}$ (mol/s)	$O_{2\text{sto.c}}$ (mol/s)	$O_{2\text{ava.c}}$ (mol/s)	$\Phi_c$
1100	N <sub>2</sub>	0.5	0.42	0.341	0.0020	0.0014	1.377
1100	N <sub>2</sub>	3	2.55	0.385	0.0020	0.0098	0.199
1100	N <sub>2</sub>	6	5.20	0.432	0.0020	0.0225	0.087

**Tab. 11: Values of equivalence ratio for volatiles and char oxidation stages for char particles size  $d_p=90-125 \mu\text{m}$  in continuous fed tests**

T (°C)	Diluent gas	$Y_{O_2}$ (% dry)	$Y_{O_{2w}}$ (% wet)	$G_{\text{gas}}$ (mol/s)	$O_{2\text{sto.c}}$ (mol/s)	$O_{2\text{ava.c}}$ (mol/s)	$\Phi_c$
1100	N <sub>2</sub>	6	5.20	0.432	0.0019	0.0225	0.084

**Tab. 12: Values of equivalence ratio for volatiles and char oxidation stages for char particles size  $d_p=45-90 \mu\text{m}$  in continuous fed tests**

T (°C)	Diluent gas	$Y_{O_2}$ (% dry)	$Y_{O_{2w}}$ (% wet)	$G_{\text{gas}}$ (mol/s)	$O_{2\text{sto.c}}$ (mol/s)	$O_{2\text{ava.c}}$ (mol/s)	$\Phi_c$
1100	N <sub>2</sub>	6	5.20	0.432	0.0018	0.0225	0.081

**Tab. 13: Values of equivalence ratio for volatiles and char oxidation stages for biomass particles in continuous fed tests**

T (°C)	Diluent gas	$Y_{O_2}$ (% dry)	$Y_{O_{2w}}$ (% wet)	$G_{\text{gas}}$ (mol/s)	$O_{2\text{sto.c}}$ (mol/s)	$O_{2\text{ava.c}}$ (mol/s)	$\Phi_c$
900	N <sub>2</sub>	0.5	0.42	0.396	0.0013	0.0017	0.765
900	N <sub>2</sub>	3	2.60	0.427	0.0013	0.0111	0.116
900	N <sub>2</sub>	6	5.31	0.501	0.0013	0.0266	0.048

It is possible noting as the value of equivalence ratio is always lower than 1 if  $Y_{O_2} > 0.5\%$ , then in practice all the experimental tests are in excess of oxygen than the stoichiometric value and then the environment is oxidizing. This means that there are conditions to have complete oxidation of volatiles matter and char.

In the case of pulsed fed tests the available oxygen amount was evaluated considering all the oxygen amount contained in the IPFR reactor while coal particles are inside it. With this assumption a residence time ( $\tau$ ) of the coal particles inside the IPFR must be evaluated as shown in the paragraph above. The available amount of oxygen in pulsed fed tests ( $O_{2\text{ava.p}}$ ) is evaluated as:

$$O_{2\text{ava.p}} = \tau * G_{\text{gas}} * Y_{O_{2w}} \quad (18)$$

where:

$G_{\text{gas}}$  is the molar gas flow in each test

$Y_{O_{2w}}$  is the molar oxygen gas fraction in each test (wet).

The stoichiometric molar amount of oxygen needed ( $O_{2\text{sto.p}}$ ) is evaluated on the base of the amount of carbon and hydrogen contained in the volume of coal fed with every pulse. The procedure used in this case is then the same of that used for continuous feed tests, with the only one difference that a molar amount is calculated instead of a molar flow.

Calculated values of equivalence ratio in pulsed fed tests are shown in Tab. 14-Tab. 18.

**Tab. 14: Values of equivalence ratio for volatiles and char oxidation stages for coal particles size  $d_p > 125 \mu\text{m}$  in pulsed fed tests**

T (°C)	Diluent gas	Y <sub>O2</sub> (%dry)	Y <sub>O2w</sub> (%wet)	G <sub>gas</sub> (mol/s)	O <sub>2sto,p</sub> (mol)	O <sub>2ava,p</sub> (mol)	Φ <sub>p</sub>
1100	N <sub>2</sub>	0.5	0.43	0.361	0.0197	0.0012	16.031
1100	N <sub>2</sub>	3	2.59	0.405	0.0197	0.0084	2.351
1100	N <sub>2</sub>	6	5.28	0.464	0.0197	0.0196	1.005
1100	N <sub>2</sub>	9	7.97	0.490	0.0197	0.0313	0.629
900	N <sub>2</sub>	0.5	0.42	0.351	0.0197	0.0012	16.740
900	N <sub>2</sub>	3	2.56	0.389	0.0197	0.0080	2.470
900	N <sub>2</sub>	6	5.28	0.473	0.0197	0.0200	0.986

**Tab. 15: Values of equivalence ratio for volatiles and char oxidation stages for coal particles size d<sub>p</sub>=38-90 μm in pulsed fed tests**

T (°C)	Diluent gas	Y <sub>O2</sub> (%dry)	Y <sub>O2w</sub> (%wet)	G <sub>gas</sub> (mol/s)	O <sub>2sto,p</sub> (mol)	O <sub>2ava,p</sub> (mol)	Φ <sub>p</sub>
1100	N <sub>2</sub>	0.5	0.43	0.366	0.0194	0.0012	15.611
1100	N <sub>2</sub>	3	2.59	0.411	0.0194	0.0085	2.289
1100	N <sub>2</sub>	6	5.29	0.475	0.0194	0.0201	0.968
1100	N <sub>2</sub>	9	7.97	0.497	0.0194	0.0317	0.613
1100	CO <sub>2</sub>	3	1.89	0.183	0.0194	0.0058	3.368
1100	CO <sub>2</sub>	6	4.13	0.187	0.0194	0.0131	1.479
1100	CO <sub>2</sub>	9	6.91	0.193	0.0194	0.0226	0.859
900	N <sub>2</sub>	0.5	0.44	0.425	0.0194	0.0015	13.131
900	N <sub>2</sub>	3	2.65	0.507	0.0194	0.0107	1.813
900	N <sub>2</sub>	6	5.28	0.473	0.0194	0.0200	0.973

**Tab. 16: Values of equivalence ratio for volatiles and char oxidation stages for char particles size d<sub>p</sub>=90-125 μm in pulsed fed tests**

T (°C)	Diluent gas	Y <sub>O2</sub> (%dry)	Y <sub>O2w</sub> (%wet)	G <sub>gas</sub> (mol/s)	O <sub>2sto,p</sub> (mol)	O <sub>2ava,p</sub> (mol)	Φ <sub>p</sub>
1100	N <sub>2</sub>	6	5.28	0.475	0.0200	0.0201	0.997

**Tab. 17: Values of equivalence ratio for volatiles and char oxidation stages for char particles size d<sub>p</sub>=45-90 μm in pulsed fed tests**

T (°C)	Diluent gas	Y <sub>O2</sub> (%dry)	Y <sub>O2w</sub> (%wet)	G <sub>gas</sub> (mol/s)	O <sub>2sto,p</sub> (mol)	O <sub>2ava,p</sub> (mol)	Φ <sub>p</sub>
1100	N <sub>2</sub>	6	5.28	0.475	0.0193	0.0201	0.961

**Tab. 18: Values of equivalence ratio for volatiles and char oxidation stages for biomass particles in continuous fed tests**

T (°C)	Diluent gas	Y <sub>O2</sub> (%dry)	Y <sub>O2w</sub> (%wet)	G <sub>gas</sub> (mol/s)	O <sub>2sto,p</sub> (mol)	O <sub>2ava,p</sub> (mol)	Φ <sub>p</sub>
900	N <sub>2</sub>	0.5	0.42	0.351	0.0063	0.0012	5.368
900	N <sub>2</sub>	3	2.56	0.392	0.0063	0.0080	0.785
900	N <sub>2</sub>	6	5.25	0.459	0.0063	0.0193	0.327

It is possible noting as the value of equivalence ratio is bigger than 1 if Y<sub>O2</sub>=0.5% or Y<sub>O2</sub>=3%, while it is lower for higher oxygen fractions.

#### 4.6 Calculus of the group number in each test

The numerical particle density of coal particles has fundamental role on the combustion process inside the reactor. In fact if the feed stream (carrier gas and entrained solid coal particles) is low dense the trend is of single particle combustion, with no or little influence between the flames of two near particles. On the other hand if the feed stream is dense there is an important interaction between the flames of two or more near particles because of there is competition for the needed oxygen for the oxidation. Than, in this last case, there is the trend to form a flames union, originating an only one big flame that surrounds all the particles. This is called group combustion and the trend is more marked more the feed stream is dense in coal particles. To discriminate if there is or not interaction between near particles two parameters can be evaluated: the group number and the numerical particle density. Those parameters are defined as shown in Eq.19 and Eq. 20 [11]:

$$G = \frac{3 * \rho_g * R_c^2}{a^2 * \rho_p * \frac{m_g}{m_p}} \quad (19)$$

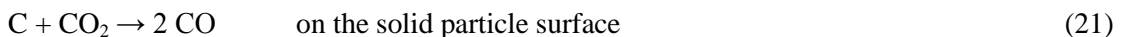
$$G = 4\pi n R_c^2 a \quad (20)$$

where:

- G is the group number in cylindrical geometry
- $\rho_g$  is the carrier gas density
- $R_c$  is the radius of the cylinder of the carrier gas
- a is the radius of the solid fuel particles
- $\rho_p$  is the solid fuel particles density
- $m_g$  is the massive flow of the carrier gas
- $m_p$  is the massive flow of the solid fuel particles
- n is the numerical particle density.

All gas parameters are evaluated for the cold carrier gas and not for the hot gas mixture inside the IPFR. This is justified because of the great uncertainty about the gas properties at the ignition point of the coal particles inside the IPFR. For this reason to calculate the group number for the cold carrier gas is a good approach and it is the mode adopted in other similar experimental works [12], [13].

The carbon oxidation is normally modelled using a double film model:



In this case on the base of the calculated value of G there is the possibility to estimate the coal particles mode of combustion inside the IPFR. If:

- $G < 0.3$  combustion of single coal particles (Fig. 12/a)
- $0.3 < G < 2$  combustion of single particles with a single flame for each particle and low interaction between particles (Fig. 12/b)
- $2 < G < 4$  tendency to group combustion of the coal particles with an only one big flame in the inner zone and single flames externally (Fig. 12/c)
- $4 < G < 100$  group combustion with union of all the single flames (Fig. 12/e)
- $G > 100$  sheath combustion – combustion as the cloud was an only one single big particle (Fig. 12/f).



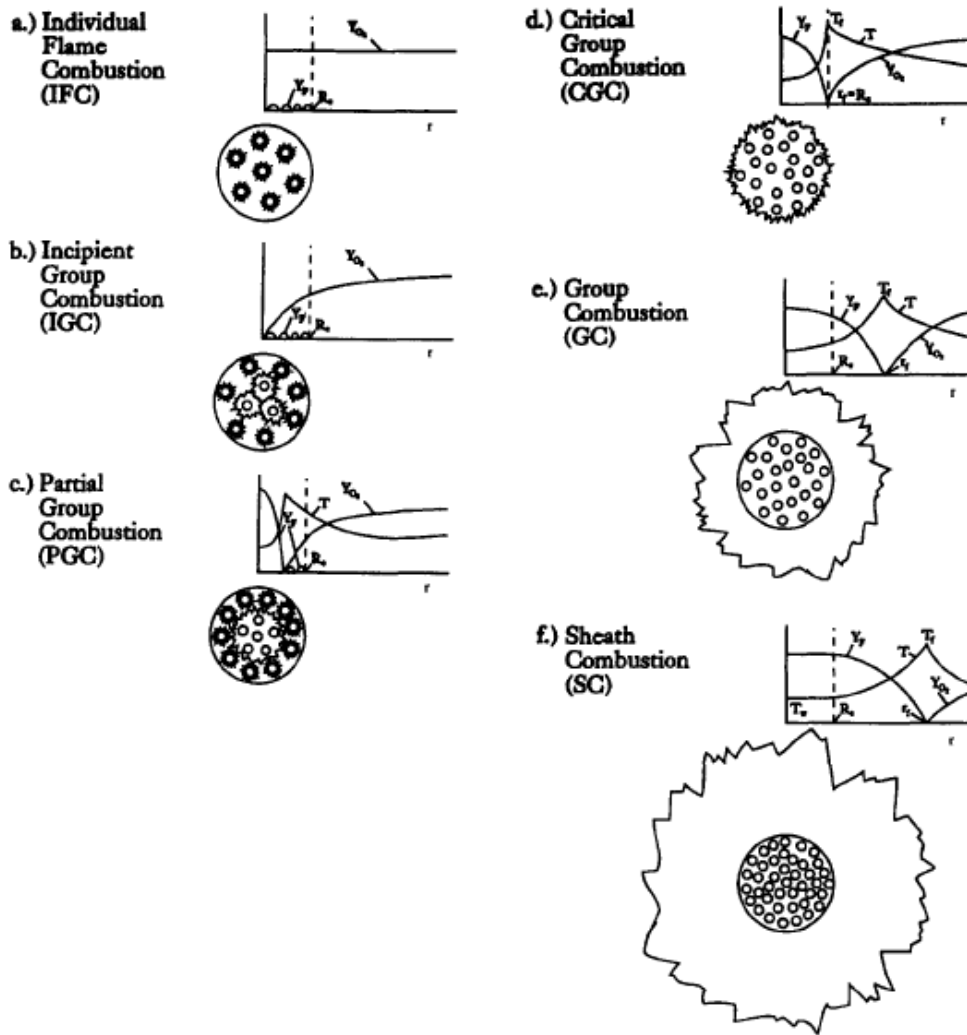


Fig. 12: Model of the interactions between coal particles during combustion varying the group number

The group number was evaluated both for continuous fed tests and for pulsed fed ones. Obviously for the case of pulsed feed an equivalent value of massive flow previously calculated was used.

Parameters used for the calculus of the group number in case of continuous feed of pulverized coal are shown in Tab. 19, while values of group number and numerical particle density are shown in Tab. 20.

Tab. 19: Parameters used for the evaluation of the group number in tests with continuous feed of pulverized coal

Parameter	Value	Unit of measure	
$R_c$	0.35	cm	Radius of the feed probe
$\rho_p$	1500	kg/m <sup>3</sup>	Coal particles density
a	65 (for $d_p > 125$ ) 32 (for $d_p = 38-90$ )	$\mu\text{m}$	Radius of coal particles
$m_p$	110	g/h	Pulverized coal massive flow
$T_g$	20	$^{\circ}\text{C}$	Carrier gas temperature
$V_{cN}$	1.2	Nm <sup>3</sup> /h	Volumetric flow of carrier gas
$x_n$	0.895	-	Molar fraction of nitrogen in carrier gas

$x_o$	0.105	-	Molar fraction of oxygen in carrier gas
$\rho_g$	1.182	kg/m <sup>3</sup>	Carrier gas density
$m_g$	1522	g/h	Carrier gas massive flow

**Tab. 20: Group number and numerical particle density for tests with continuous feed of pulverized coal**

Particles size ( $\mu\text{m}$ )	G	n (m <sup>-3</sup> )
$d_p > 125$	0.50	$4.95 \cdot 10^7$
$d_p = 38-90$	2.04	$4.15 \cdot 10^8$

It is possible noting as the evaluated group numbers for these tests are low, in particular:  
 for particles size  $d_p > 125 \mu\text{m}$   $0.3 < G < 2$  it is a case of single flames combustion with very low interaction between near particles  
 for particles size  $d_p = 38-90 \mu\text{m}$   $2 < G < 4$  it is a case of union of flames in the inner zone and single flames externally.

Then there is an appreciable difference in the coal particles mode of combustion varying the particles size.

Parameters used for the calculus of the group number in case of pulsed feed of pulverized coal are shown in Tab. 21, while values of group number and numerical particle density are shown in Tab. 22.

**Tab. 21: Parameters used for the evaluation of the group number in tests with continuous feed of pulverized coal**

Parameter	Value	Unit of measure	
$R_c$	0.35	cm	Radius of the feed probe
$\rho_p$	1500	kg/m <sup>3</sup>	Coal particles density
$\rho_b$	1200	kg/m <sup>3</sup>	Bulk density of the volume of coal fed in each pulse
a	65 (for $d_p > 125$ ) 32 (for $d_p = 38-90$ )	$\mu\text{m}$	Radius of coal particles
$V_p$	250	mm <sup>3</sup>	Volume of pulverized coal fed for each pulse
$t_c$	0.5	s	Discharge time of the coal fed pulse
$T_g$	20	°C	Carrier gas temperature
$V_{cN}$	1.2	Nm <sup>3</sup> /h	Volumetric flow of carrier gas
$x_n$	1	-	Molar fraction of nitrogen in carrier gas
$\rho_g$	1.182	kg/m <sup>3</sup>	Carrier gas density
$m_g$	1499	g/h	Carrier gas massive flow
$m_p$	2160	g/h	Equivalent massive flow of coal in pulsed fed tests

**Tab. 22: Group number and numerical particle density for tests with pulsed feed of pulverized coal**

Particles size ( $\mu\text{m}$ )	G	n (m <sup>-3</sup> )
$d_p > 125$	9.7	$9.72 \cdot 10^8$
$d_p = 38-90$	40.1	$8.15 \cdot 10^9$

It is possible noting as the evaluated group numbers for these tests are high, for both cases  $4 < G < 100$  then there is group combustion with union of single flames in both cases.

Concluding in continuous fed tests there is a combustion mode of single particles for big particles ( $d_p > 125 \mu\text{m}$ ), interaction between near particles for small particles ( $d_p = 38-90 \mu\text{m}$ ) with a inner big flame and externally single flames and always group combustion with an only one big flame in case of pulse fed tests. In case of pulsed fed tests the feed stream is dense and then it should be considered as on only one big cloud burning as an only one big particle. Obviously the cloud is generated by the volatiles matter ejected from the single coal particles.

---

## 5 Signals analysis of continuous fed tests

### 5.1 Signals form and data treatment

In continuous fed tests four lateral optical probes are present at different heights. Examining the registered signals it is possible to interpret phenomena in course. However signals have many problems that make complex the immediate analysis:

the absolute value of the signal depends from the stage of signal compensation during the acquisition, then it has not importance

the characteristic frequencies analysis shows the presence of common frequencies in signals of probes not depending from coal combustion phenomena but from reactor's dynamics or probes dynamics and frequencies that are always present and due to optics and electronics (as 50-100-120-150-200-250-350 Hz) (Fig. 13). Probes signals have to be analyzed as couples, because the compensation stage was conducted on couple of optical probes.

In order to eliminate these problems a stage of preliminary treatment of the signal is needed. A procedure of elimination of common frequencies (with a relevant amplitude) and of typical frequencies of optics and electronics was adopted. The following method was used:

conversion of signals data series from the temporal domain to the frequency domain using the Fast Fourier Transform (FFT) respecting the Nyquist restriction on the limit frequency [14] obtaining for every probe's signal a spectrum similar to those shown in Fig. 13

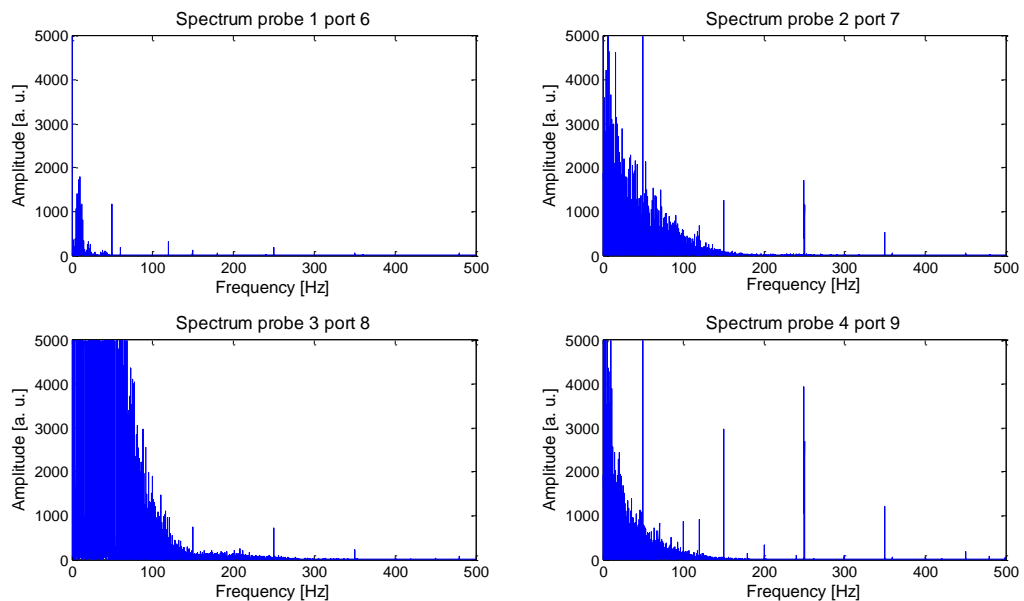


Fig. 13: Example of frequency spectrum for signals of continuous fed tests

identification of common frequencies with relevant amplitude ( $>300$ ) present in both optical probes compensated coupled

the value of amplitude of the these frequencies was decreased and to avoid the risk to invert the phase of the signal (like could be possible if it was set at value 0) it was set to the value of 100

the amplitude of the typical frequencies due to optics and electronics was set at the medium value of the amplitude in the following 3 Hz, so it has a value similar to the surrounding noise. Proceeding in this way spectrums are modified as shown in Fig. 14

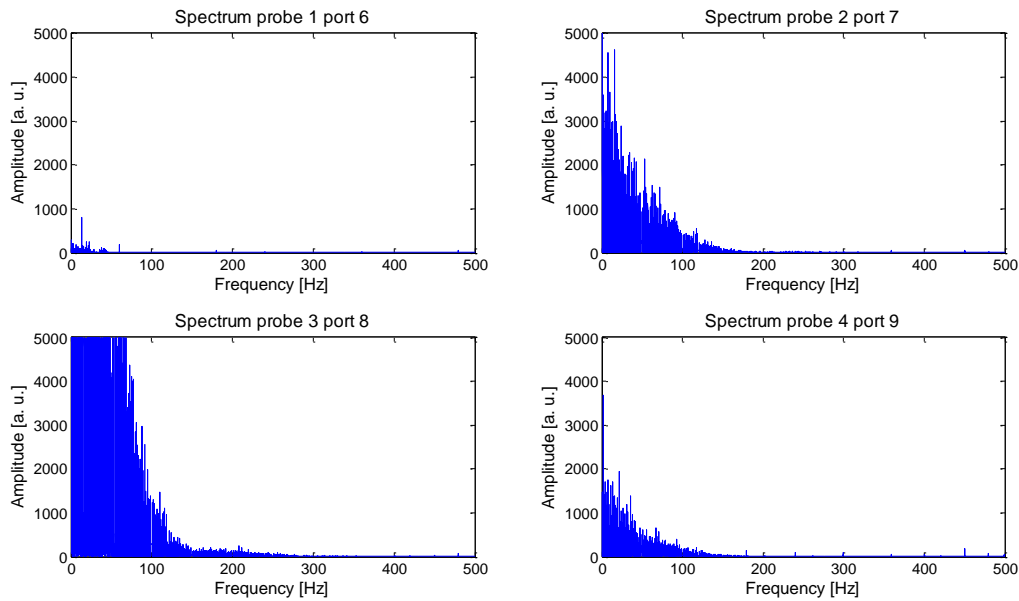


Fig. 14: Example of modified frequency spectrum for signals of continuous fed tests

treated signal is reconverted in temporal domain using the Inverse Fast Fourier Transform (IFFT).

Passing to the frequency domain, modifying the amplitude of some frequencies and coming back to the temporal domain the informations about the absolute value of the signals are lost, but the informations on the signals dynamics rest. The previous statement can be easily verified in Fig. 15

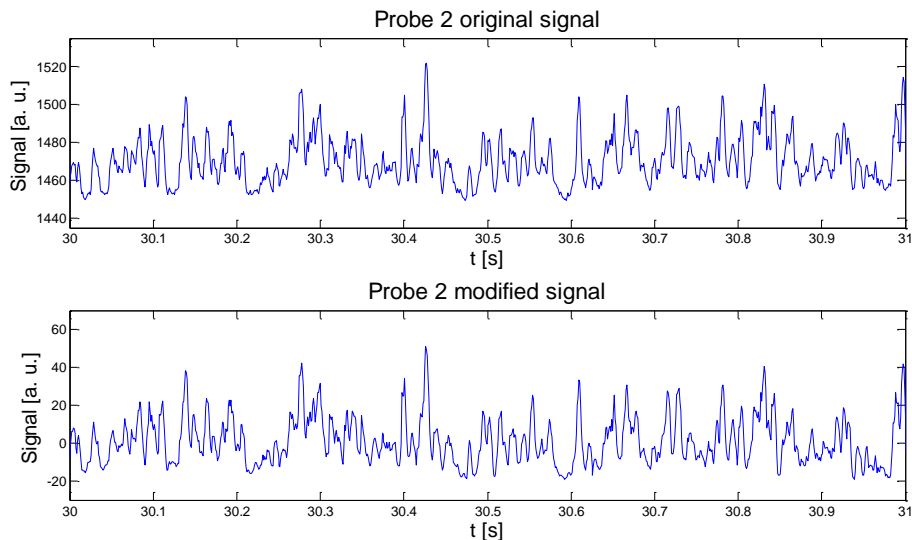


Fig. 15: Example of original and modified signal

The following figures are all of signals treated as described above.

It is interesting to note that the spectrum given by the ODC system reveals the characteristic inertial decay, with a slope of order  $-5/3$  in two-logarithmic scale (Fig. 16) with the big conservative but instable scales decompose in little scales, confirming the probes capability to reveal the fluid-dynamic state of the process. The characteristic decay of  $-5/3$  is typical of not reactive homogeneous gases (Kolmogorov law), characteristics not really true for analyzed gases.

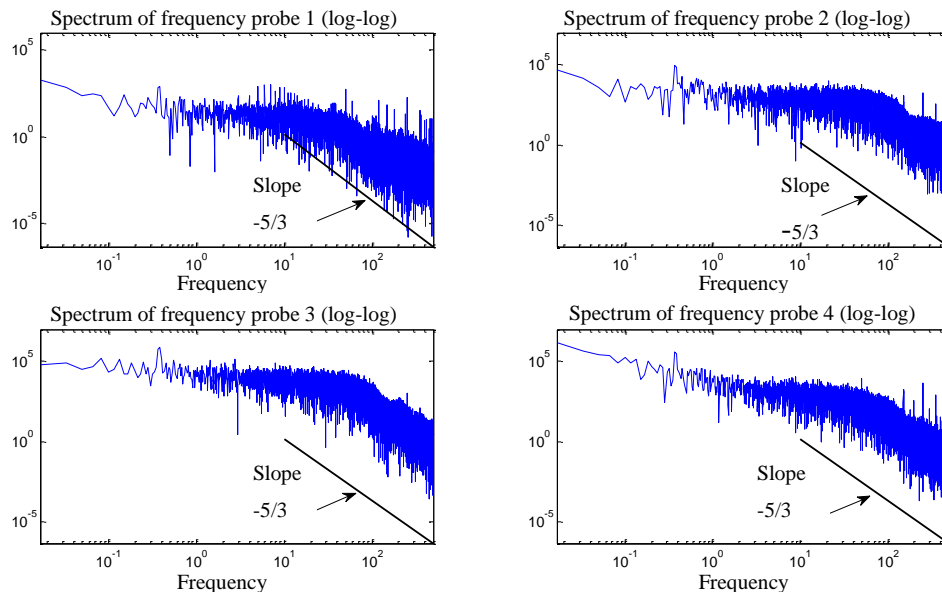


Fig. 16: Spectrums slope in two-logarithmic scale

Experimental tests were conducted in different operating conditions and then it is very interesting to search differences in the signals dynamics from a condition to another. Signals have a very oscillating and not regular dynamics, in fact there are many relevant frequencies. Also the probes position and the fed solid fuel have influence on the signal dynamics, because different processes at different heights happen. Particular care was dedicated at devolatilization and volatiles oxidation phenomena.

To highlight the increase/decrease in signal dynamics (and then of the process) varying operating conditions in following figures two parameters for the data comparison are reported:

- the standard deviation of the signal ( $\sigma_{st}$ ), that represents an index of the dynamics of the signal
- the frequency of significant peaks in the signals ( $f$ ) (number of peaks/second).

A peak is significant if its amplitude, after pre-treatment of the signal, exceeds the medium value of the signal of four times the standard deviation. The choice of four times the standard deviation derives from many tries to find the best threshold value to highlight the variation.

## 5.2 Tests with coal

### 5.2.1 Validation of the probes capability to diagnose the pulverized coal transit

Before analyzing probes signals varying operating conditions it is important to validate the probes capability to diagnose the transit of the pulverized coal particles inside the IPFR. For this reason some tests with a time of signal acquisition higher than coal feed injection time were made. In these tests probes observe the internal of IPFR in different stages:

- before coal injection, with presence of only hot gases coming from the pre-heater
- during coal injection
- after coal injection was stopped.

Obviously a difference in signals must be present in correspondence of coal injection. In following figures some examples of signals in these tests are reported showing both probes signals and coal feed.

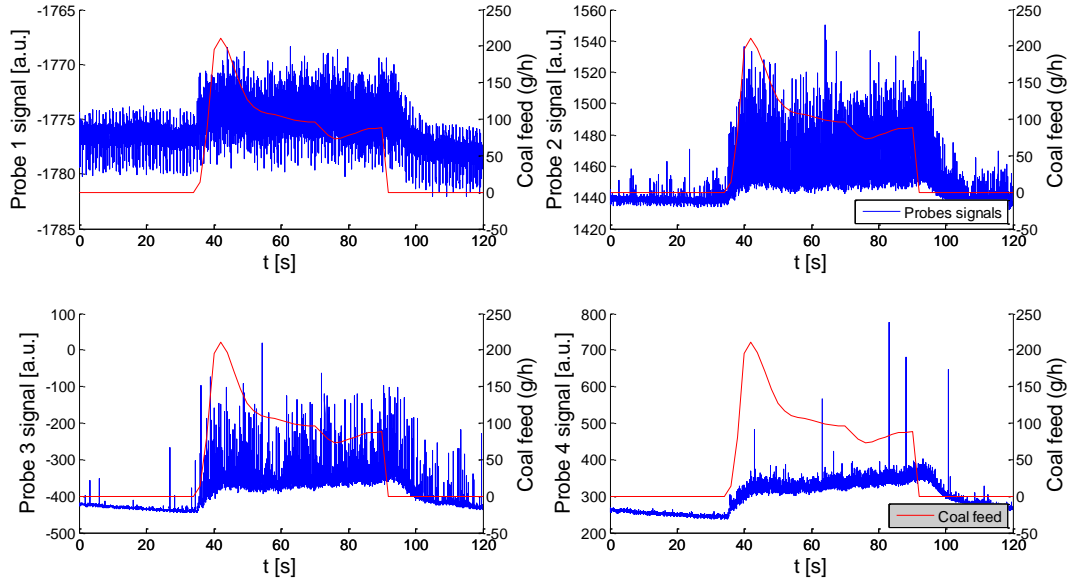


Fig. 17: Detail of probes signals varying coal feed

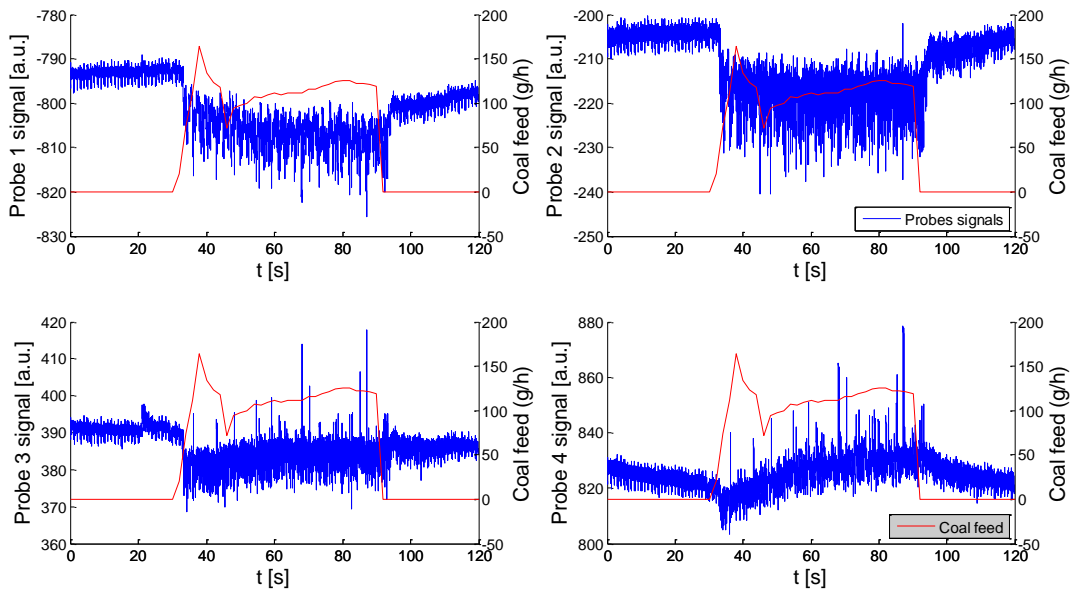


Fig. 18: Detail of probes signals varying coal feed

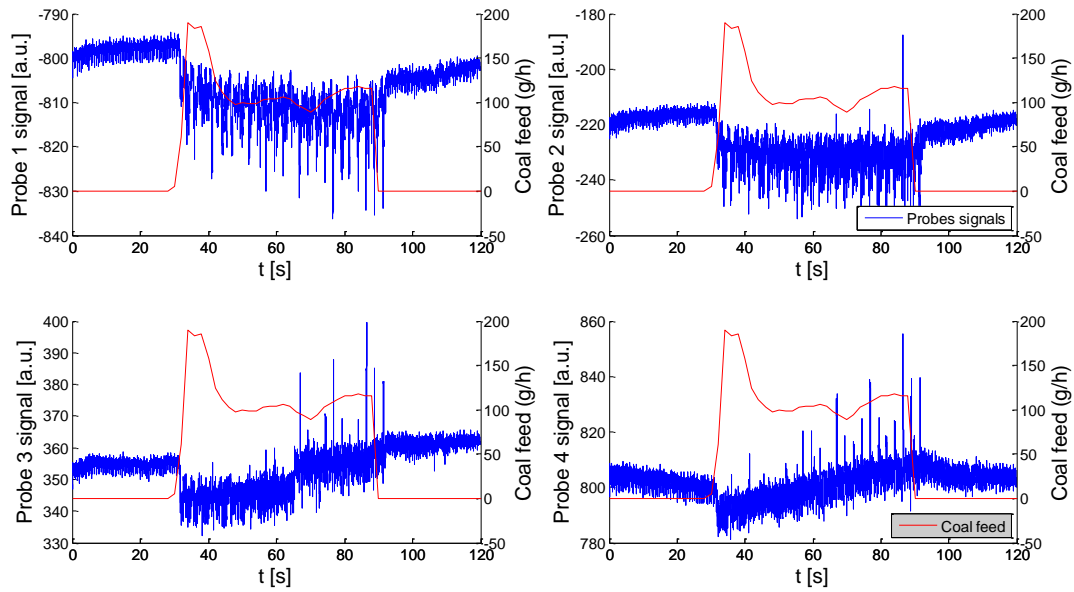


Fig. 19: Detail of probes signals varying coal feed

Examining probes signals is immediate to note as signals vary in correspondence of the coal feed, then this is the confirm that probes can diagnose the pulverized coal transit and combustion in the IPFR.

### 5.2.2 Effect of the reactor temperature

The reactor temperature has an important effect on the coal devolatilization process, because it has influence on pyrolysis kinetics, diffusion and volatiles oxidation. Tests at 900°C and 1100°C remarkably differ in signal dynamics and intensity for the same particles size and oxygen gas fraction. At 900°C the particles heating rate is lower than at 1100°C, then it is reasonable to attend a higher time of devolatilization beginning. As consequence of this at 900°C the signal should be more dynamic for higher distances from the fuel injection. In Fig. 20 and Fig. 21 are shown signals of two tests with the same particles size ( $d_p > 125 \mu\text{m}$ ), the same oxygen fraction in hot gases ( $Y_{O_2} = 6\%$ ) and the same carrier gas (pure nitrogen). Values of standard deviation and significant peaks frequency are shown above every probe signal figure.



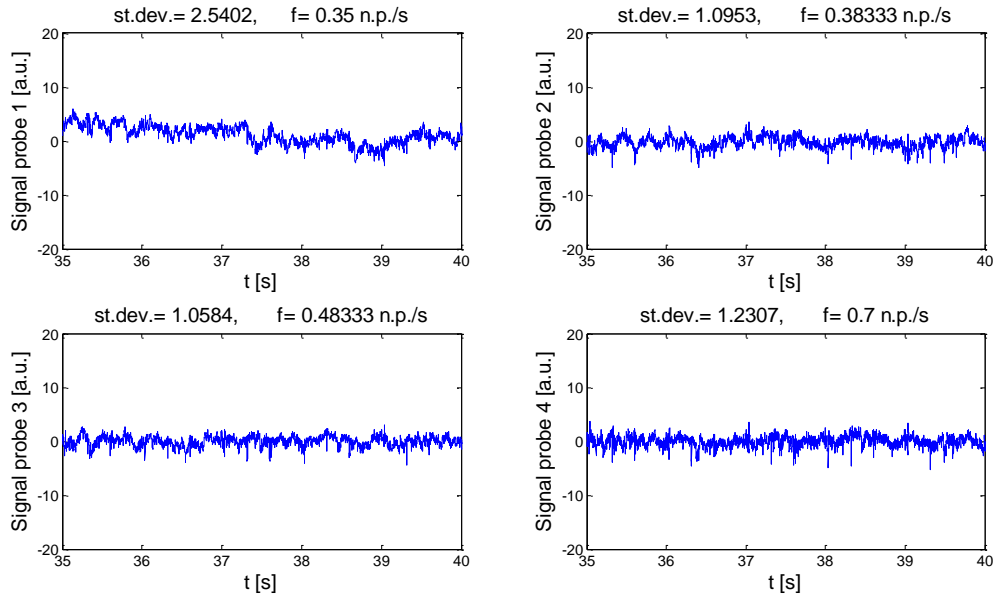


Fig. 20: Detail of probes signals at T=900°C

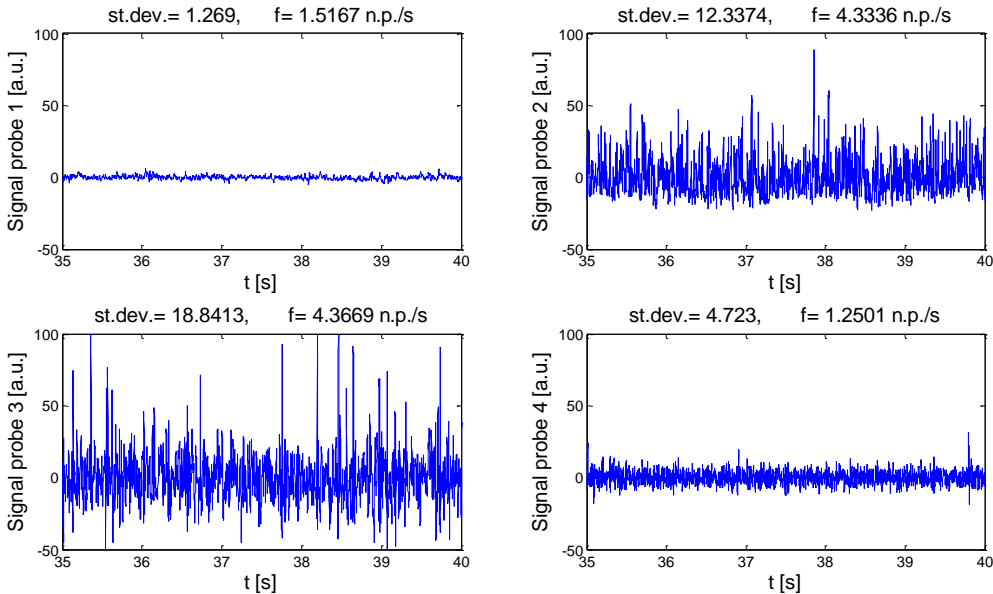


Fig. 21: Detail of probes signals at T=1100°C

It is easy to note like in case of tests at T=1100°C probes 1 and 2 registered a signal very dynamic, full of radiant emissions. On the contrary for the tests at T=900°C signal is very less dynamic and the signals of the four probes are very more similar than the case at higher temperature. These statements are confirmed by the exam of the two performance indexes: standard deviation and significant peaks frequency. In the case at T=1100°C the standard deviation for probes 2 and 3 is very high with a higher value for the probe 3, while the frequencies are very similar. The probe 1 has both indexes very low, while probe 4 has a discrete value of standard deviation and a low frequency. As consequence at T=1100°C the process is more dynamic between the port 7 (probe 2) and the port 8 (probe 3), then from about 25 cm to 50 cm after the coal injection. In case of tests at T=900°C the signals of all probes have standard deviation and significant peaks frequency very low, then there is not a particularly relevant dynamics between the coal injection and the port 9 (probe 4) at 75 cm of distance. These observations can be interpreted considering the different particles heating rate

for the different reactor temperature and the slower pyrolysis kinetics, diffusion and volatiles oxidation.

### 5.2.3 Effect of the oxygen gas fraction

The oxygen gas fraction acts prevalently on the volatiles ignition than on the stage of devolatilization. The ODCs however are optical probes and are able to detect only phenomena that involve an increase in temperature and radiation, then an ejection of volatiles without ignition for oxygen lack can't be detected. For this reason a more dynamic and intense signal increasing the oxygen fraction is attended, because of the volatiles cloud ignition is favourite. Examples of probes signal for the same particles size ( $d_p > 125 \mu\text{m}$ ) and the same temperature ( $T=1100^\circ\text{C}$ ) for different oxygen gas fractions are shown in Fig. 22- Fig. 24.

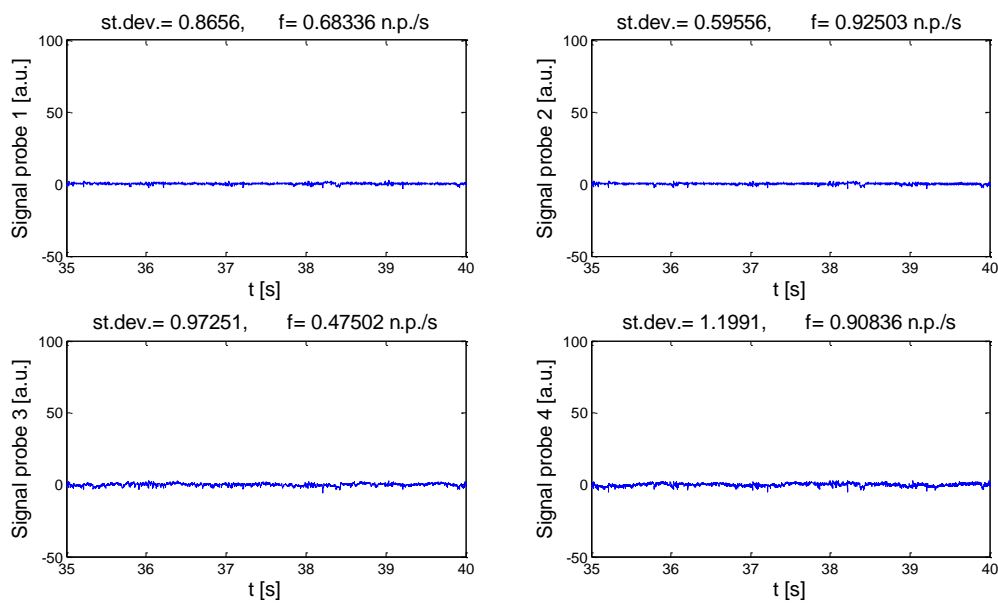


Fig. 22: Detail of probes signals for  $Y_{O_2}=0.5\%$

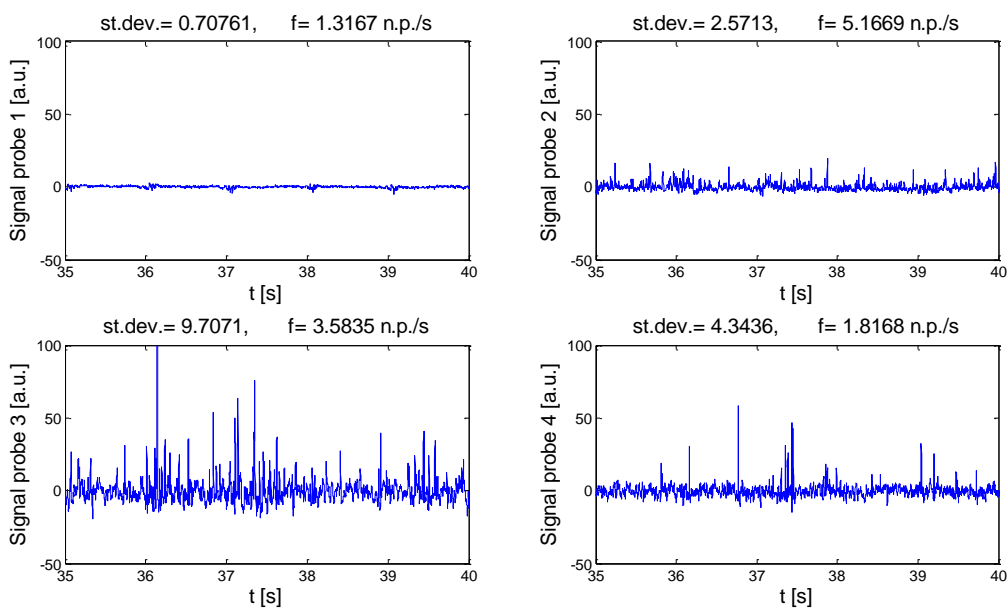


Fig. 23: Detail of probes signals for  $Y_{O_2}=3\%$

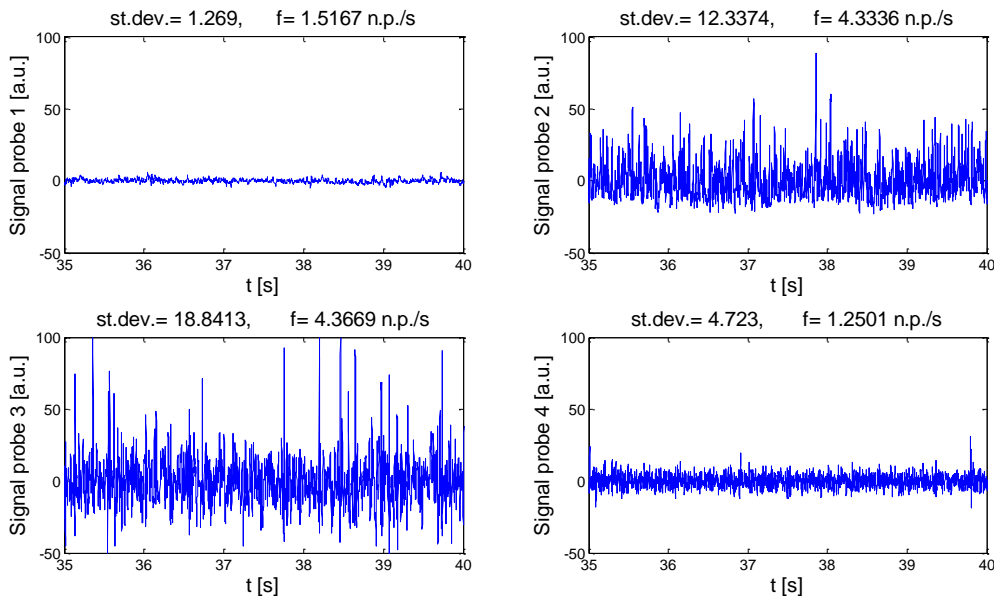


Fig. 24: Detail of probes signals for  $Y_{O_2}=6\%$

The analysis of these signals clearly shows like the signal is very more dynamic and intense if the oxygen fraction increases. In particular there is a great difference between the case  $Y_{O_2}=0.5\%$  and  $Y_{O_2}=3\%$ , in fact in the first case the oxygen fraction is probably not sufficient to cause the ignition of a significant amount of volatiles that surely have been ejected from the coal particles. Performance parameters confirm these observations. For the test with  $Y_{O_2}=0.5\%$ , in fact, both indexes are very low and about constant for all the four probes. For the test with  $Y_{O_2}=3\%$  instead the probe 1 in the port 6 (12.5 cm before the coal injection) has no dynamics, the probe 2 (port 7, 25 cm after the injection) has a significant dynamics and the probe 3 (port 8, 50 cm after injection) has the most great dynamics. It is possible noting as for the probe 3 the standard deviation is very higher than for probe 2, while the frequency of significant peaks is lower. To understand this difference it is important considering that the standard deviation is proportional at the intensity of the process in course, while the significant peaks frequency is proportional at the number of events detected from the probe position. Probe 4 signal has a discrete dynamics with a high standard deviation. On this base it should be noted like the process has a great dynamics between 25 cm and 75 cm after the coal injection. Examining signals of the test with  $Y_{O_2}=6\%$  there is a similar situation, also this time the probe 3 has the greatest dynamics like performance indexes confirm. However there is an important difference between the case with  $Y_{O_2}=3\%$  and  $Y_{O_2}=6\%$ , in the least case in fact the probe 2 has a very high dynamics, not very lower than probe 3. Also probe 4 signal is more dynamic than the case with  $Y_{O_2}=3\%$ . In the end it is possible to affirm that the process dynamics shows itself faster, then for lower distances from the coal injection.

#### 5.2.4 Effect of the particles size

Pulverized coal particles size has a particular importance because of the smallest particles are subjected to a faster heating and then it is possible that time for ignition of volatiles and char are lower. As consequence of this the smallest particles should show a significant dynamic signal before than big ones. In Fig. 25 and Fig. 26 are shown signals for different coal particles size ( $d_p=38-90 \mu\text{m}$  e  $d_p>125 \mu\text{m}$ ) for the same temperature conditions ( $T=1100^\circ\text{C}$ ) and oxygen fraction in hot gases ( $Y_{O_2}=6\%$ ).

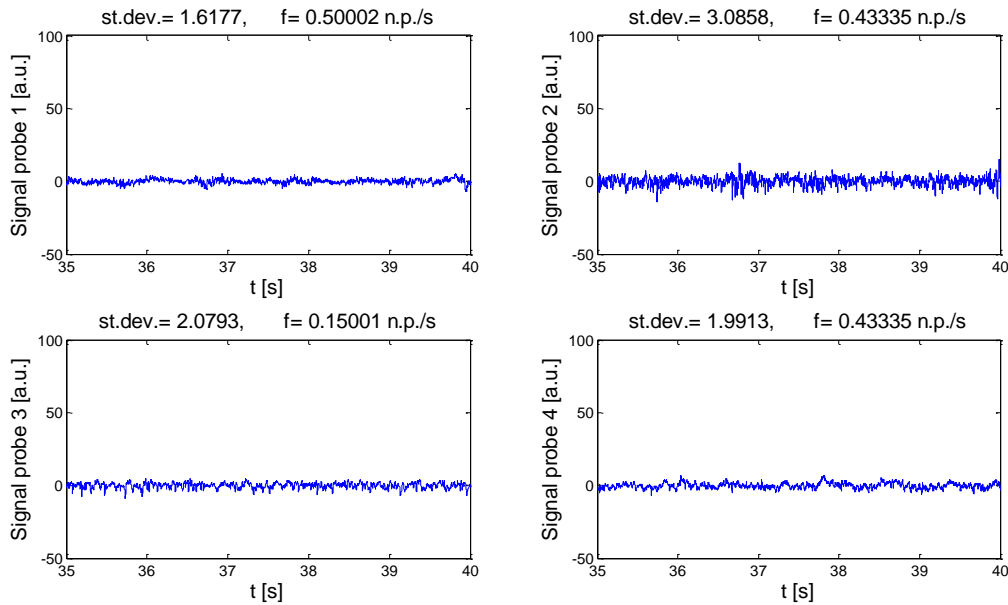


Fig. 25: Detail of probes signals for SA coal  $d_p=38-90 \mu\text{m}$

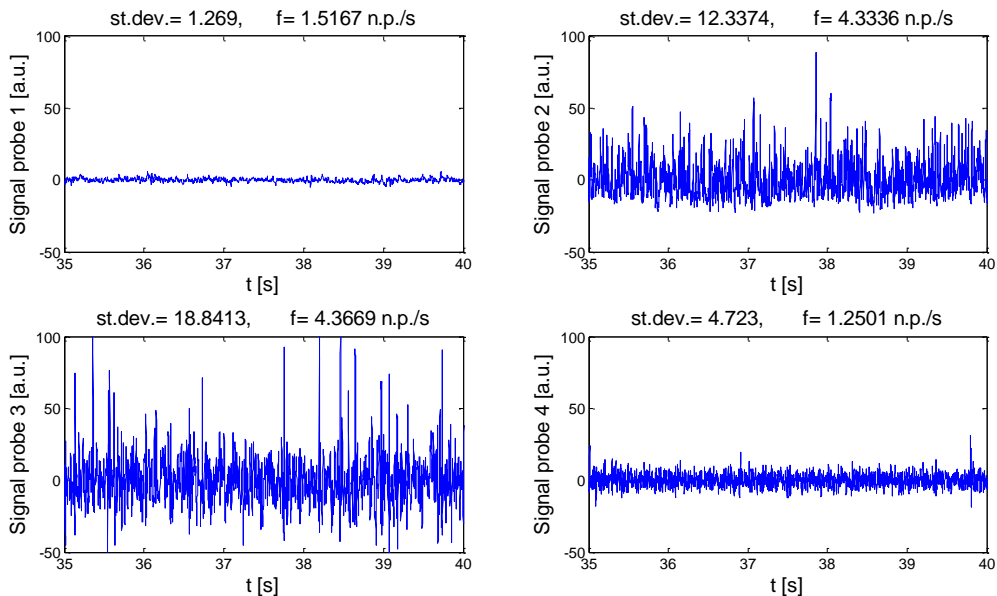


Fig. 26: Detail of probes signals for SA coal  $d_p>125 \mu\text{m}$

Examining signals and performance parameters it is possible to make some considerations. Taking the significant peaks number as comparative way it is notable as tests with small particles size have a small value of this index (Fig. 25). On this base it would seem no probes show a significant dynamics. Actually observing the standard deviation values it is possible to see as this index is quite high for all four signals and it is particularly elevated for the probe 2, decreasing then for probes 3 and 4. Comparing standard deviation values of this test with values of test with the biggest particles size it should be noted as they are lower, in fact in the second (Fig. 26) case there are very intense peaks. As consequence of this the evaluation of the significant peaks in tests with small particles size is very more difficult than for big particles where they are very marked and distinct from the surrounding noise. The standard deviation instead is a more direct measure of the signal dynamics and then it is a more reliable comparative index. In fact observing the signals in case of small particles size ( $d_p=38-90 \mu\text{m}$ ) the most dynamic probe signal is for the probe 2 (port 7), while for big

particles size ( $d_p > 125 \mu\text{m}$ ) the most dynamic signal is for the probe 3 (port 8). Standard deviation values highlight these aspects. Then the oxidizing process is faster for the smaller particles size because the most intense dynamics is nearer at the injection point, while the signal is very more intense for the big particles size.

### 5.2.5 Effect of gaseous atmosphere composition

Analyzing signals of tests in oxy-fuel conditions an important characteristic emerges: detected signal is very less intense than in conventional conditions. This fact can be noted from signals registered during the transition from a combustion environment to the other: passing from conventional conditions to oxy-fuel with the same gaseous oxygen fraction ( $Y_{O_2}=6\%$ ) there is a great decrease in signal dynamics. In fact both signal intensity and swaying decrease. Fig. 27 shows signals of probes 3 and 4 during a transition and the contemporary carbon dioxide measure inside the IPFR.

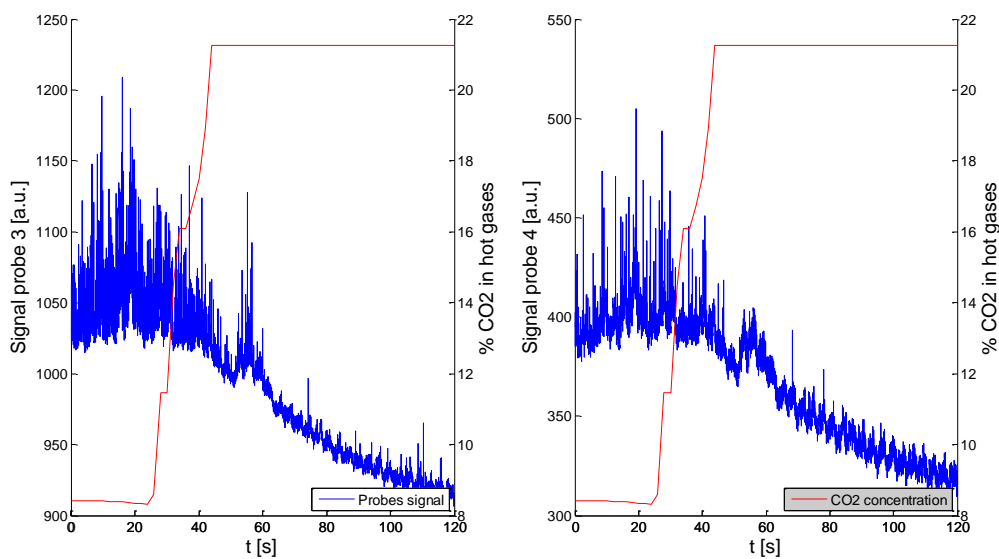


Fig. 27: Signal during transition from conventional combustion to oxy-fuel with  $Y_{O_2}=6\%$ ,  $T=1100^\circ\text{C}$ , coal particles size  $d_p > 125 \mu\text{m}$

As maximum value of 21% for carbon dioxide concentration value is shown, this corresponds to the full scale value of the measure on-line instrument. Actually the true  $\text{CO}_2$  concentration is about 92%.

In these figures signals of probes 3 and 4 are shown, because the other two probes in transition tests were positioned inside the gas pre-heater. It is possible seeing as passing to oxy-fuel conditions signal becomes very less dynamic than in conventional conditions. This observation could induce to think that in oxy-fuel coal reactivity with the hot oxidizing gases is lower. To have a wide analysis it is useful to examine also tests in stationary regime of two tests with the same reactor gas temperature ( $T=1100^\circ\text{C}$ ), oxygen concentration ( $Y_{O_2}=6\%$ ) and pulverized coal particles size ( $d_p > 125 \mu\text{m}$ ).

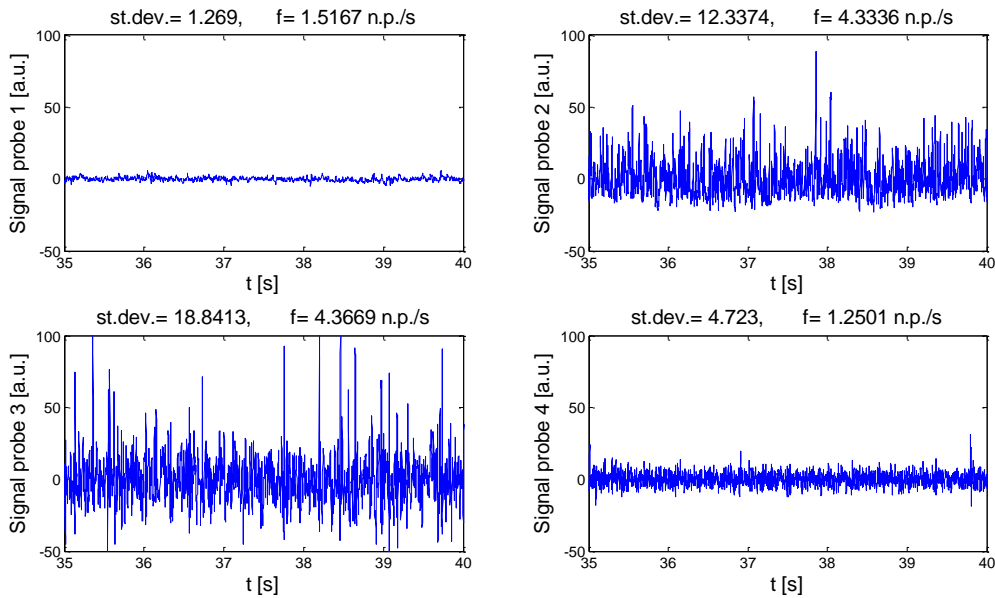


Fig. 28: Detail of probes signals for conventional combustion

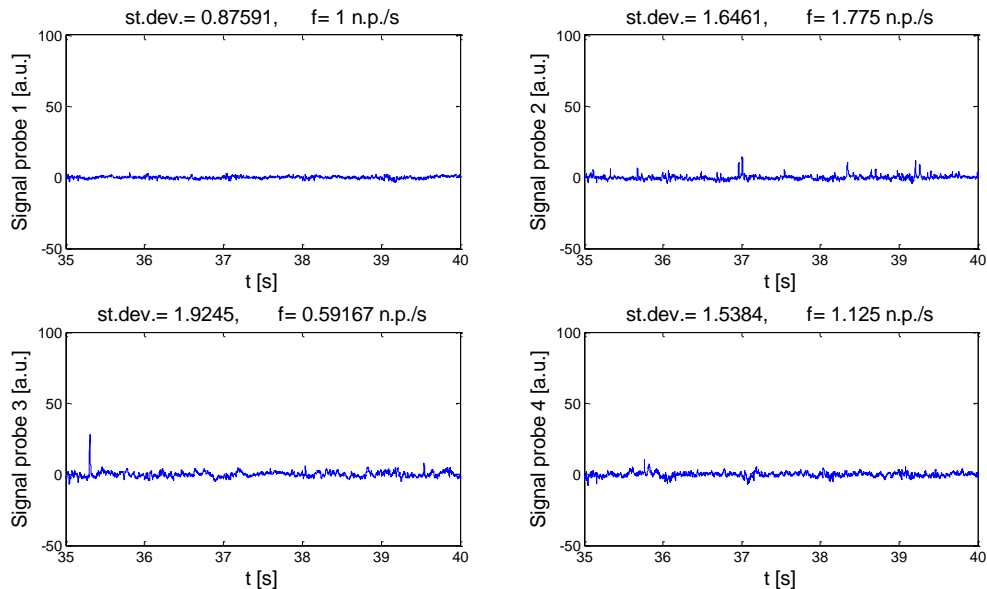


Fig. 29: Detail of probes signals for oxy-fuel combustion

Observing signals and examining performance indexes it is possible noting as in oxy-fuel dynamics is very lower, confirming previous observations. This fact could be due to a higher ignition delay in oxy-fuel conditions [4] and to a lower flame temperature during volatiles oxidation in oxy-fuel [4], [15].

### 5.2.6 Effect of the carrier gas composition

To examine the effect of the carrier gas composition signals of two tests where carrier gas is the only one different operating variable are analyzed. Both tests were conducted at  $T=1100^{\circ}\text{C}$  and with small coal particles size ( $d_p=38-90\ \mu\text{m}$ ) and  $Y_{\text{O}_2}=6\%$ . In the first experimental test carrier gas was made of pure nitrogen while in the second case a mixture of 50% nitrogen and 50% air was used (then the oxygen fraction in the second case was about 10%). The oxygen presence in carrier gas is important because increases the amount of

oxygen available for the ignition of volatiles and char. Beside the oxygen fed with the carrier gas is immediately near to the coal particles and then it is already available to the ignition without waiting the diffusion from the hot gases bulk. For this reason a decrease in ignition times in case of presence of oxygen in carrier gas is attended and a confirm is searched in probes signals.

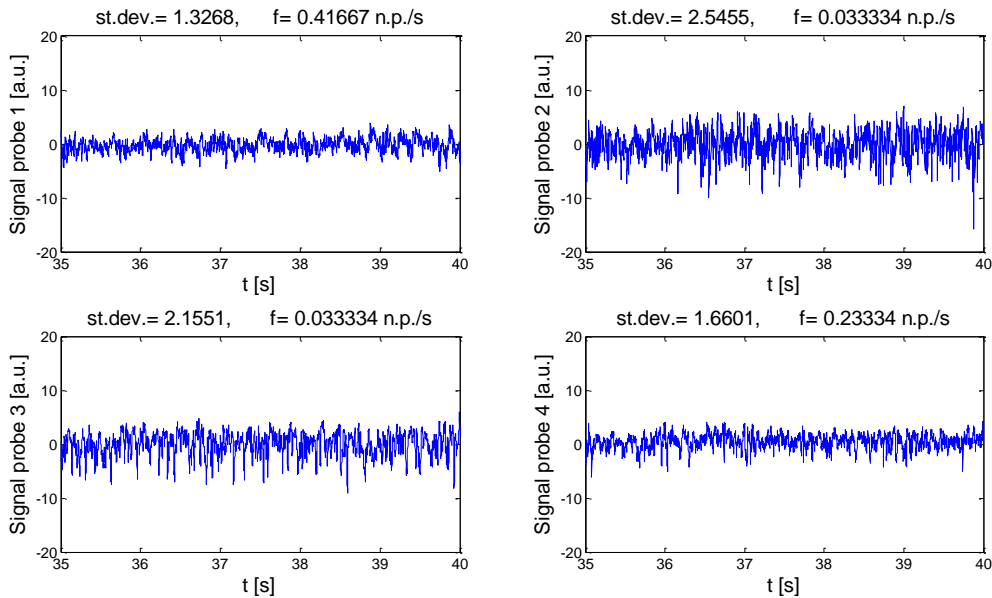


Fig. 30: Detail of probes signals with pure nitrogen as carrier gas

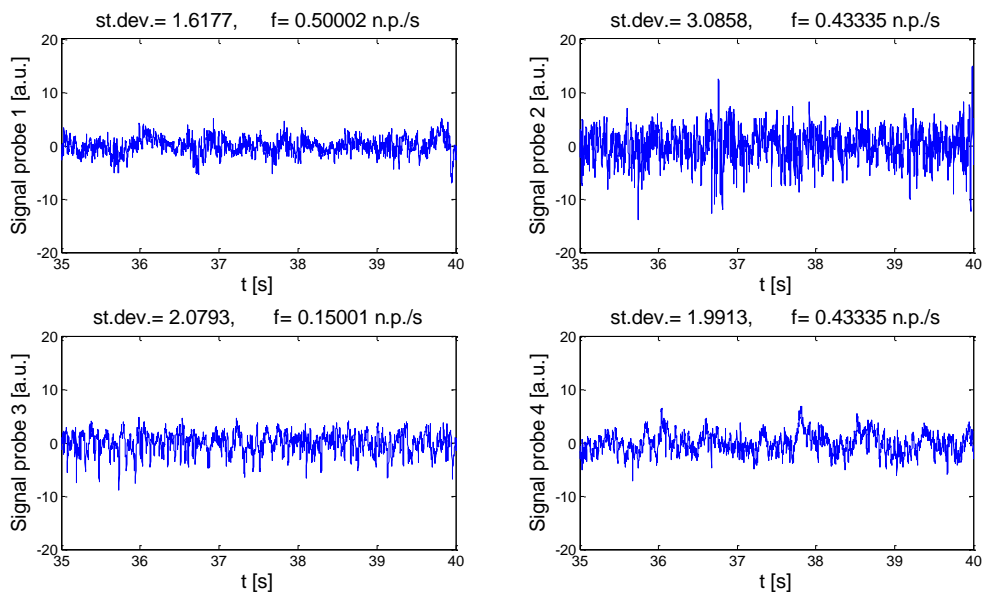


Fig. 31: Detail of probes signals with mixture nitrogen-air as carrier gas

Carrier gas flows inside the IPFR with a higher velocity than the hot gases coming from the gas pre-heater, so there is a jet effect which causes a flow of hot gases toward the feed coal stream. This fact increases the gas mixing and the contact between coal particles and oxygen, more than the alone diffusion of oxygen could do. However nearly the point of coal injection the only one oxygen available for the ignition is that contained in the carrier gas, then particular care must be focused on the probe 1 signal and less on the probe 2. The other probes signals are very similar for both the conditions because of the jet effect and diffusion a big

amount of oxygen is available for those distances. In fact examining the performance indexes no particular differences are present. Probe 1 signal in case of carrier gas containing oxygen is slightly more dynamic as the standard deviation highlights being a bit higher, the same thing is for the probe 2. However there is not a big difference probably because the carrier gas entering in the IPFR is cold and particles ignition happen when coal meets hot oxidizing gases. A time is needed to heat the carrier gas and the oxygen that contains, so that time probably compensate the time needed for the oxygen diffusion from the bulk.

### 5.2.7 Peaks analysis

In many signals, especially for those with the big particles size, it is possible noting a lot of peaks. On the base of the group number a different mode of combustion is revealed for the two particles size tested. In fact in case of small particles size there is a tendency to form an only one big flame in the inner zone with little single flames externally. On the other hand in case of big particles many single flames with little interactions are expected. Every of these little flames could be caused by the ignition of volatiles ejected by the coal particles during devolatilization stage. It is very interesting to understand the reasons that cause the presence of these peaks examining what are the operating conditions in which this presence is greater. Firstly tests with a reactor temperature of 1100°C are analyzed. For these tests different concentrations of oxygen in hot gases ( $Y_{O_2}=0.5; 3; 6\%$ ) were tried with different conditions of lack/excess of oxygen. Probes see a trunk of cone in front of them with a minimum diameter of 4 cm and maximum of 7 cm. Assuming a medium value of particles velocity of 6 m/s the residence time of the particles in the region that the probes can see is about 9 ms. This value is the time needed at the solid particles to cover the medium diameter of the trunk of cone seen by the probes. Obviously this is a medium value because of particles are injected in the IPFR with a velocity near to 9.3 m/s which decreases along the reactor through the gas exit.

In signals of tests with big particles size ( $d_p > 125 \mu m$ ) peaks are clearly present in case of probes 2, 3 and 4 at the ports 7, 8 and 9 while the coal injection is from the port 5. In Fig. 32a/b the significant peaks number distribution is shown for tests with  $Y_{O_2}=3\%$  and  $Y_{O_2}=6\%$ , those where there is an oxygen excess (Tab. 9).

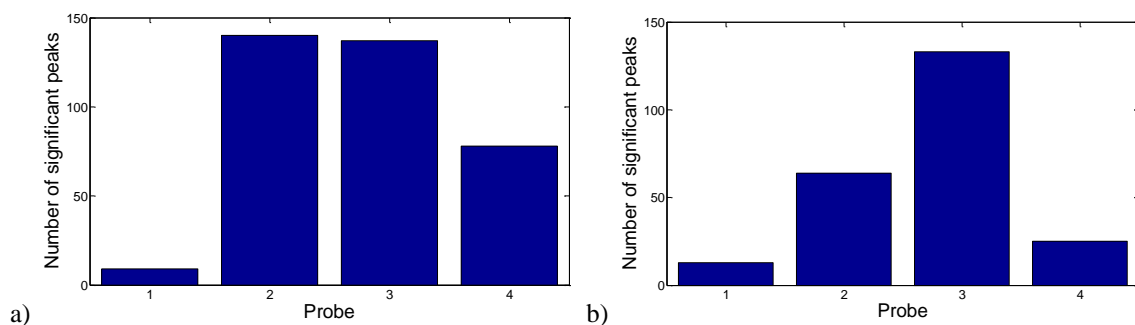


Fig. 32: Significant number peaks distribution for tests with a)  $Y_{O_2}=3\%$ , b)  $Y_{O_2}=6\%$

Much care is needed examining Fig. 32, in fact a fast observation could induce to think that in case of lower oxygen concentration the phenomena is faster and the presence of peaks is higher. This is due from the observation that the probe 2 has a high number of significant peaks in case  $Y_{O_2}=3\%$  (Fig. 32a). On the other hand in case with  $Y_{O_2}=6\%$  this number is very lower (Fig. 32b). To understand this fact it is needed a study of the peaks distribution: in case of low oxygen fraction every peak is sufficiently far from the others to be counted a time (Fig. 34), in case of high oxygen fraction many peaks are near and then more peaks are



counted a single time (Fig. 33). This is very important for signals where the presence of peaks is very high such as probe 2. Another simple consideration can be done: the phenomena of peaks presence is very important for probes 2 and 3, while there low peaks for probe 1 and a good number for probe 4 (Fig. 35). This means that the phenomena needs a time to start (low peaks for probe 1 and many for probe 2), then has a maximum in its activity and then decreases along the reactor (less peaks for probe 4 than for probe 3). Where peaks are present they have a temporal extension of 7-15 ms, then this can be higher than the medium residence time of a solid particle in front of the probes. This could mean that more ignited particles transit at little distance in front of the probes, so more near peaks derive from more oxidizing stages of more particles. On the other hand if the peak extension is lower than the particle residence time in front of the probe the particle volatile oxidation could happen completely in that moment. Examples of signals and peaks for various probes are shown in following figures for the highest oxygen fraction in hot gases ( $Y_{O_2}=6\%$ ).

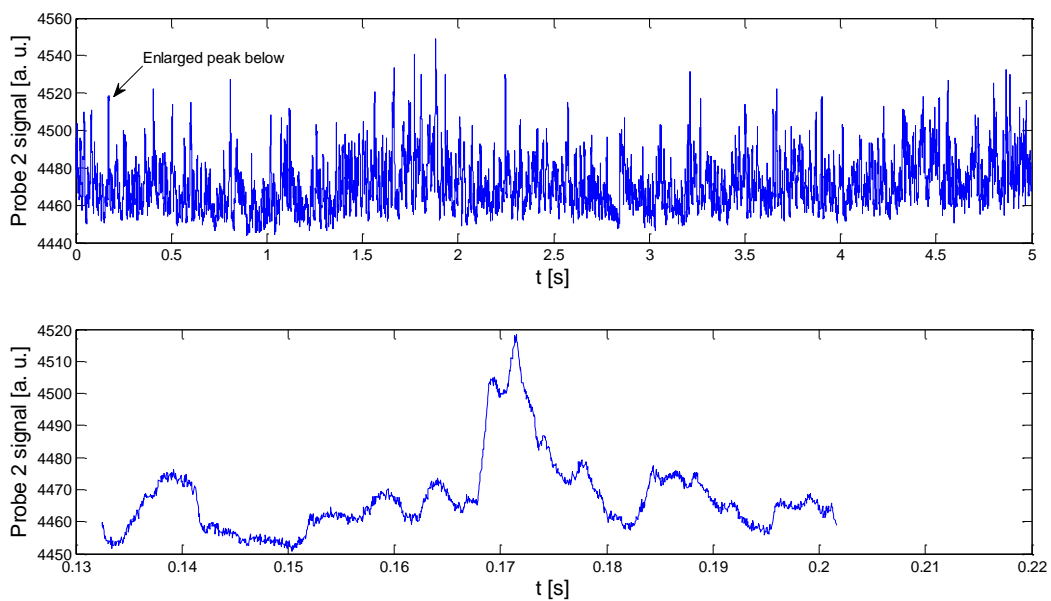


Fig. 33: Detail of signal of probe 2 for test with  $T=1100^{\circ}\text{C}$ ,  $Y_{O_2}=6\%$ , coal  $d_p > 125 \mu\text{m}$

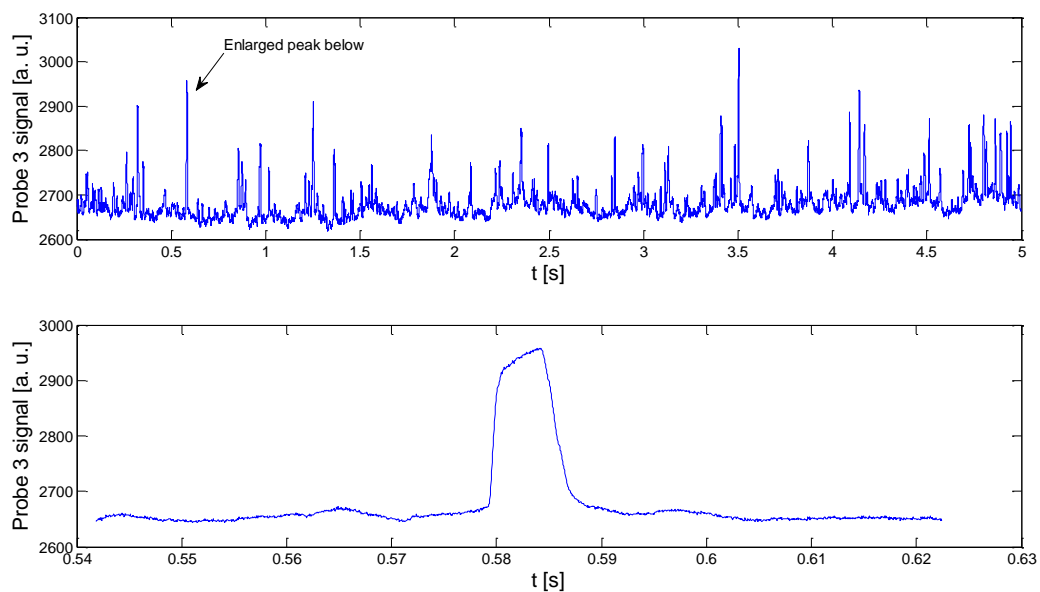


Fig. 34: Detail of signal of probe 3 for test with  $T=1100^{\circ}\text{C}$ ,  $Y_{O_2}=6\%$ , coal  $d_p > 125 \mu\text{m}$

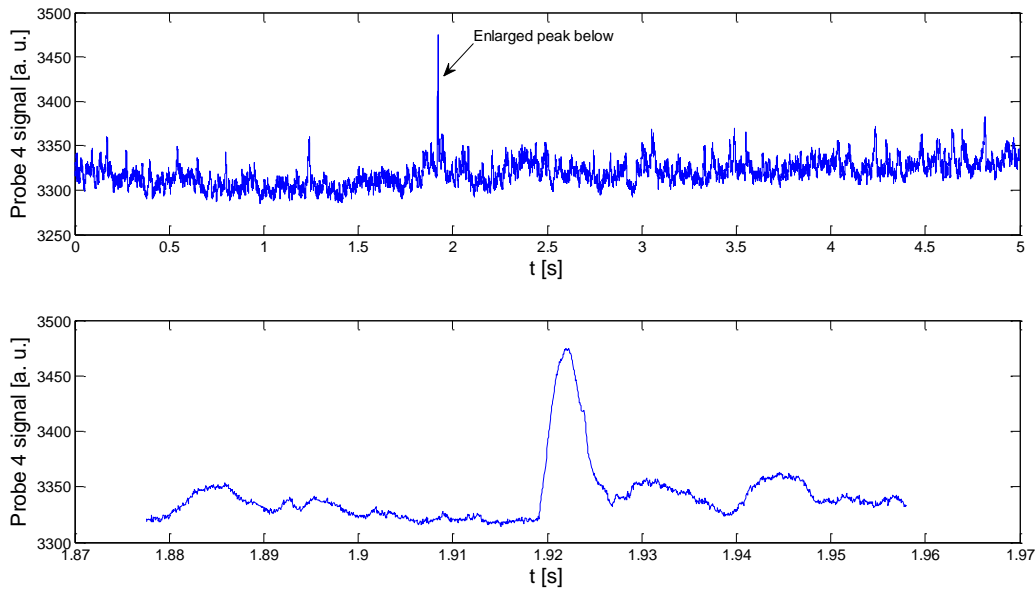


Fig. 35: Detail of signal of probe 4 for test with  $T=1100^{\circ}\text{C}$ ,  $Y_{\text{O}_2}=6\%$ , coal  $d_p>125\ \mu\text{m}$

Similar considerations are valid also for test with  $Y_{\text{O}_2}=3\%$ , while in test with lack of oxygen than the stoichiometric value ( $Y_{\text{O}_2}=0.5\%$ ) shows no significant peak (Fig. 36).

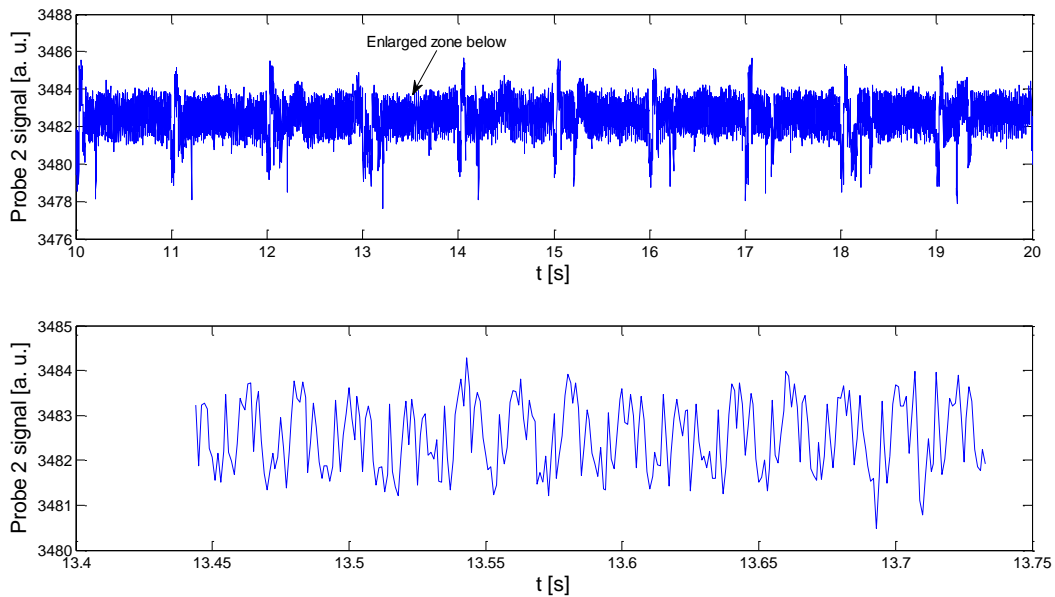


Fig. 36: Detail of signal of probe 2 for test with  $T=1100^{\circ}\text{C}$ ,  $Y_{\text{O}_2}=0.5\%$ , coal  $d_p>125\ \mu\text{m}$

Signals of tests in the same conditions ( $T=1100^{\circ}\text{C}$ ) of the previous but with the small particles size ( $d_p=38-90\ \mu\text{m}$ ) shows peaks not very intense. This can be observed from signals of probe 1 (Fig. 37) and 2 (Fig. 38) with a high oxygen fraction ( $Y_{\text{O}_2}=6\%$ ).

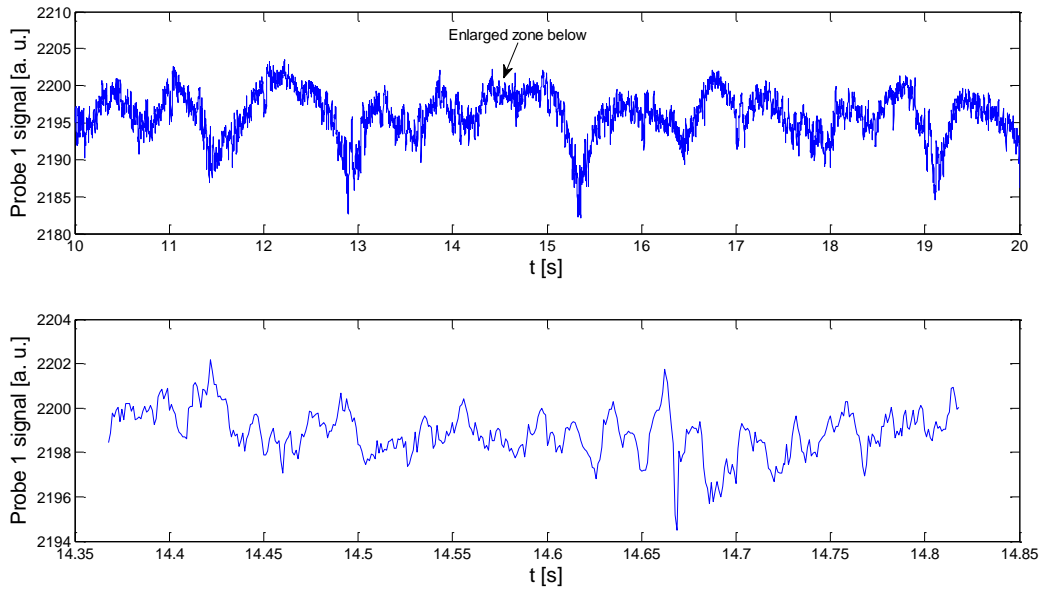


Fig. 37: Detail of signal of probe 1 for test with  $T=1100^{\circ}\text{C}$ ,  $Y_{\text{O}_2}=6\%$ , coal  $d_p=38-90 \mu\text{m}$

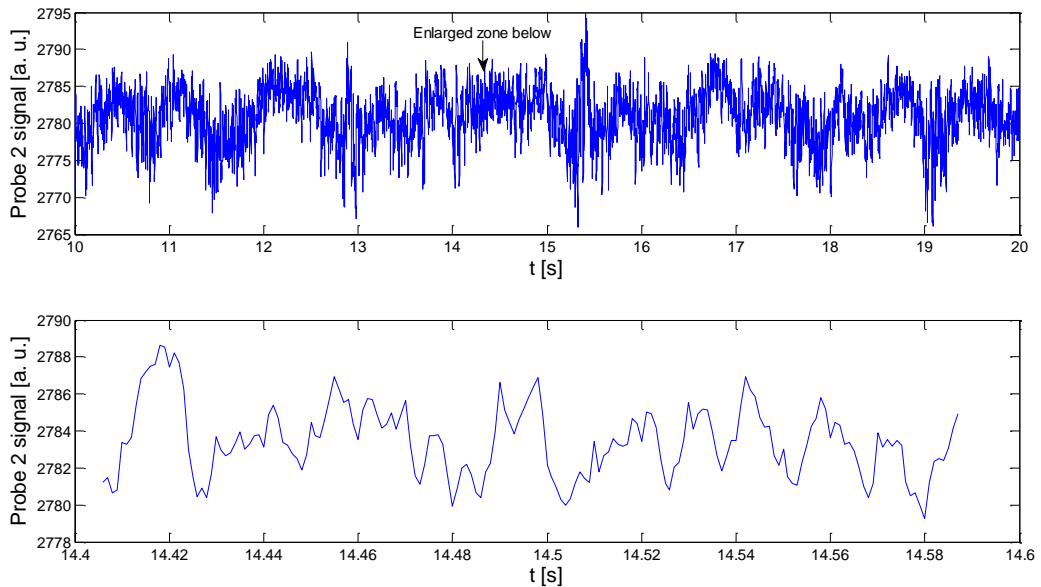


Fig. 38: Detail of signal of probe 2 for test with  $T=1100^{\circ}\text{C}$ ,  $Y_{\text{O}_2}=6\%$ , coal  $d_p=38-90 \mu\text{m}$

It is possible noting like in these tests peaks are observable from the port 6 where probe 1 was placed, then before than in tests with the bigger particles size when peaks are visible from the port 7. In these tests peaks are lower in intensity but they have the same extension of 7-15 ms of the previous tests, indicating that the phenomena that originates them is probably the same. Also in this case if there is a lack in oxygen peaks are not present in appreciable amount. Examining signals of tests at lower temperature ( $T=900^{\circ}\text{C}$ ) for big particles size ( $d_p>125 \mu\text{m}$ ) an important thing is noted: also with a high excess of oxygen in hot gases signals don't show a significant amount of peaks. This can be noted from signals of probe 2 (Fig. 39) and 4 (Fig. 40).

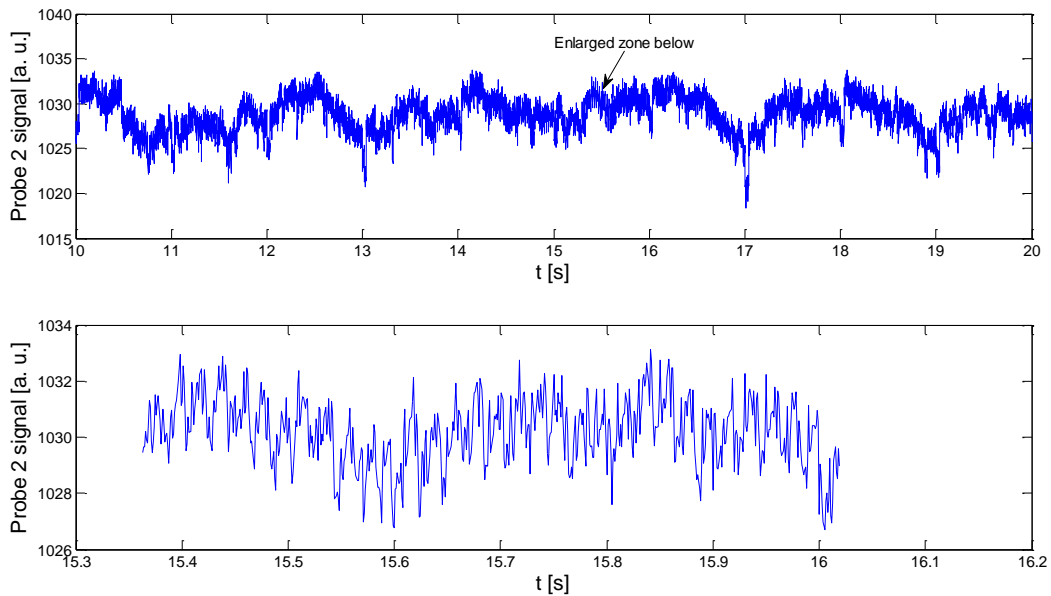


Fig. 39: Detail of signal of probe 2 for test with  $T=900^{\circ}\text{C}$ ,  $Y_{\text{O}_2}=6\%$ , coal  $d_p>125\ \mu\text{m}$

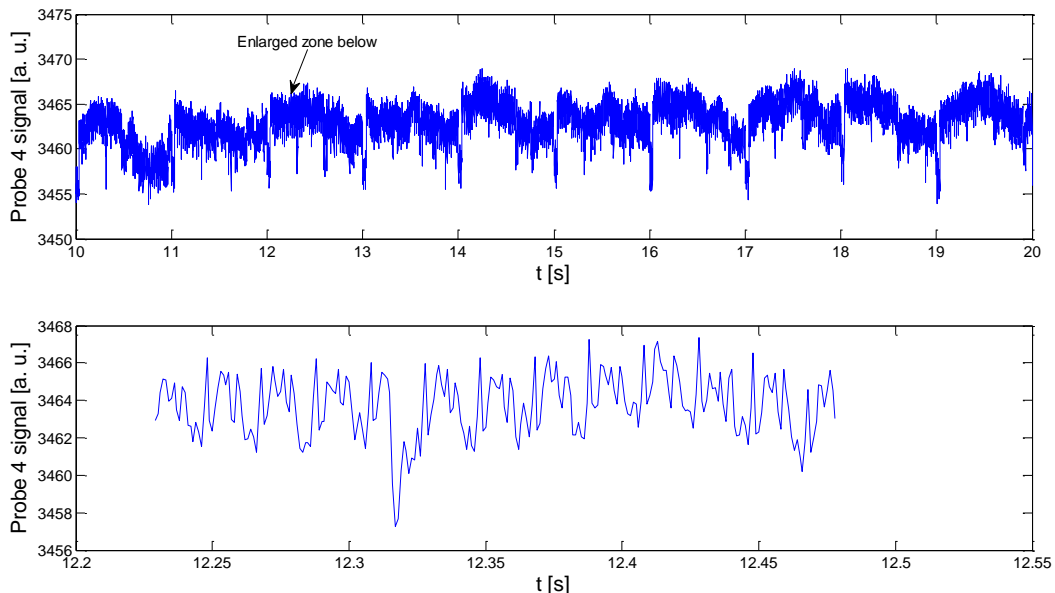


Fig. 40: Detail of signal of probe 4 for test with  $T=900^{\circ}\text{C}$ ,  $Y_{\text{O}_2}=6\%$ , coal  $d_p>125\ \mu\text{m}$

In practice no signals show peaks because the small oscillations have an extension of 2-5 ms and not 7-15 ms like in case at higher reactor temperature, then they are caused by the noise during the acquisition.

As result of this analysis ODC probes can observe the combustion process and signals generated are characterized by the presence of peaks. Observing signals for different operating conditions the following indications can be obtained:

- in case of strong lack of oxygen (tests with  $Y_{\text{O}_2}=0.5\%$ ) there is not a significant amount of peaks in probes signals

- peaks in signals of tests at high reactor temperature ( $T=1100^{\circ}\text{C}$ ) are consistent for both particles size with the same temporal extension (7-15 ms), but in case of small particles they are present at lower distances from the coal injection and are lower in intensity

- at low temperature ( $T=900^{\circ}\text{C}$ ) peaks are difficult to observe in signals

fitting of some peaks highlights as they have an initial stage that can be fitted with an exponential trend, a following stationary stage and in the end a negative exponential stage.

All these observations could induce to think that peaks are originated by volatiles oxidation stage for some reasons:

if there is a lack in oxygen there are not peaks in signals, this is consistent with the greater difficulty of a combustion process due to the slower oxygen diffusion of oxygen from the bulk and the incapacity to realize a complete oxidation

for bigger particles size peaks are more intense but peaks form and extension are the same, the higher intensity could be due to the higher flame temperature during volatiles oxidation stage of bigger particles [3]

at lower reactor temperature peaks are not observable, but must be considered that at  $T=900^{\circ}\text{C}$  both devolatilization and volatiles oxidation stages are slower and then possible peaks presence could be noted by probes placed at higher distances from the coal injection.

Other experimental tests with another probes disposition could confirm or not this hypothesis.

These effects are consistent with an experimental study of literature [16] where a stage of volatiles pre-ignition is noted with a great luminous emission before char ignition. All volatiles oxidation process is evaluated in 7-15 ms, a time consistent with other experimental studies [3], [4] that obtain values of 10-25 ms. Those studies analyzed single particles oxidation, but the continuous feed conditions used in these tests are not to far from it as the low group number highlights.

---

### 5.3 Tests with char

#### 5.3.1 Effect of the particles size

Experimental tests were conducted with the same reactor temperature ( $T=1100^{\circ}\text{C}$ ) and oxygen concentration in hot gases ( $Y_{\text{O}_2}=6\%$ ), only char particles size was varied. Two sizes were tried:  $d_p=90\text{-}125\ \mu\text{m}$  (Fig. 41) and  $d_p=45\text{-}90\ \mu\text{m}$  (Fig. 42).

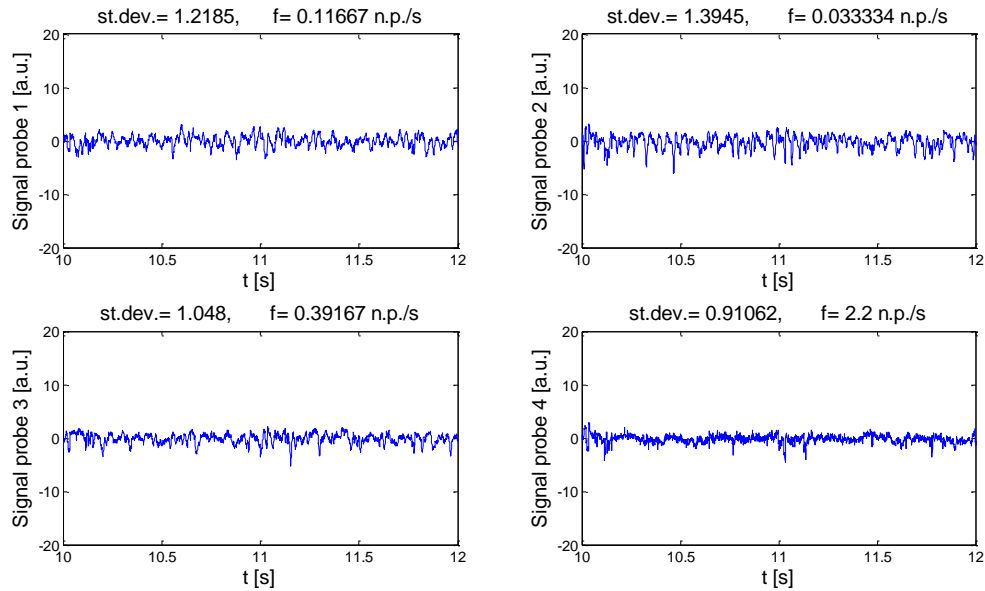


Fig. 41: Details of probes signals for test with coal  $d_p=90\text{-}125\ \mu\text{m}$

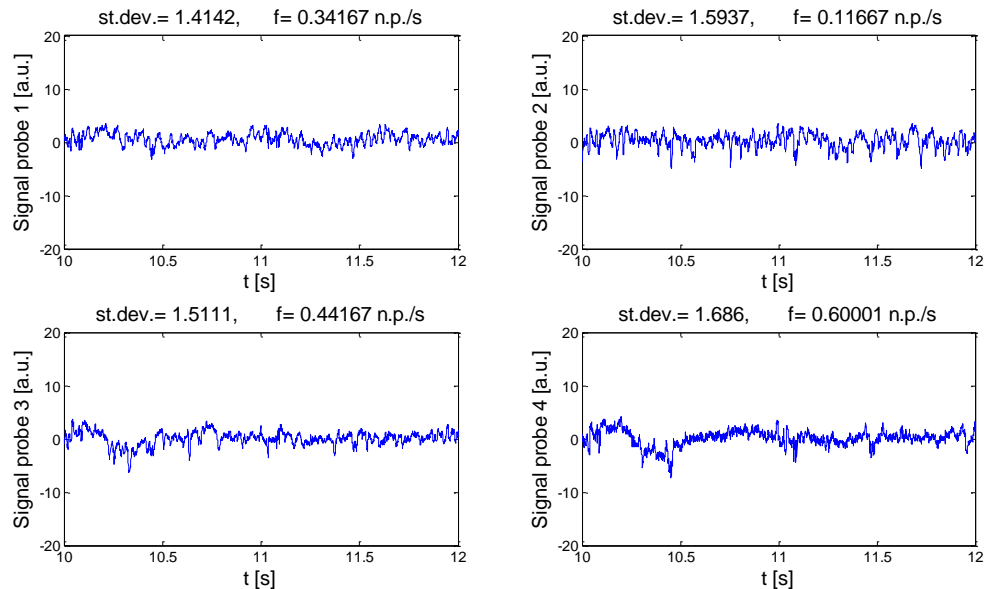


Fig. 42: Details of probes signals for test with coal  $d_p=45\text{-}90\ \mu\text{m}$

Examining signals shown in figures there are not particular differences between signals varying char particles size. It could seem that probes see no relevant phenomena, then if char oxidation happen is not characterized by luminous emission as volatiles oxidation. This is consistent with other experimental studies 0. On the other char oxidation could happen for higher distances from coal injection where there are not probes that can see it.

## 5.4 Tests with biomass

### 5.4.1 Effect of the oxygen gas fraction

Tests were conducted at a reactor temperature of 900°C varying the oxygen fraction in hot gases. Like in tests on coal an increase in signal dynamic is expected increasing the oxygen fraction. Some examples are shown in Fig. 43, Fig. 44 and Fig. 45.

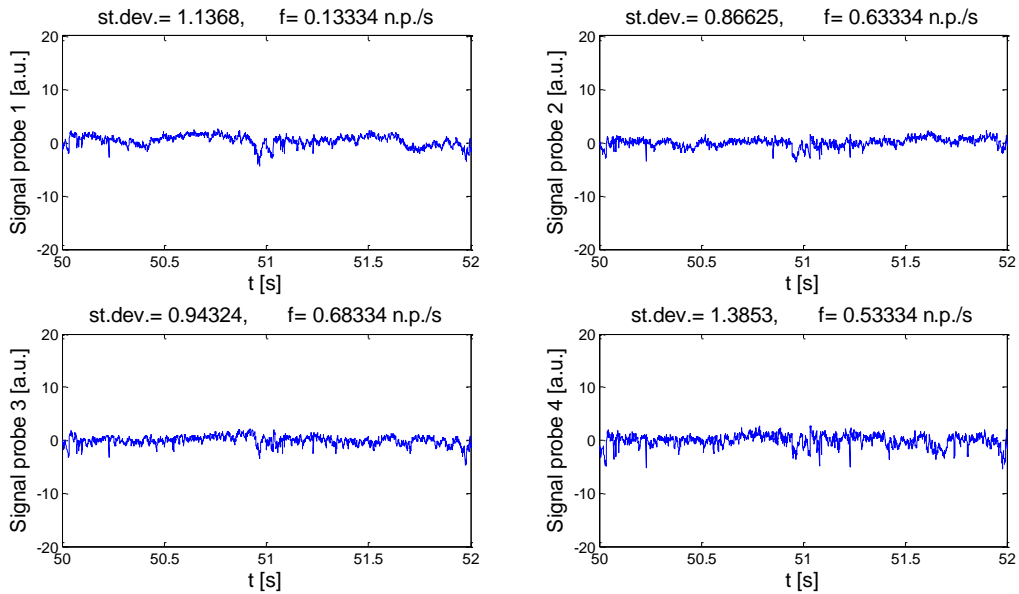


Fig. 43: Details of probes signals for test with  $Y_{O_2}=0.5\%$

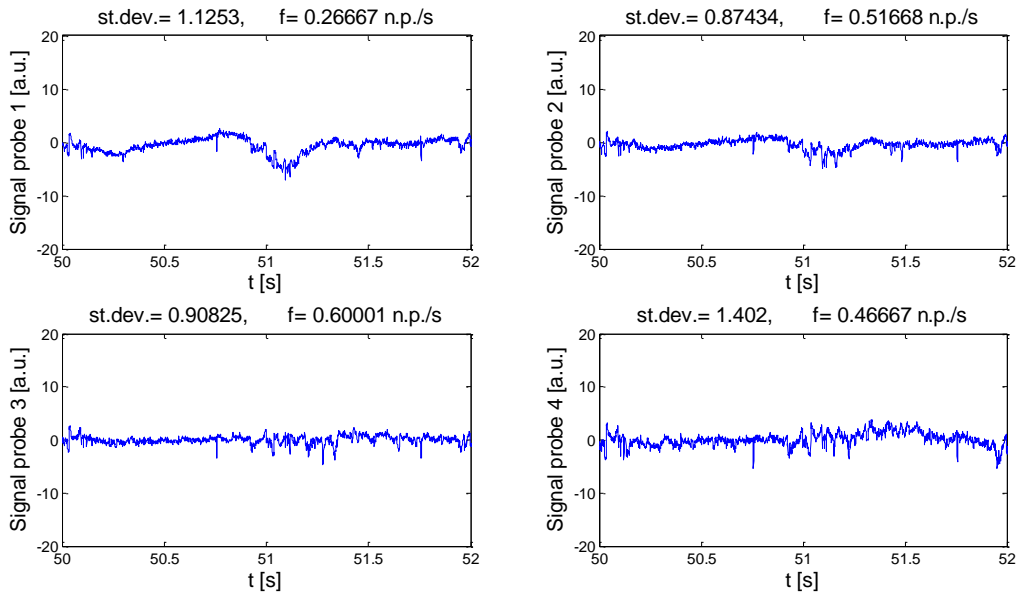


Fig. 44: Details of probes signals for test with  $Y_{O_2}=3\%$

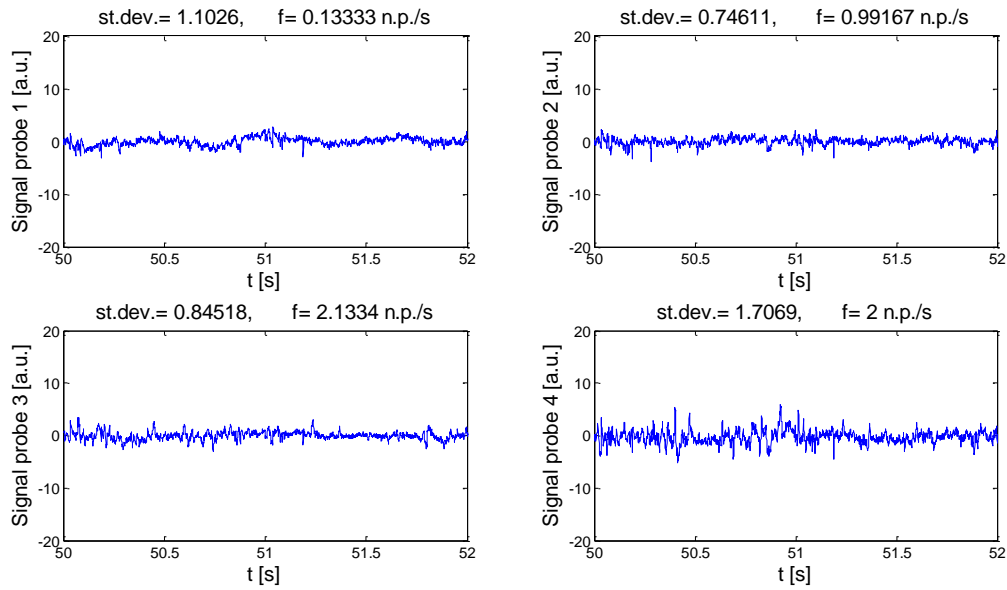


Fig. 45: Details of probes signals for test with  $Y_{O_2}=6\%$

It is possible observing like signals dynamic is the same for all the conditions tested, indicating that no probes see a luminous emission. This could induce to think that volatiles ignition happen for higher distances from coal injection where there are not probes, or that volatiles ignition for biomass is not luminous.



## 6 Signals analysis of pulsed fed tests

### 6.1 Signals form and data treatment

Pulsed fed tests were made both in April and in September session, then with different probes dispositions. In April session four probes were placed laterally, while in September tests one of them was placed axially on the bottom of the IPFR. Obviously lateral probes give a signal containing spatial informations and the probe on the bottom gives a temporal information.

Due to the signal acquisition and compensation stage the absolute value of the signal has not sense, while its variation is a measure of the energy detected by the probes. For this reason a preliminary data treatment is needed. Due to the signals simplicity a simple data treatment of detrend is sufficient. This operation consists in the subtraction from the signal of the best fitting straight line of the signal itself. In case like this of complex signals with frequent variation during the time Matlab<sup>®</sup> divides the signals in intervals and subtracts the values of the least square lines that better fit every part. In this way the absolute value of the signal is lost but its form and variations rest uncharged, so its dynamics is unaltered. This kind of operation allows to consider like 0 the radiation value emitted by reactors walls and then every variation is due to the solid fuel particles transit. If a variation is negative is given by the transit of not ignited particles because they are colder than the walls, on the other hand ignited particles are hotter than walls and then variation is positive. Obviously these statements derive from the fact that the level of detected signal is higher if energy content is higher, then high temperature mean high energy and then high radiation. As confirm of the dynamics maintenance during detrend data treatment noting Fig. 46.

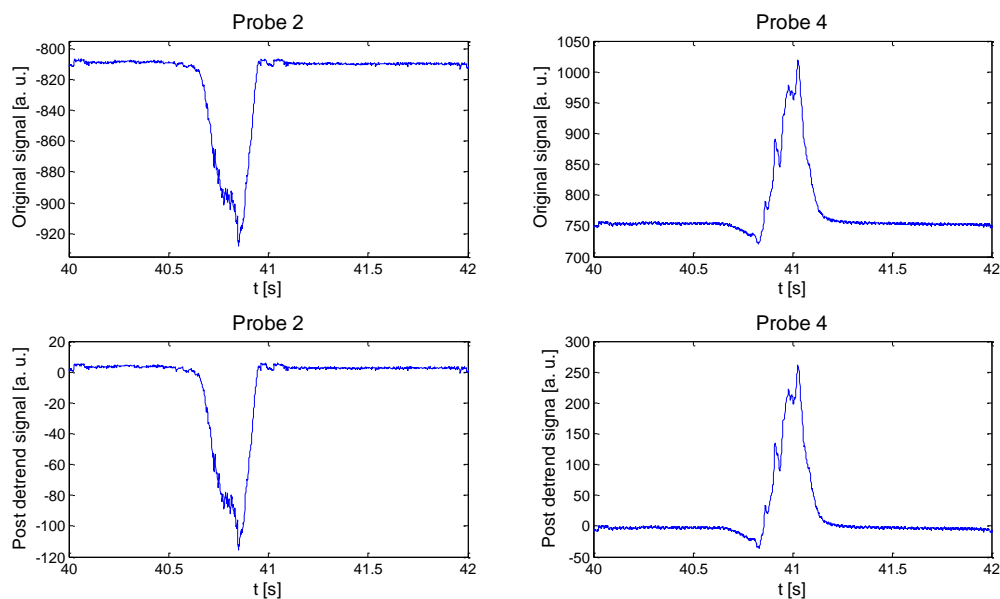


Fig. 46: Comparison between original and treated signals

All following figures are obtained with the previous described data treatment and are taken from September tests than probe 1 is from the bottom, probe 2 is in port 6, probe 3 in port 8, probe 4 in port 10 and coal injection from port 5.

Lateral signals can be:

signal with negative variation from the reactor walls level if solid coal particles are not ignited then are colder and absorb radiation (Fig. 46-probe 2)

signal with positive variation from the reactor walls if solid coal particles are ignited then are hotter and emit radiation (Fig. 46-probe 4).

Signal detected by the bottom probe is completely different and more complex. It has a characteristic form observable in Fig. 47 for a test with feed of pulverized coal. Varying fuel and operating conditions the signal curve form changes slightly. In Fig. 47 are also shown some frames registered with a camera.

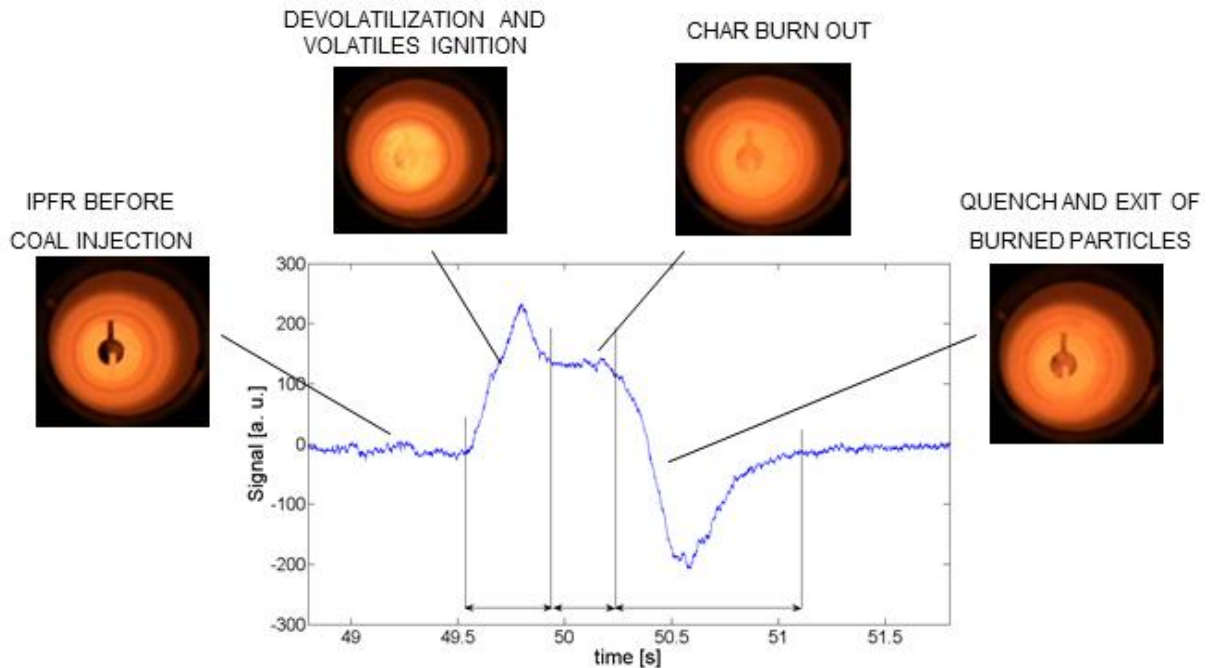


Fig. 47: Example of signal of the bottom probe

Some sections can be observed:

section 1: signal increases quickly from a constant value (given by reactor walls) until a maximum, then decreases. In this period particles have a temperature sufficient to start devolatilization and then volatiles ignition with luminous emission that decreases with volatiles consumption

section 2: signal keeps constant at a quasi stationary value, in this period a partial char oxidation occurs and the emission is less luminous and intense

section 3: due to the quench particles temperature decreases quickly and then char oxidation is stopped. Cold particles cover the least reactor section absorbing walls radiation and when are exited from the IPFR signals comes back to the constant value of 0.

Section 1 then is due to the devolatilization and volatiles oxidation stage with homogeneous ignition.

It is possible to note like from signal there is not the capability to identify the moment when coal injection occurs, this is due to the high distance from the optical probe and the feed probe (over 3.3 m) and the low volume of coal fed ( $250 \text{ mm}^3$ ).

## 6.2 Tests with coal

### 6.2.1 Effect of the reactor temperature

Keeping constant all other operating conditions and varying the IPFR temperature an increase in processes kinetics is expected. This statement is true also for devolatilization and

volatiles/char oxidation stages. To analyze this fact in following figures are shown lateral probes signals for the same conditions ( $Y_{O_2}=3\%$ ,  $d_p=38-90\ \mu\text{m}$ ) and different temperature:  $T=900^\circ\text{C}$  in Fig. 48 and  $T=1100^\circ\text{C}$  in Fig. 49.

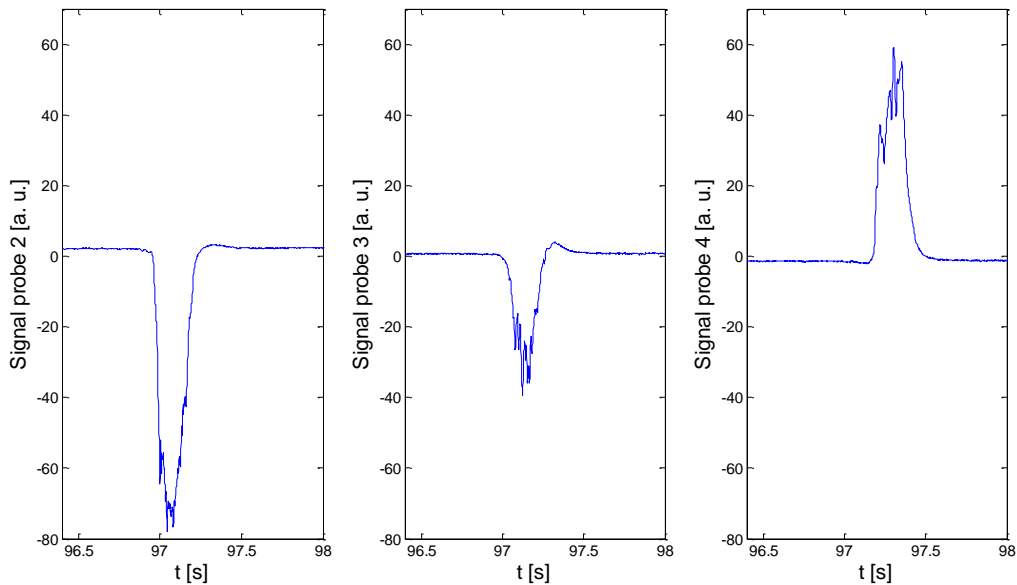


Fig. 48: Details of probes signals for test with  $T=900^\circ\text{C}$

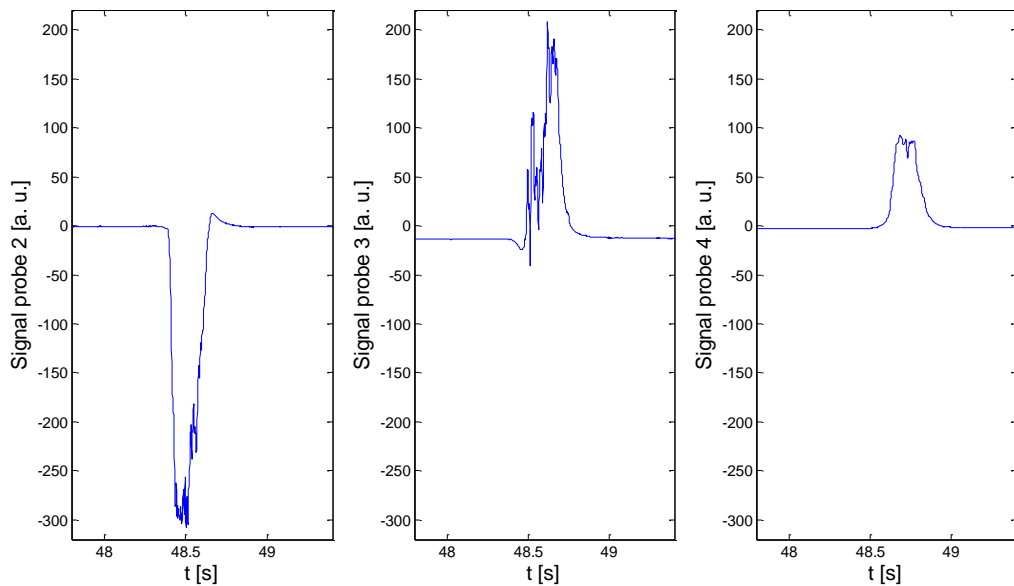


Fig. 49: Details of probes signals for test with  $T=1100^\circ\text{C}$

For both tests probe 2 (port 6, 12.65 cm after coal injection) reveals a negative signal and the probe 4 (port 10, 100.3 cm after coal injection) reveals a positive signal. The difference is in the probe 3 signal (port 8): for  $T=900^\circ\text{C}$  is negative while for  $T=1100^\circ\text{C}$  is positive. This difference is very important because means that volatiles ignition occurs before for higher temperature. This confirms the expectations and was already partially observed for continuous fed test. Then an increase in IPFR gases temperature reduces times for devolatilization and ignition.

### 6.2.2 Effect of the oxygen gas fraction

Analyzing continuous fed tests an increase of signal dynamics with oxygen gas fraction was observed and this is a good base to examine pulsed fed tests signals. In fact in this case a reduction of time for ignition is expected increasing oxygen fraction and this should be visible in a movement of signals of emission through probes more near to the coal injection point. In the following figures many signals of different tests are shown varying oxygen gas fraction and keeping constant reactor temperature ( $T=1100^{\circ}\text{C}$ ) and pulverized coal particles size ( $d_p=38-90\ \mu\text{m}$ ).

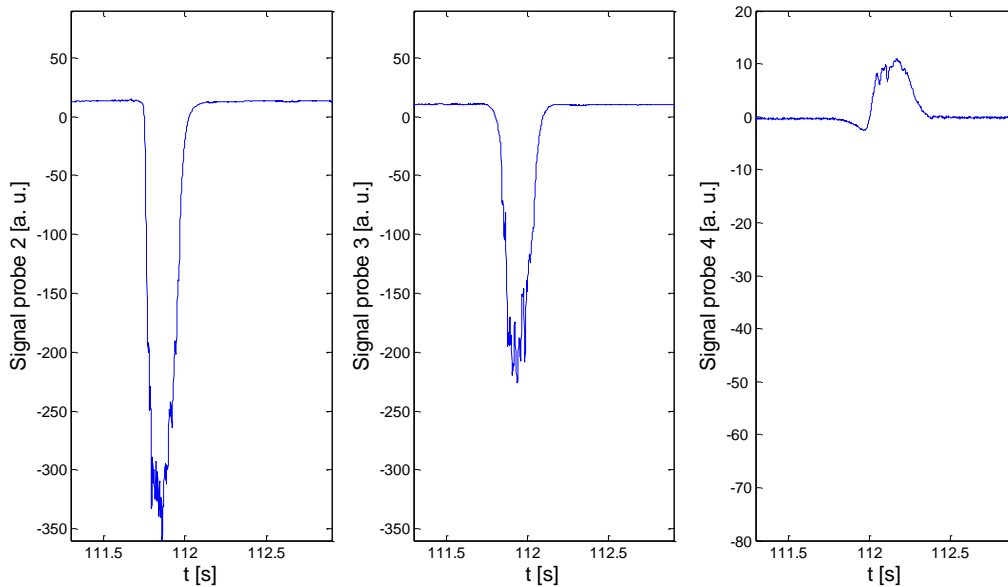


Fig. 50: Details of probes signals for test with  $Y_{O_2}=0.5\%$

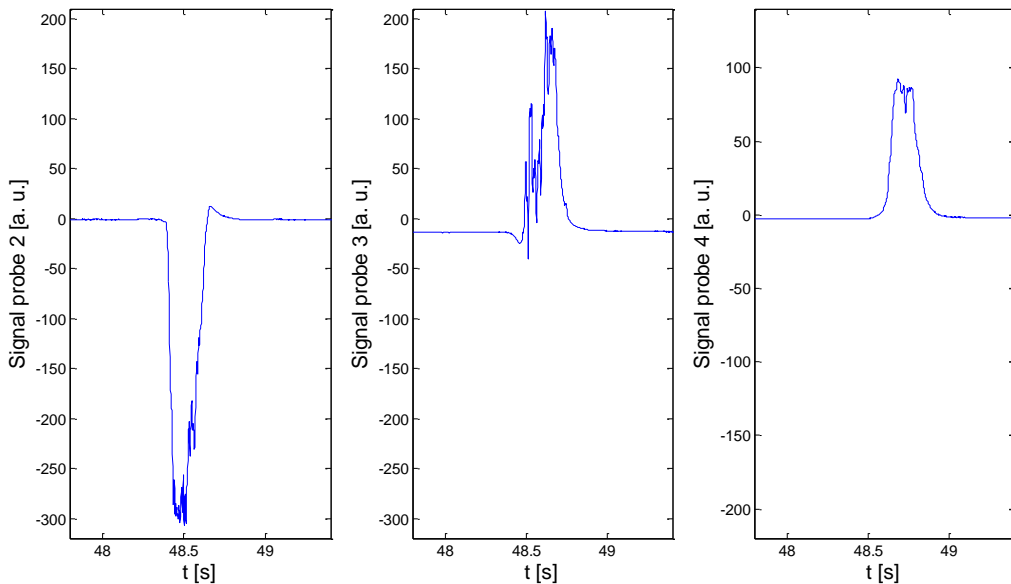


Fig. 51: Details of probes signals for test with  $Y_{O_2}=3\%$

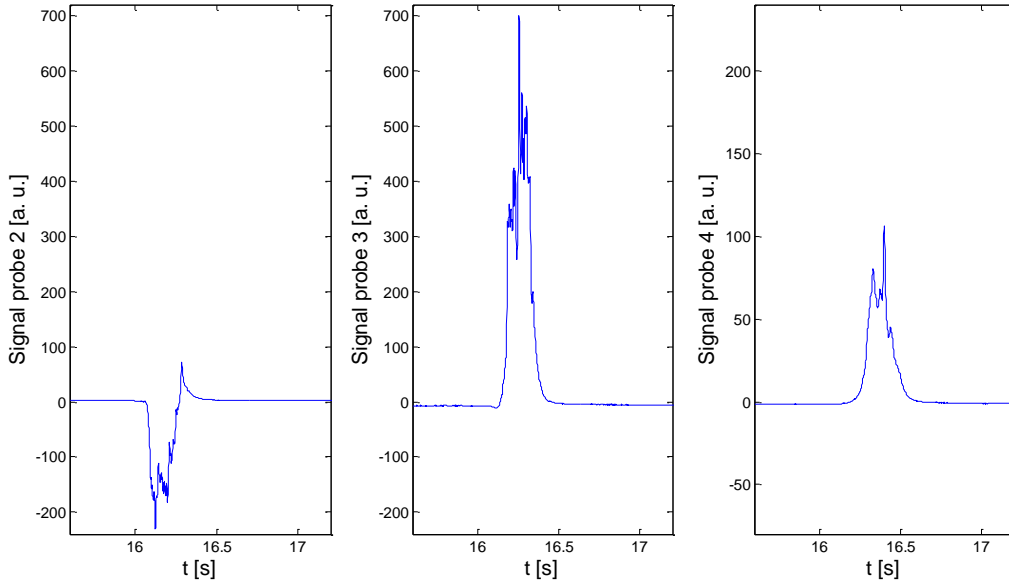


Fig. 52: Details of probes signals for test with  $Y_{O_2}=6\%$

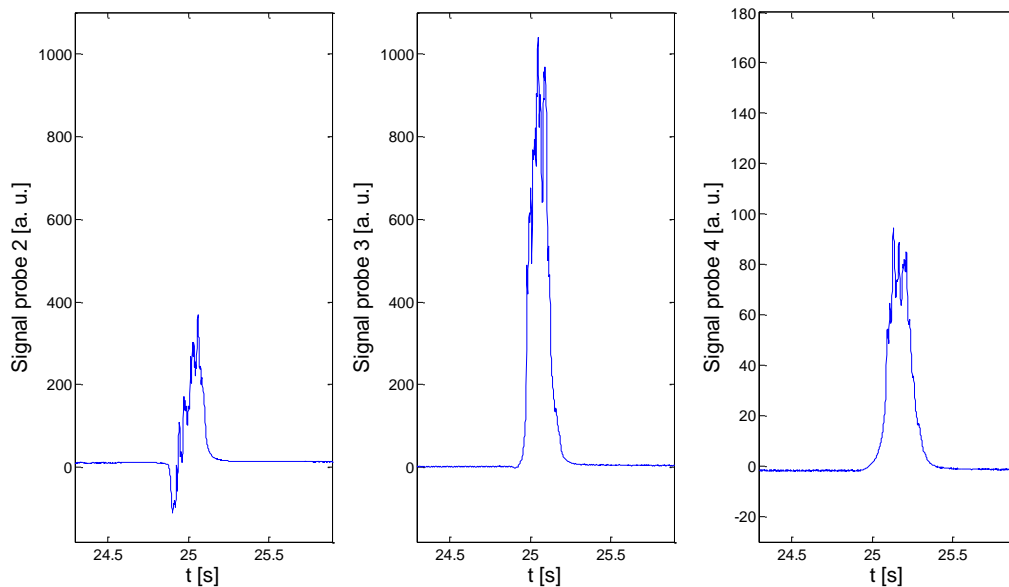


Fig. 53: Details of probes signals for test with  $Y_{O_2}=9\%$

From these figures appears like increasing oxygen fraction in hot gases emission phenomena tends to show itself quickly. In particular in case of a big lack of oxygen ( $Y_{O_2}=0.5\%$ , Fig. 50) only probe 4 shows a tiny emission, while cases with higher oxygen fraction ( $Y_{O_2}=3\%$  and  $Y_{O_2}=6\%$ ) (Fig. 51 and Fig. 52) show probes 3 and 4 in emission and for the highest oxygen excess ( $Y_{O_2}=9\%$ , Fig. 53) all probes show emission signals. Ignition is favoured by high oxygen concentration because there is a greater diffusion of oxygen from the bulk to ejected volatiles and the char surface and probes signals reveal it. Further considerations derive from the exam of signals of the probe from the bottom of the IPFR (Fig. 54).

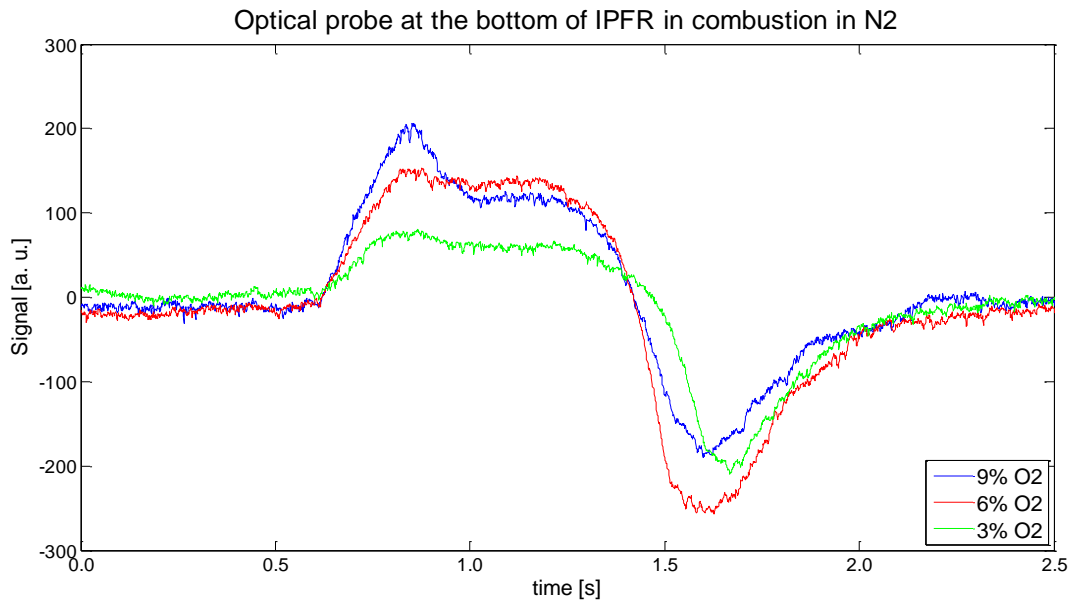


Fig. 54: Comparison of bottom probe signals varying oxygen gas concentration

Some observations can be made:

- the intensity of the maximum of the signal corresponding to volatiles oxidation increases with the increase in oxygen gas fraction, the same order is for signals of lateral probe 4
- the slope of the signal in the initial stage of volatiles oxidation increases with the increase of oxygen gas fraction and this effect is very clear
- signal of test with  $Y_{O_2}=9\%$  shows a very different intensity between the volatiles oxidation and the char oxidation stages, in other cases this is less clear
- also the slope during the quench stage is different for the three cases but a direct relation with the oxygen gas fraction is not so clear.

### 6.2.3 Effect of the particles size

From the exam of the continuous fed tests an influence of the coal particles size on the ignition time was revealed, in fact it was lower for smaller particles. To confirm or not this observation a comparison of signals of tests at the same operating conditions ( $T=1100^{\circ}\text{C}$ ,  $Y_{O_2}=6\%$ ) and different coal particles size is shown.

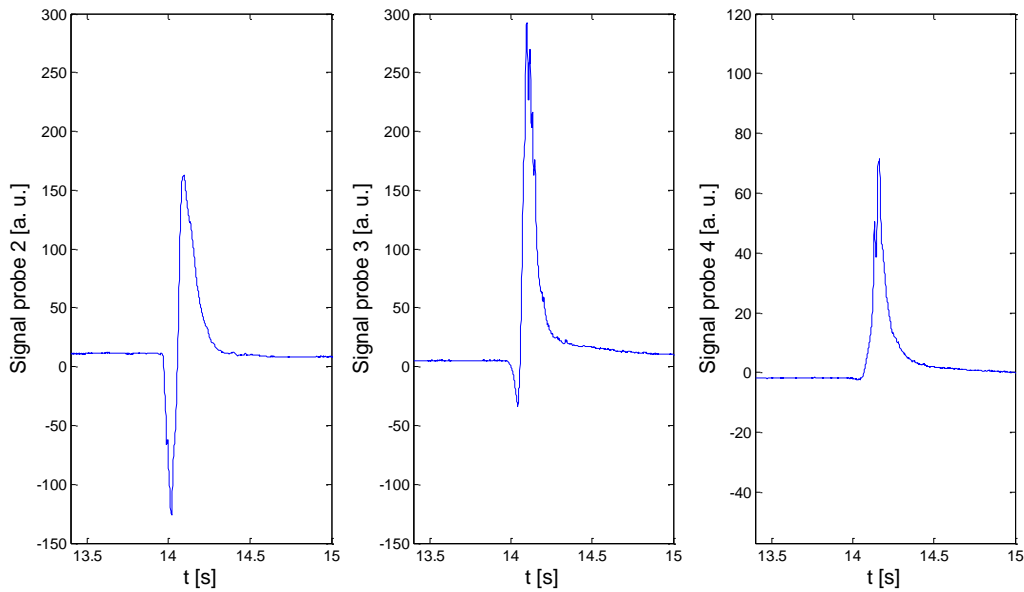


Fig. 55: Details of probes signals for test with coal  $d_p > 125 \mu\text{m}$

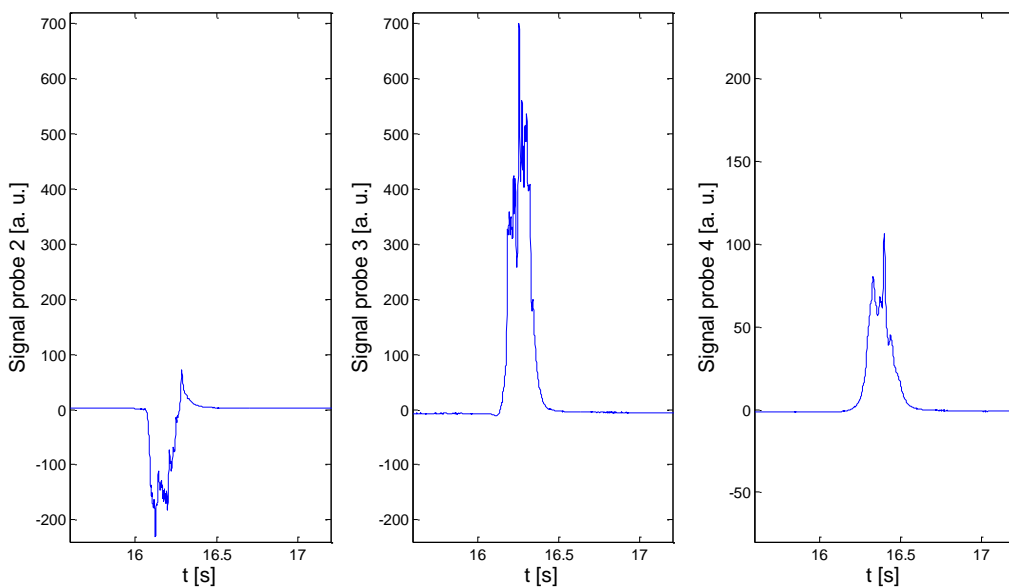
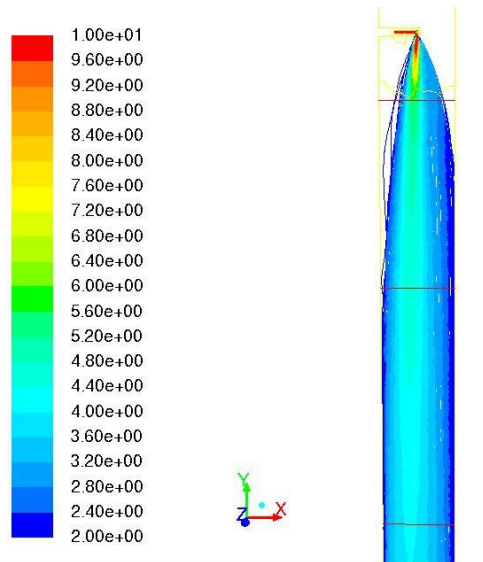


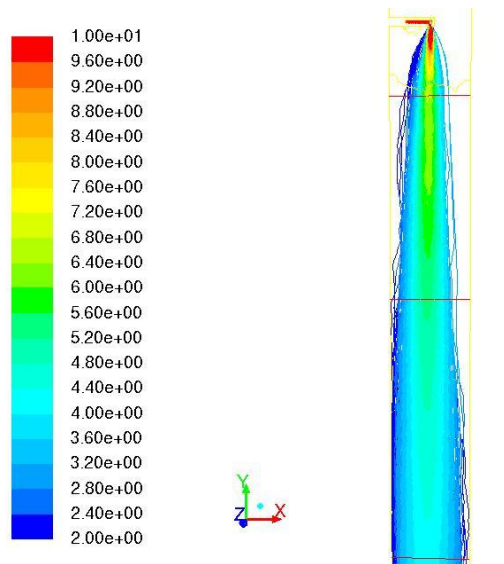
Fig. 56: Details of probes signals for test with coal  $d_p = 38-90 \mu\text{m}$

Thermic history of particles is strongly influenced by their size because in lower particles high temperatures are more quickly reached. Examining probes signals a surprise appears: signals of probes 3 and 4 are positive for both tests, but probe 2 signal is positive for big particles (Fig. 55) and negative for small ones (Fig. 56). This fact is not easily understandable because the difference in group number calculated for the feed conditions ( $G=9.7$  for big particles and  $G=40.1$  for small ones) is not sufficient to explain an inversion from the expectations. A better interpretation of this can be made observing the distribution of the coal fed particles injected inside the IPFR obtained modelling these cases with Ansys 13<sup>®</sup> and in particular with the software Fluent<sup>®</sup>.



Particle Traces Colored by Velocity Magnitude (m/s)

Fig. 57: Particle traces for test with coal  $d_p > 125 \mu\text{m}$



Particle Traces Colored by Velocity Magnitude (m/s)

Fig. 58: Particle traces for test with coal  $d_p = 38-90 \mu\text{m}$

Analyzing these figures it is clear like for the particular form of the feed probe the biggest particles tend to enlarge to the reactor walls very quickly, especially to the wall at the opposite side than the coal injection (Fig. 57). These coal particles are very slow and then the volatiles oxidation occurs for the same time of the inner particles but for lower distances from the coal injection point (Fig. 59). On the contrary small particles tend to follow the carrier gas flow and volatiles oxidation occurs in an only one region (Fig. 60).



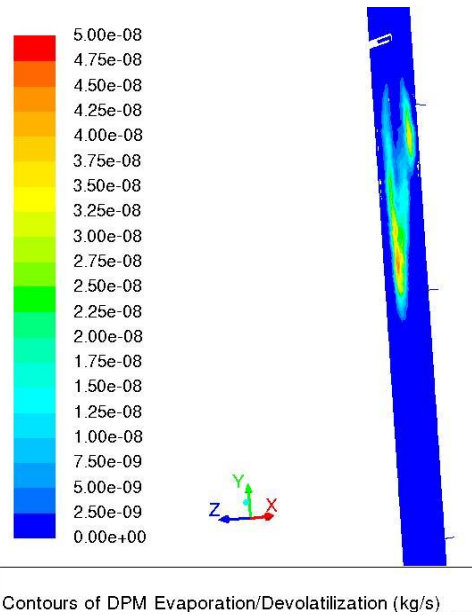


Fig. 59: Contour of devolatilization rate for test with coal  $d_p > 125 \mu\text{m}$

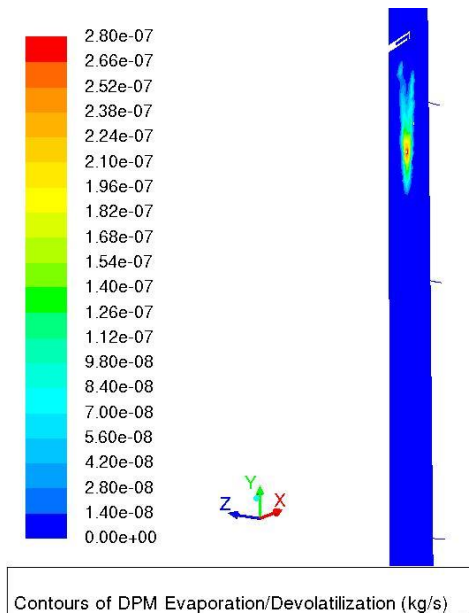


Fig. 60: Contour of devolatilization rate for test with coal  $d_p = 38-90 \mu\text{m}$

Lines at the right side of the IPFR represent the lateral ODC probes positions. As is visible devolatilization (and then volatiles oxidation and then emission) occurs quickly for small particles. However a fraction of big particles in case of  $d_p > 125 \mu\text{m}$  is subjected to devolatilization in the zone in front of the probe 2 (Fig. 59) (the first lateral probe), so this is seen by the probe (Fig. 55). Concluding then volatiles oxidation is quicker for smaller particles but in case of very big particles they have an inertia sufficient to abandon the gas flow and to go through the reactor walls slowly, so a part of them is subjected to volatiles oxidation in front of the first lateral probe. However this is only a little fraction of the injected particles and volatiles oxidation occurs for a little distance from coal injection point but after a longer time than for smaller particles (due to the very low velocity of the very big particles). Lateral probes signals then have a big limitation: their informations are only spatial and sometimes can be misleading.

Further informations can be get analyzing the signals of the bottom probe. Examples are shown in Fig. 61 and Fig. 62.

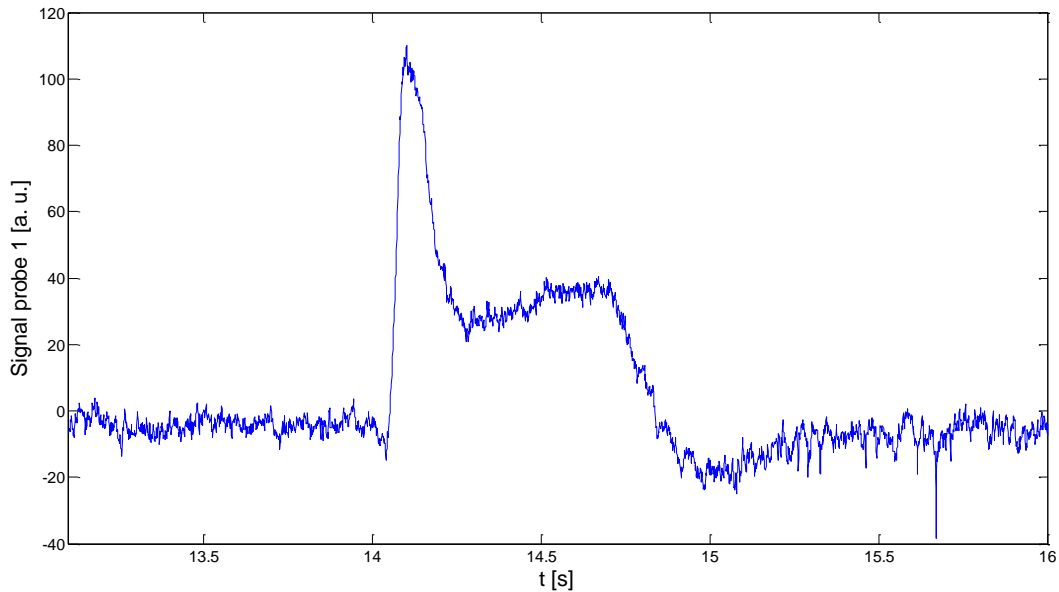


Fig. 61: Detail of bottom probe for test with coal  $d_p > 125 \mu\text{m}$

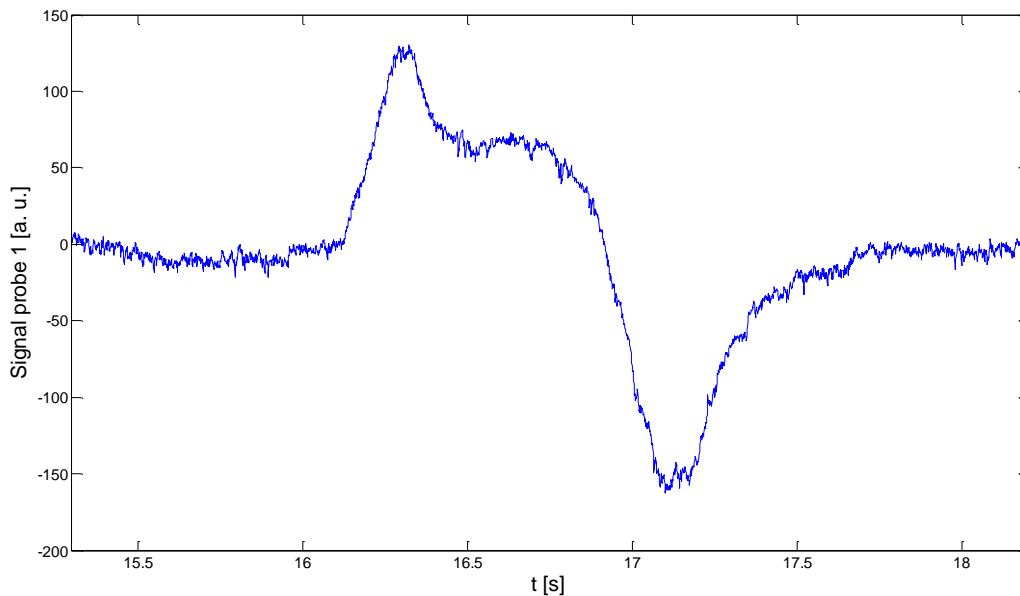


Fig. 62: Detail of bottom probe for test with coal  $d_p = 38-90 \mu\text{m}$

In case of bigger coal particles there is a greater difference between peak of volatiles oxidation and quasi stationary stage of char oxidation than in case of smaller particles. Beside in case of bigger particles the slope of the volatiles oxidation peak is higher. These observations are consistent with those made for peaks of continuous fed tests.

#### 6.2.4 Effect of gaseous atmosphere composition

To compare the effect of the gaseous atmosphere composition signals of lateral probes in tests with the same operating conditions ( $T=1100^\circ\text{C}$ ;  $Y_{\text{O}_2}=9\%$ ;  $d_p=38-90 \mu\text{m}$ ) and different

diluent gas are shown. Fig. 63 shows signals of conventional combustion (diluent gas N<sub>2</sub>) while Fig. 64 shows signals of oxy-fuel combustion (diluent gas CO<sub>2</sub>).

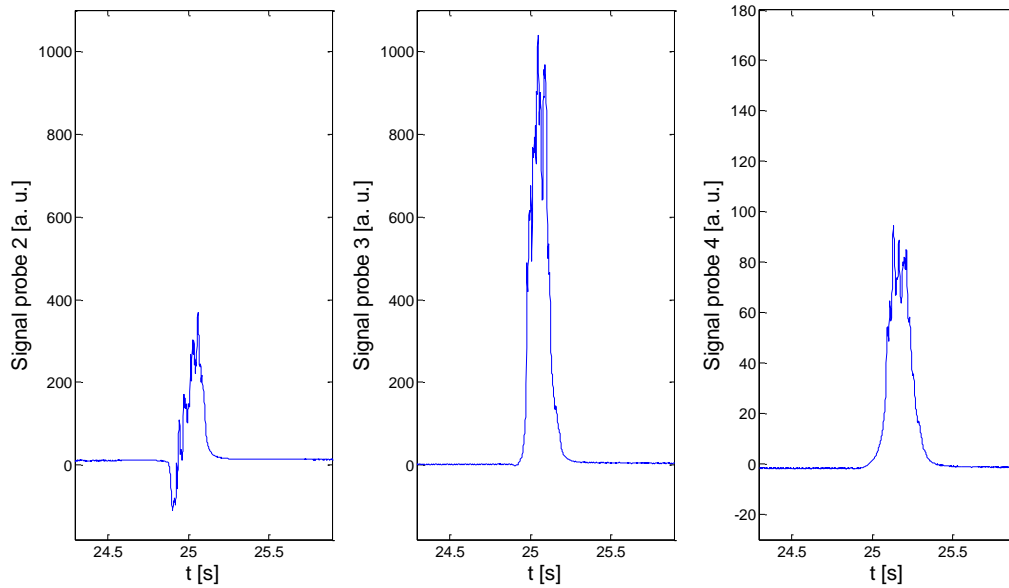


Fig. 63: Details of probes signals for test of conventional combustion

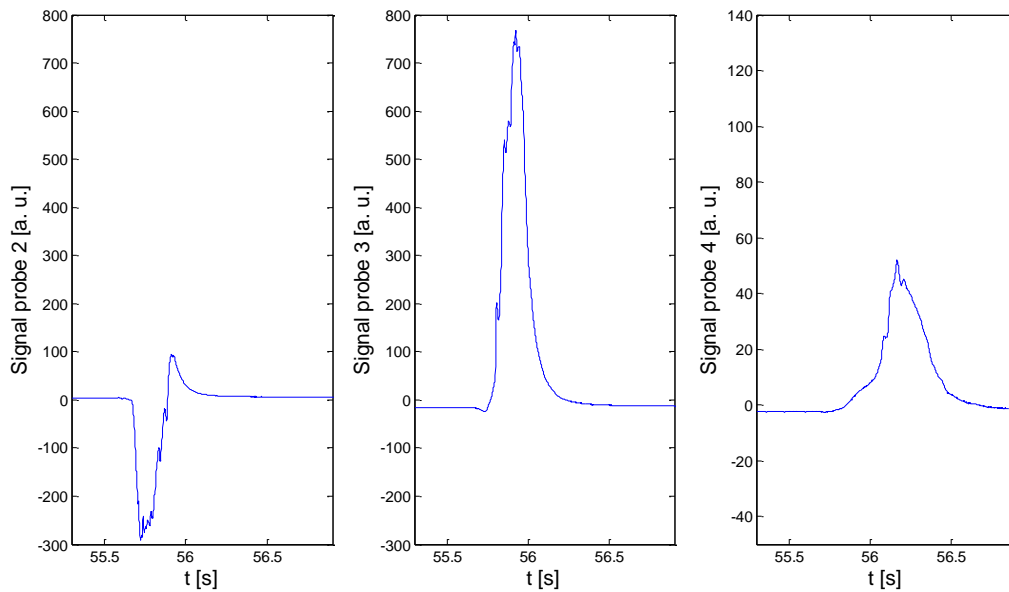


Fig. 64: Details of probes signals for test of oxy-fuel combustion

Examining signals of tests with the diluent gas as only one difference it is possible noting like the signal of the probe 2 (port 6) is the most different. In fact in case of nitrogen as diluent gas (Fig. 63) that signal is completely of emission, while in oxy-fuel combustion (Fig. 64) it is of absorption. Concluding ignition process in oxy-fuel conditions is slower than for conventional combustion. Beside it should be noted like substituting nitrogen with carbon dioxide radiant properties of hot gaseous mixture change strongly because atmospheric transmissivity ( $\tau_a$ ) decreases:

$$\tau_a = 1 - \alpha_w - \alpha_c \quad (23)$$

where  $\alpha_w$  and  $\alpha_c$  are the absorbencies of water and carbon dioxide. In conventional combustion these substances are present but the most of the gas mixture is made of nitrogen that is a transparent gas for radiations. In oxy-fuel instead the most of the gas is made of carbon dioxide that absorbs part of the emitted radiations and then contributes to signal attenuation. However there is a difference in signals varying diluent gas but for pulsed fed tests is less clear than for continuous fed tests.

The difference in bottom probe signal varying oxygen fraction in hot gases is analyzed also in case of oxy-fuel combustion (Fig. 65).

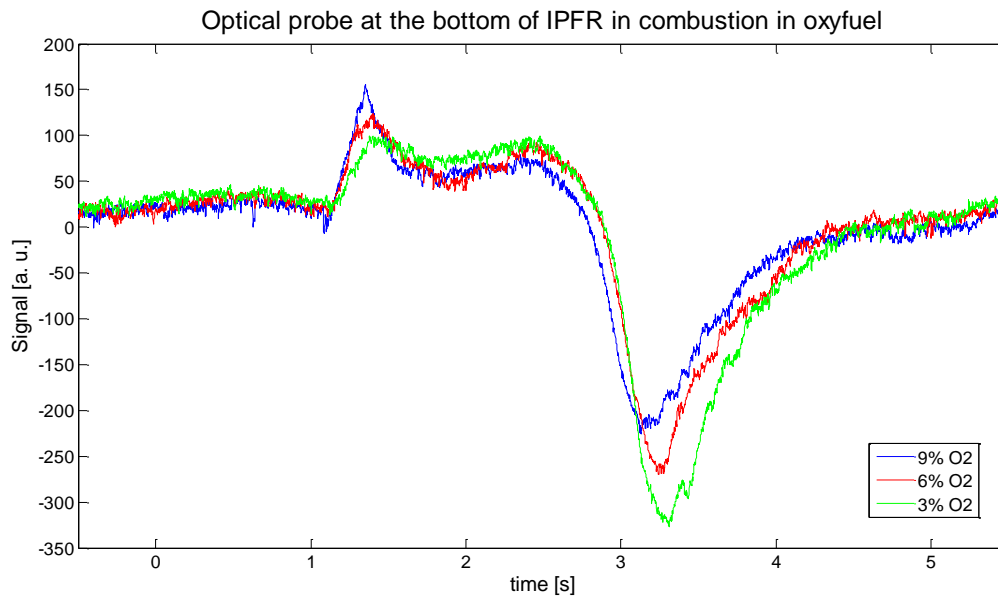


Fig. 65: Comparison of bottom probe signals varying oxygen gas concentration

The effect of the difference oxygen fraction in hot gaseous mixture in oxy-fuel conditions is the same than for conventional combustion:

- the intensity of the volatiles oxidation peak increases increasing oxygen fraction
- the slope of the peak increases increasing oxygen concentration
- the difference of intensity between volatiles oxidation peak and char oxidation stage decreases decreasing the oxygen fraction.

### 6.2.5 Determination of ignition delay

The ignition delay of the coal particles' clouds for all the conditions tested was evaluated by relating the lateral and the bottom probes' signals. The ignition delay was calculated as the time interval between coal injection and the time at which the signal seen by the bottom probe starts to increase considerably. This latter condition represents a state of initial ignition that can be related to volatile oxidation and could be easily determined from the signal analysis. Coal injection was not directly determined because the fed coal particles are too little and too far from the bottom probe (placed about 4 m above the coal injection) to cause an important decrease of the signal. So the injection time was determined with the aid of the first lateral probe. This probe was placed only 0.1265 m below of the coal injection point, thus it could reveal the passage of a group of (cold) solid particles through a well decrease of the signal. Particles were injected at a velocity of around 9.3 m/s; however it should be considered the jet decay when evaluating the particle velocity at downstream positions. As a matter of fact, the particle velocity may be estimated by the comparison of signals taken at the different lateral ports. In particular it was evaluated a particle velocity of about 6.1 m/s

between the first lateral probe (0.1265 m below coal injection) and the second one (0.503 m below coal injection). Subsequently it was assumed that particles flowed with a medium velocity of about 8 m/s between the coal injection and the first lateral probe. With this hypothesis the time between coal injection and the transit of the first coal particles in front of the first probe was evaluated to be of about 16 ms, from the ratio between the distance from injection to first probe and the mean velocity. Therefore the coal injection time could be determined by subtracting 16 ms from the time the particles started to be seen by the first lateral probe.

Ignition delay results as well as relative errors (evaluated from the standard deviation of the data) are reported in Fig. 66 for  $d_p = 38-90 \mu\text{m}$ . Fig. 66 shows the strong effect of reactor temperature on ignition delay at different  $Y_{O_2}$  for  $N_2$  diluent and basically confirms observations made above. Usually  $T = 1100 \text{ K}$  is considered the minimum temperature to have a fast ignition of a coal stream; however the very large difference in ignition delays between  $T = 1173 \text{ K}$  and  $T = 1373 \text{ K}$  indicates that maybe the minimum temperature is higher for the tested conditions. As far as the effect of  $O_2$  fraction is concerned, the ignition delay decreases with the  $O_2$  fraction. For instance at  $T = 1373 \text{ K}$  the ignition time decreases from 77 to 65 ms with increasing for  $Y_{O_2}$  from 6 to 9%. The observed trend is in agreement with works of [3] [7] [16].

In oxy-fuel conditions it was observed a larger ignition delay (Fig. 66b), but the influence of oxygen fraction is the same that in  $N_2$  combustion. It should be noticed that the present values of ignition delay are higher than those reported in other works [3] [7], however this may be partly imputed to the different coal tested and the different (i.e. higher) particle numerical density. As a matter of fact our high particle density was aimed at investigating fuel/gas carrier ratios not far from the typical fuel/air ratios of real boilers.

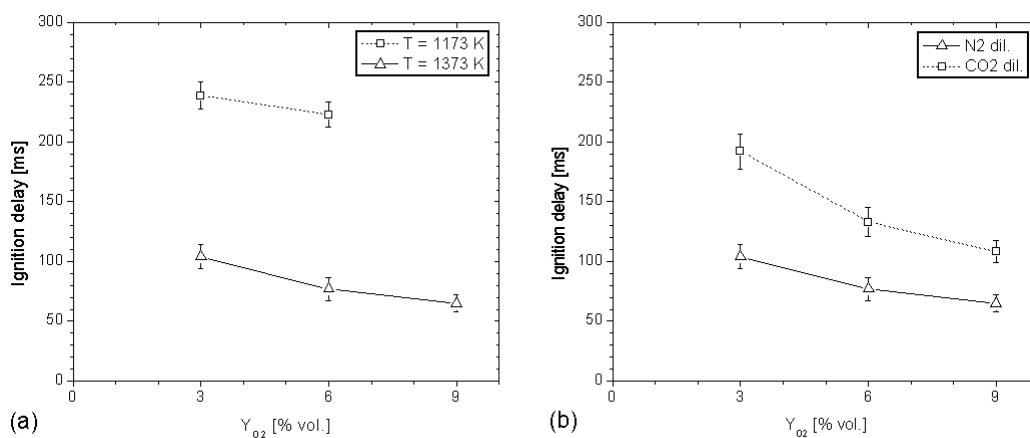


Fig. 66 Ignition delay as a function of the  $O_2$  fraction for different (a) reactor temperatures ( $N_2$  diluent) and (b) diluents ( $T = 1373 \text{ K}$ ).  $d_p = 38-90 \mu\text{m}$ .

## 6.3 Tests with char

### 6.3.1 Effect of the particles size

Two different particles size of char were analyzed during experimental tests keeping constant the operating conditions ( $T=1100^\circ\text{C}$ ;  $Y_{O_2}=6\%$  and nitrogen as diluent gas).

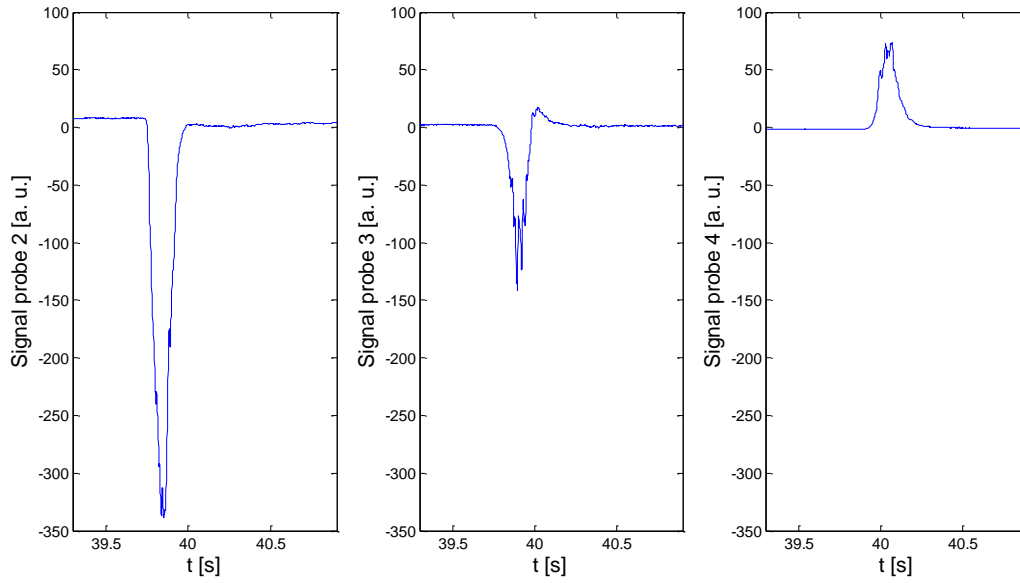


Fig. 67: Details of probes signals for test with coal  $d_p=45-90 \mu\text{m}$

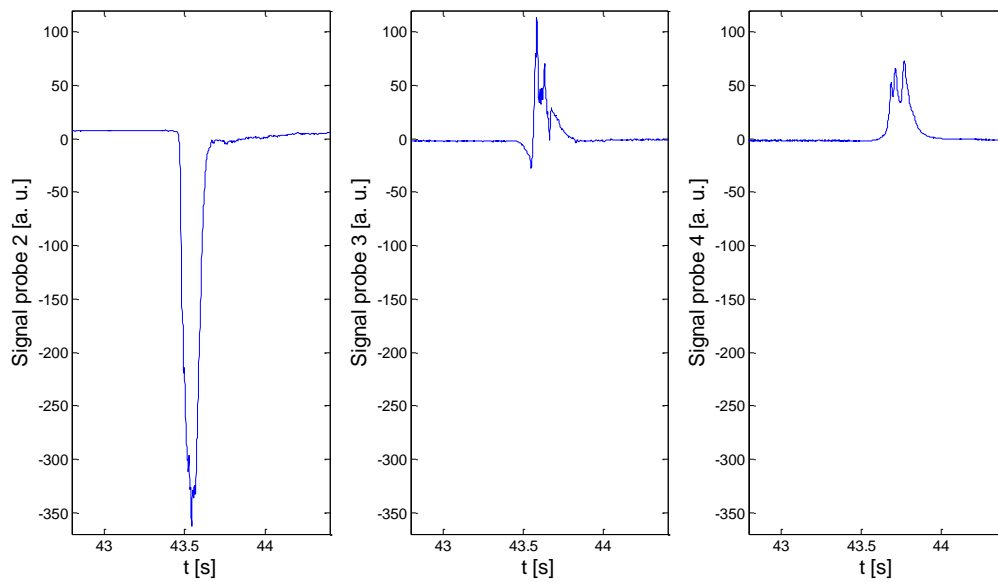


Fig. 68: Details of probes signals for test with coal  $d_p=90-125 \mu\text{m}$

For both case probe 2 signal is negative and probe 4 signal is positive. But probe 3 in case of smaller particles is completely negative (Fig. 67) while in case of bigger particles is of emission (Fig. 68). This is the same trend noted for tests on coal.

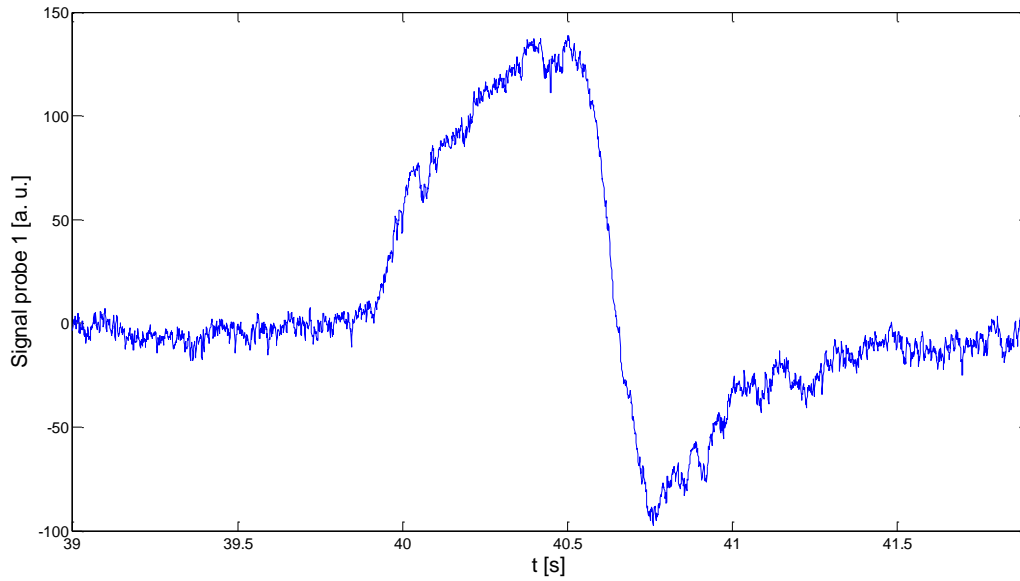


Fig. 69: Details of bottom probe signal for test with coal  $d_p=45-90 \mu\text{m}$

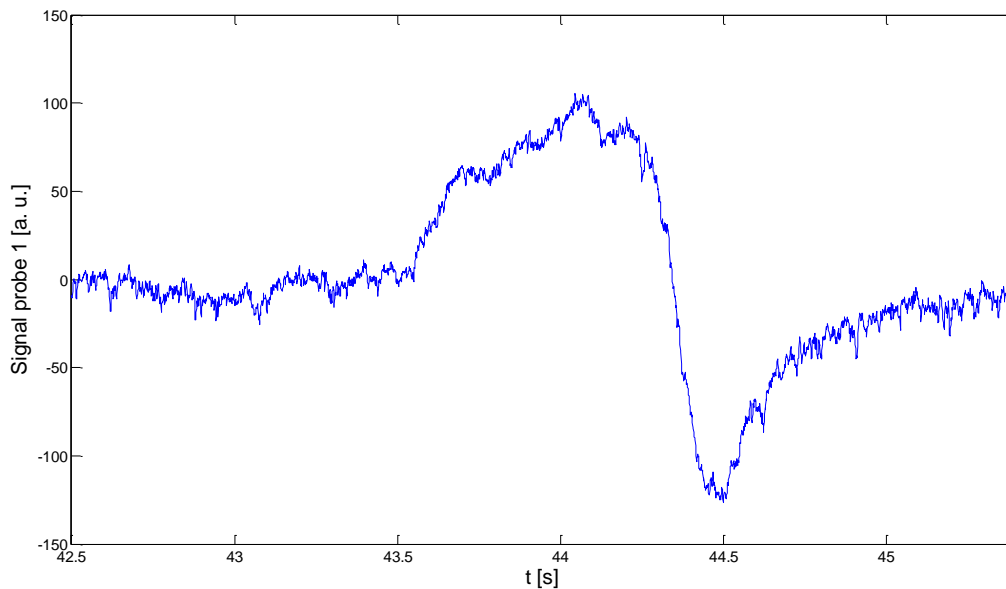


Fig. 70: Details of bottom probe signal for test with coal  $d_p=90-125 \mu\text{m}$

It is interesting to note like for both particles size the volatiles oxidation stage is not present in probe 1 signals from the IPFR bottom. This fact is consistent with the very low content of volatile matter in char. However first signals of emission registered by lateral probes are probably due to volatiles oxidation.

## 6.4 Tests with biomass

### 6.4.1 Effect of the oxygen gas fraction

Experimental tests with the same temperature of hot gases ( $T=900^\circ\text{C}$ ) were conducted varying oxygen gas fraction.

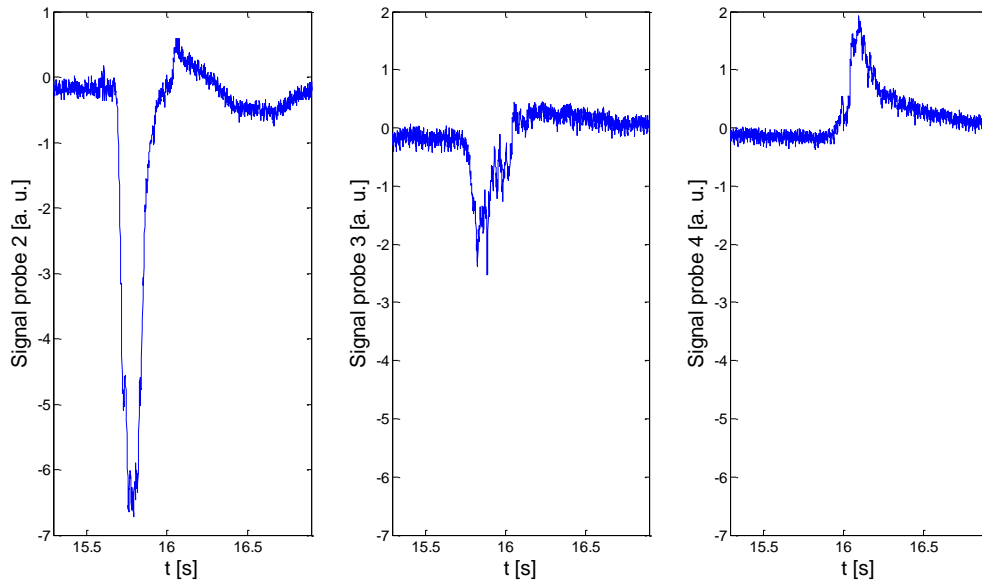


Fig. 71: Details of probes signals for test with  $Y_{O_2}=3\%$

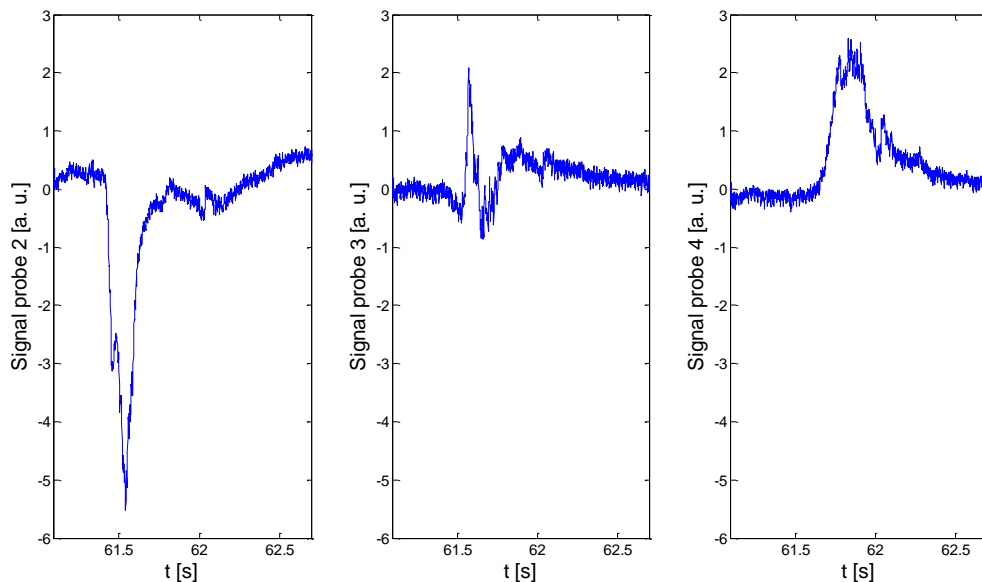


Fig. 72: Details of probes signals for test with  $Y_{O_2}=6\%$

The differences between two cases is the signal of probe 3: in case of lower oxygen content is of absorption (Fig. 71) while in case of higher oxygen content is of tiny emission (Fig. 72). Signals of probe 2 and 4 are the same : absorption the first and emission the second one. However every emission signal is not very intense in case of biomass and this contributes to speech because in case of continuous fed tests no peaks were noted considering also that in that case the mass flow of the feed was very lower (this contributes to signals attenuation). Beside the first probe to see a great emission is the probe 4 (port 10) that is placed at higher distances from fuel injection point than for continuous fed tests (the least probe was in port 9).

An exam of the effect of the oxygen concentration in hot gases on the bottom probe signal is shown in following figures.



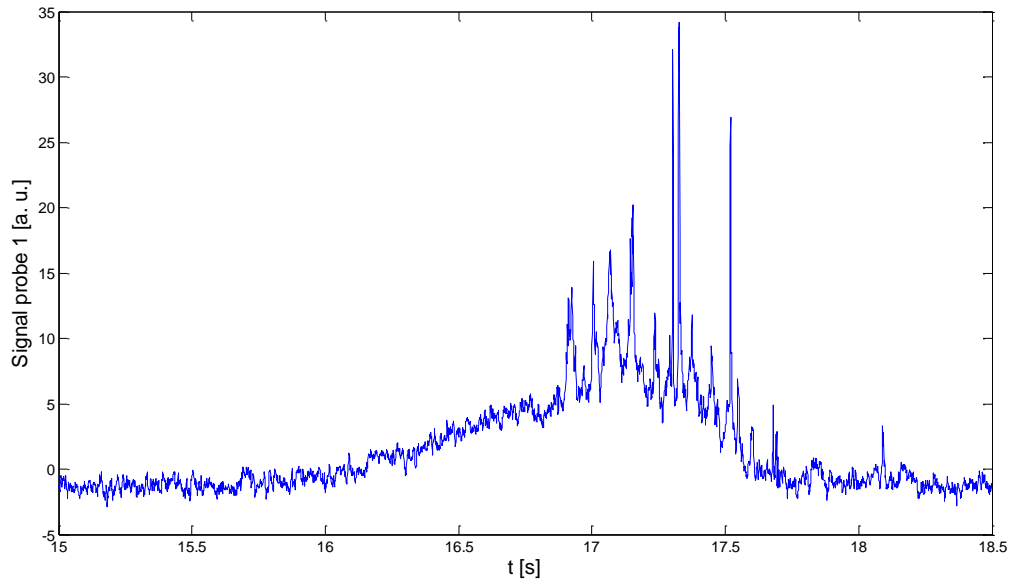


Fig. 73: Details of bottom probe signal for test with  $Y_{O_2}=3\%$

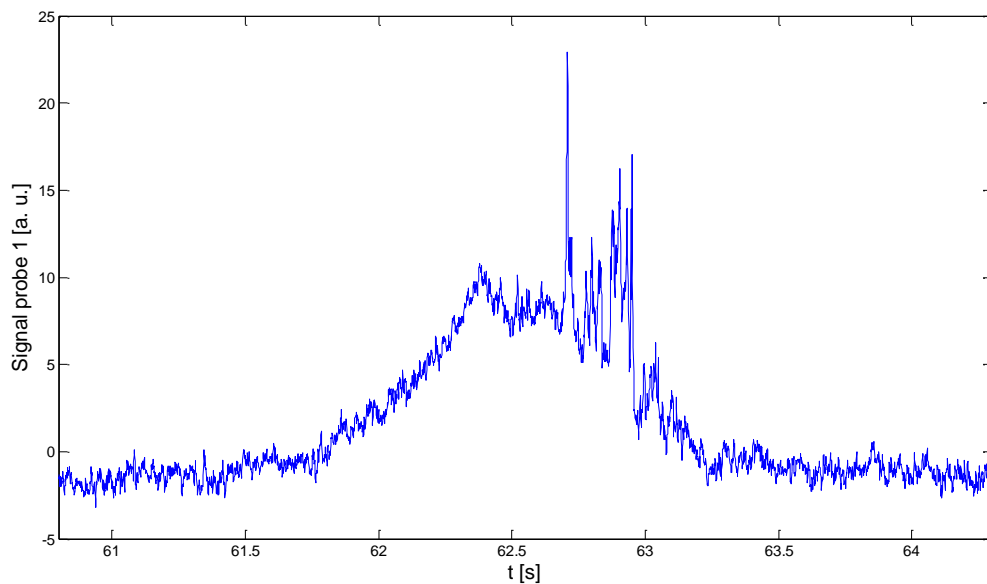


Fig. 74: Details of bottom probe signal for test with  $Y_{O_2}=6\%$

There are not particular differences between two cases. However it is interesting to examine the signal form: there are not characteristic zones, in fact there is not a clear division of volatiles oxidation and char oxidation like in coal tests. This is probably due to the biomass very high volatile content then the emission signal is due to volatiles oxidation.

## 7 Data post-processing of signals of pulsed fed experimental tests

### 7.1 Evaluation of solid particles medium velocity

#### 7.1.1 Adopted procedure

Solid fuel particles are fed to the IPFR by a carrier gas that flows in the reactor with a velocity of 9.3 m/s. Solid particles are fed with a velocity similar at the carrier gas velocity (because of their low inertia). Inside the IPFR the hot gases coming from the pre-heater flow with a velocity very lower than carrier gas velocity. Medium velocity of hot gases is function of the volumetric flow of nitrogen, oxygen, air, natural gas and carbon dioxide fed to the gas pre-heater, values that depend from the experimental test conditions. Typical values of hot gases medium velocity are shown in Tab. 23.

**Tab. 23: Hot gases medium velocity for different operating conditions of experimental tests**

Diluent gas	Temperature (°C)	Y <sub>O<sub>2</sub></sub> (% dry)	Hot gases medium velocity (m/s)
N <sub>2</sub>	1100	3	2.60
N <sub>2</sub>	1100	6	2.96
N <sub>2</sub>	1100	9	3.15
N <sub>2</sub>	900	3	2.13
N <sub>2</sub>	900	6	2.58
CO <sub>2</sub>	1100	3	1.17
CO <sub>2</sub>	1100	6	1.19
CO <sub>2</sub>	1100	9	1.23

Then fuel particles enter inside the IPFR with a velocity very higher than flue gases coming from the gas pre-heater and for big distances from the fuel injection point their velocity decreases for this reason. For very high distances solid particles have velocity very similar at hot gases one. For this reason a higher solid particles velocity is expected between port 6 and port 8 than that between port 8 and port 10, because of the lower distance from the point of injection.

Examining lateral probes signals it is possible to determine the medium velocity of fuel particles inside the reactor because of the distance from a port to another is known:

37.5 cm between port 6 and 8

50 cm between port 8 and 10.

From signals it is possible to determine the point when the fuel particles amount starts to transit in front of the probe, like in example of Fig. 75:

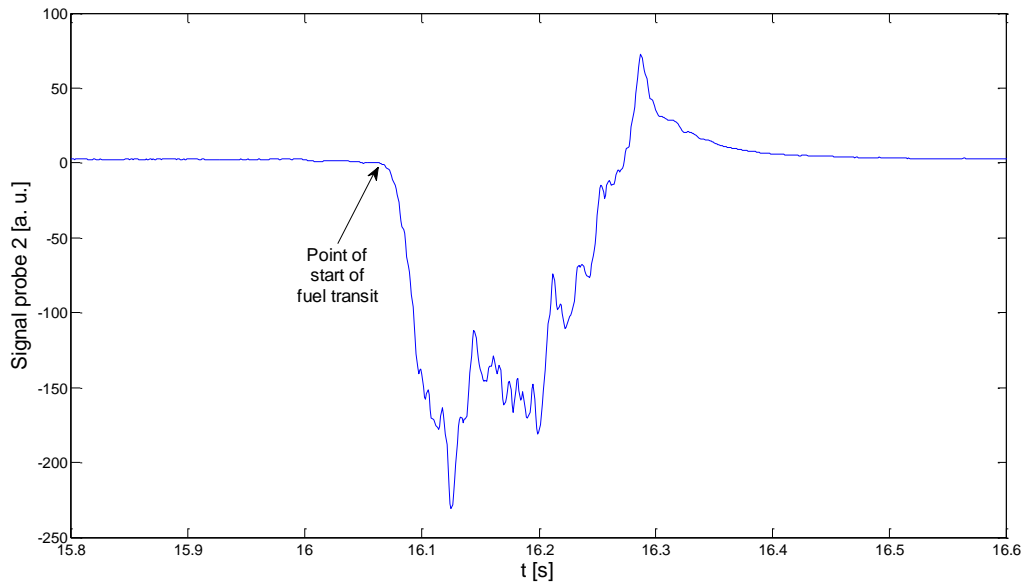


Fig. 75: Example of individuation of the point of start of fuel transit

When these points are known, the fuel particles velocity it is calculated as:

$$v = \frac{\Delta S}{\Delta t} \quad (24)$$

where:

- $\Delta S$  is the distance between two lateral probes
- $\Delta t$  is the time between the fuel transit in front of two probes.

Results shown are relative to September experimental tests.

## 7.1.2 Experimental results

### 7.1.2.1 Tests with coal

Medium velocity of coal particles are shown between port 6 and 8 and port 8 and 10 with data standard deviation.

Tab. 24: Coal particles velocity for  $d_p=38-90 \mu\text{m}$

Temperature (°C)	Y <sub>O2</sub> (%dry)	Diluent gas	Velocity port 6/8 (m/s)	Stand. Dev.(m/s)	Velocity port 8/10 (m/s)	Stand. Dev.(m/s)
1100	3	N <sub>2</sub>	5.67	0.41	4.21	0.17
1100	6	N <sub>2</sub>	6.11	0.48	5.31	0.32
1100	9	N <sub>2</sub>	5.78	0.63	5.54	0.56
1100	3	CO <sub>2</sub>	5.39	0.34	2.48	0.04
1100	6	CO <sub>2</sub>	5.21	0.54	2.87	0.85
1100	9	CO <sub>2</sub>	6.07	0.33	2.97	0.06
900	3	N <sub>2</sub>	4.59	0.32	2.73	0.08
900	6	N <sub>2</sub>	4.24	0.35	2.71	0.09

Tab. 25: Coal particles velocity for  $d_p > 125 \mu\text{m}$

Temperature (°C)	Y <sub>O2</sub> (%dry)	Diluent gas	Velocity port 6/8 (m/s)	Stand. Dev.(m/s)	Velocity port 8/10 (m/s)	Stand. Dev.(m/s)
1100	3	N <sub>2</sub>	6.30	0.42	5.49	0.29
1100	6	N <sub>2</sub>	6.64	0.45	5.74	0.32
1100	9	N <sub>2</sub>	6.44	0.65	6.02	0.28
900	3	N <sub>2</sub>	3.81	0.17	2.95	0.12
900	6	N <sub>2</sub>	3.82	0.26	2.73	0.19

Some observations can be made:

- particles velocity at 1100°C is higher than at 900°C probably because of for the same normalized volumetric flow (in Nm<sup>3</sup>/h) the real volumetric flow of hot gases is very higher and then also the coal particles is higher
- particles velocity in oxy-fuel conditions is lower especially between port 8 and 10 because of the lower hot gases volumetric flow
- in each case the coal velocity between port 6 and 8 is higher than for port 8 and 10, like expected.

#### 7.1.2.2 Tests with char of coal

Tab. 26: Char of coal particles velocity for  $d_p = 45-90 \mu\text{m}$

Temperature (°C)	Y <sub>O2</sub> (%dry)	Diluent gas	Velocity port 6/8 (m/s)	Stand. Dev.(m/s)	Velocity port 8/10 (m/s)	Stand. Dev.(m/s)
1100	6	N <sub>2</sub>	6.12	0.49	3.92	0.20

Tab. 27: Char of coal particles velocity for  $d_p = 90-125 \mu\text{m}$

Temperature (°C)	Y <sub>O2</sub> (%dry)	Diluent gas	Velocity port 6/8 (m/s)	Stand. Dev.(m/s)	Velocity port 8/10 (m/s)	Stand. Dev.(m/s)
1100	6	N <sub>2</sub>	6.01	0.31	3.68	0.21

Obtained values are very similar at those for coal in the same operating conditions.

#### 7.1.2.3 Tests with biomass

Tab. 28: Biomass particles velocity

Temperature (°C)	Y <sub>O2</sub> (%dry)	Diluent gas	Velocity port 6/8 (m/s)	Stand. Dev.(m/s)	Velocity port 8/10 (m/s)	Stand. Dev.(m/s)
900	3	N <sub>2</sub>	4.16	0.58	2.13	0.11
900	6	N <sub>2</sub>	4.06	0.54	2.96	0.19

Obtained values are very similar at those for coal in the same operating conditions.

## 8 References

- [1]. T. WALL, Y. LIU, C. SPERO, L. ELLIOT, S. KHARE, R. RATHNAM, F. ZEENATHAL, B. MOGHTADERI, B. BUHRE, C. SHENG, R. GUPTA, T. YAMADA, K. MAKINO, J. YU, *Chemical Engineering Research and Design* 87 (2009) 1003-1016.
  - [2]. A. MOLINA, C. R. SHADDIX, *Proceedings on the Combustion Institute* 31 (2007) 1905-1912.
  - [3]. P. A. BEJARANO, Y. A. LEVENDIS, *Combustion and Flame* 153 (2008) 270-287.
  - [4]. C. R. SHADDIX, A. MOLINA. *Proceedings on the Combustion Institute* 32 (2009) 2091-2098.
  - [5]. Y. LIU, M. GEIER, A. MOLINA, C. R. SHADDIX, *Greenhouse Gas Control* 55 (2011) 536-546.
  - [6]. R. BRUSCHI, E. GIACOMAZZI, S. GIAMMARTINI, E. GIULIETTI, F. MANFREDI, C. STRINGOLA, S. DANIELE, AIAA-2005-4328, 41st AIAA/ASME/SAE/ASEE Joint Propulsion Conference & Exhibit, Tucson, Arizona, USA, 10-13 July 2005
  - [7]. E. BIAGINI, M. MARCUCCI, *Review of methodologies for coal characterisation*, Report No. IFRF Doc. No. H49/y/02, International Flame Research Foundation, 2010.
  - [8]. E. BIAGINI, L. BIASCI, M. MARCUCCI, *Description of the Isothermal Plug Flow Reactor and experimental procedures for combustion studies on solid fuels*, Report No. IFRF Doc. No. G03/y/03, International Flame Research Foundation, 2010.
  - [9]. E. GIACOMAZZI, G. TROIANI, E. GIULIETTI, R. BRUSCHI, *Experiments in Fluids*, Springer Berlin / Heidelberg, vol./issue 44/4, pp. 557-564, 2008.
  - [10]. R. BRUSCHI, C. STRINGOLA, M. NOBILI, La metodologia ODC applicata alla verifica delle condizioni di funzionamento flameless di un reattore ad ossicombustione di slurry di carbone, Report No. Report RSE/2009/104 ENEA Ricerca Sistema Elettrico, 2009.
  - [11]. K. ANNAMALAI, W. RYAN, S. DHANAPALAN, *Progress in Energy and Combustion Science* 20 (1994) 487-618.
  - [12]. Y. LIU, M. GEIER, A. MOLINA, C. R. SHADDIX, *Greenhouse Gas Control* 55 (2011) 536-546.
  - [13]. M. RUIZ, K. ANNAMALAI, K. DAHDAH, IN: W. L. GROSSHANDLER, H. G. SEMERJIAN (Eds), ASME HTD-Vol. 148, *Heat and mass transfer in fires and combustion systems*, 1990, p. 16-26.
  - [14]. W. H. PRESS, S. A. TEUKOLSKY, W. T. VETTERLING, B. P. FLANNERY, *Numerical Recipes in Fortran 77: the art of scientific computing*, second ed., Cambridge University Press, Cambridge, 1992, pp. 490-504.
  - [15]. P. A. BEJARANO, Y. A. LEVENDIS, *Combustion and Flame* 153 (2008) 270-287.
  - [16]. L. ZHANG, E. BINNER, Y. QIAO, C. Z. LI, *Fuel* 89 (2010) 2703-2712.
- Y. A. LEVENDIS, K. JOSHI, R. KHATAMI, A. F. SAROFIM, *Combustion and Flame* 158 (2011) 452-465.
-